We are committed to providing accessible customer service.
If you need accessible formats or communications supports, please contact us.

Nous tenons à améliorer l'accessibilité des services à la clientèle.
Si vous avez besoin de formats accessibles ou d'aide à la communication, veuillez nous contacter.

Ontario

REPORT ON PROCESSING & ANALYSIS OF

VTEM 30 HZ EM AND MAGNETICS DATA

WABASSI-MAX PROJECT, ONTARIO

FOR

NORTHERN SHIELD RESOURCES

OCTOBER 2010

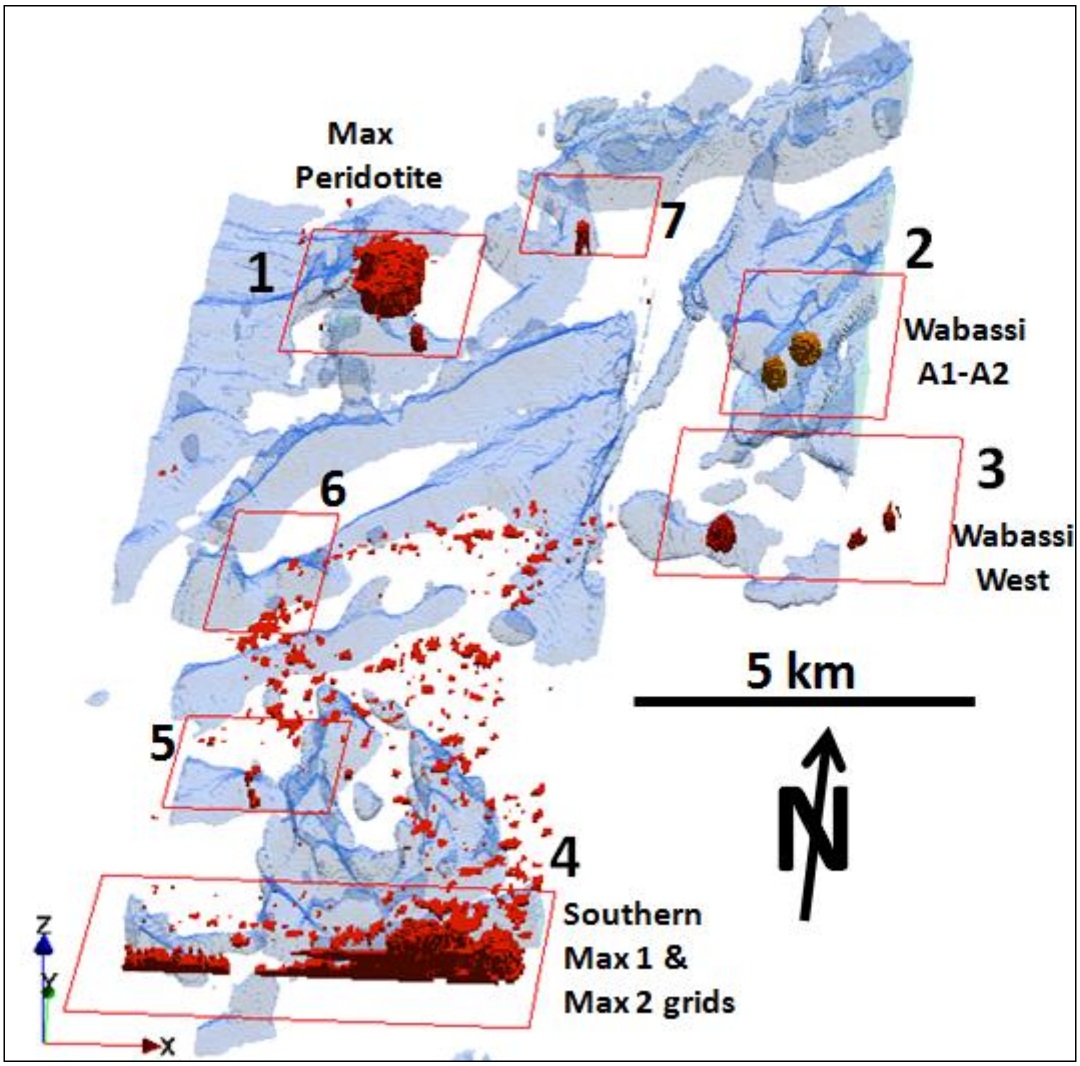

Condor Consulting
Lakewood Colorado
USA

.

CONTENTS

1. Summary 3

2. Introduction 4

3. Exploration History and Deposit Model 6

4. Processing, Analysis Techniques and Products 9
   Processing 9
      EM Data Processing 9
      Magnetic Data Processing 10
   Analysis 10
      Anomaly Shapes 10
      Picking 11
      Magnetics 11
      Target Zones 11
   Products 12
      Table 4-1 Survey Products 12

5. Geophysical Interpretation 15
   Target Zones and Targeting 15
      Summary 15
      Assessment 16
      Plate Modeling and Drill Targeting 20

6. Priority Target Zone Discussion 22
      TZ 1 23
      TZ 2 24
      TZ 3 29
      TZ 4 36

7. Conclusions 40

8. References 42

9. Appendixes 43
   Appendix A-List of Picked EM Anomalies 44
   Appendix B-Notes on Maxwell Modeling 54
   Appendix C- “Fly to drill Templates” 55
   Appendix D-Notes on Magnetic Modeling 71
   Appendix E-Wabassi-Max historic drill hole list 72

Appendix F- VTEM Target Plate Parameters..73
Appendix G- VTEM Target Drill Hole Parameters..75
Appendix H- InfiniTEM Target Plate and Drill Hole Parameters.....................................76
Appendix I-Archive DVD..77

1. Summary

This report covers the processing and analysis of three VTEM EM and magnetic surveys carried out by Geotech Ltd. in 2008 and 2010. Two of the surveys were carried out for Northern Shield Resources on their Wabassi and High Bank Camp blocks and a third block (made up of two sub-blocks called Max 1 and Max 2) was flown for East-West Resources in 2008 and was then optioned by Northern Shield Resources. The properties are located approximately 50 km southwest of the Lamon Lake Camp, near Ogoki Post, NW Ontario.

The report also includes the re-analysis of ground EM data collected over the Wabassi grid by Abitibi Geophysics for comparison with the VTEM outcomes.

The processing of the EM data includes Layered Earth Inversions (LEI), time constant (AdTau) analysis and 3D gridding of the LEIs results. Maxwell plate modeling was also performed on specific targets selected by the client. Mag3D modeling was carried out on the stitched (merged) magnetic grid from the three original surveys. Drilling information was provided by Northern Shield Resources and has been displayed in the products provided.

Based on this assessment, seven Target Zones were identified of which the top four Zones were Maxwell modeled and proposed drill holes defined. Plates were also prioritized on having higher associated Mag3D responses and in the case of the drilled Max peridotite and Wabassi A1-A2 sites, being located in gaps between existing drill holes.

The VTEM data is of sufficient quality that direct drilling of the airborne results can be undertaken for selected larger target plates. For the smaller targets of limited spatial extent, the proposed borehole collars were sighted as best as possible using the available VTEM coordinates and UTM transformed InfiniTEM coordinates. If accurate differential GPS sighting of drill holes in the field indicates that collar elevations are off by more than a few meters for the XY coordinates provided over the smaller plates, it's recommended that the drill hole trajectories be adjusted to reflect the more accurate Z coordinate.

2. Introduction

Geotech Ltd. conducted three VTEM EM and magnetic surveys in 2008 and 2010 covering the Max (then held by East-West Resources), Wabassi, and High Bank Camp (or Wabassi West). These are detailed in reports by Prikhodko (2008) and Legault et al (2009) and Au et al (2009). The total survey distance is 2 355 km as seen in Figure 1. The breakdown is shown below:

- Max-1247 lkm
- Wabassi-741 lkm
- High Bank Camp-367 lkm

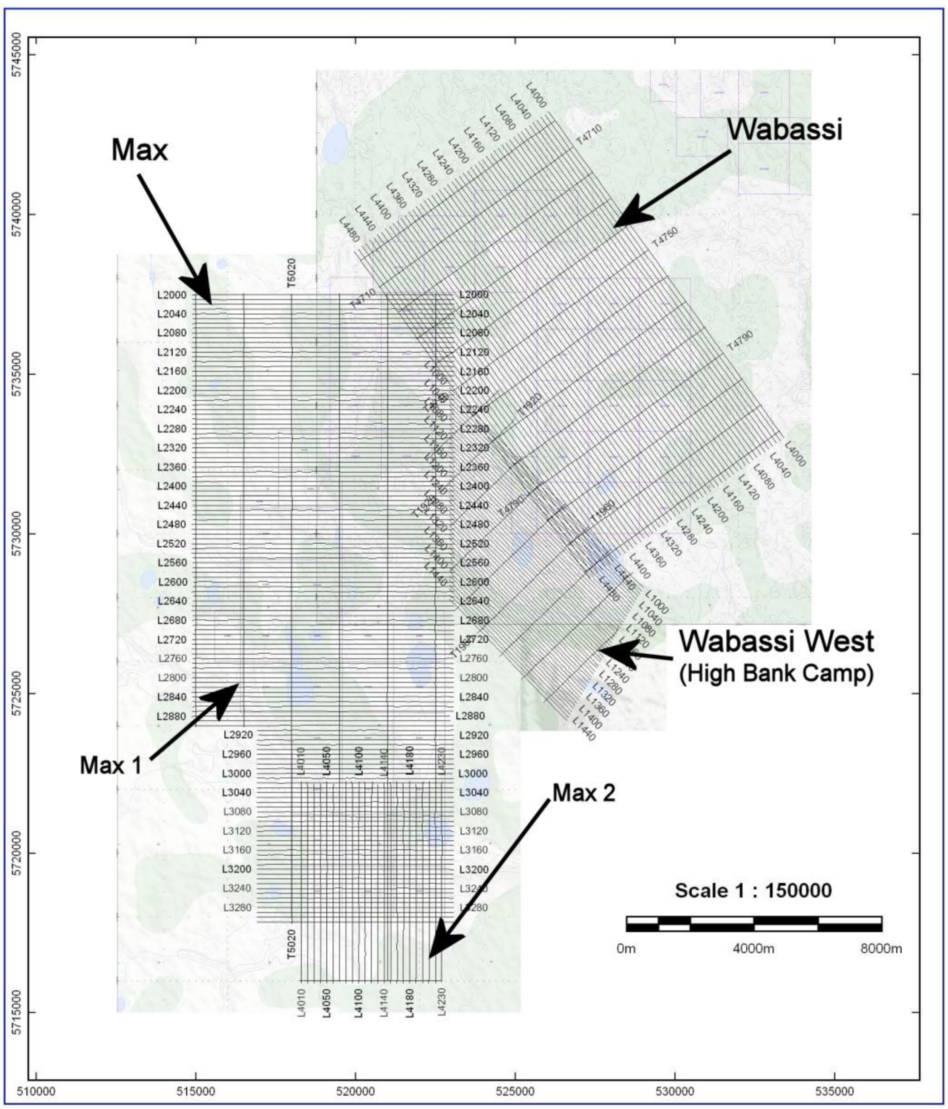

Figure 1: VTEM flight blocks.

In July 2010 Northern Shield Resources (Northern Shield) commissioned Condor Consulting Inc (Condor) to undertake an independent assessment of the survey outcomes. Condor had earlier carried out an independent assessment of ground and borehole EM results over the Wabassi A1-A2 target area. This was reported on earlier (Cunion and Witherly 2010). At the client's request, some further examination of the ground and airborne results has been undertaken so as to try and rationalize the two sets of results. The outcome of this assessment is also included in this report.

3. Exploration History and Deposit Model

Exploration History

A comprehensive on-line background data search with the Ontario Geological Survey indicates little past exploration work has taken place in the immediate four grid area. The most detailed geologic assessment of the area is from the Northern Shield website: http://www.northern-shield.com/wabassi.html as is quoted below:

The Wabassi and Max properties are located in northwestern Ontario, 60 km south of the High-bank Lake project and 100 km south of the Ring of Fire Ni-Cu-PGE and Chromite deposits. The properties are being explored for reef-hosted PGE and massive sulphide Ni-Cu-PGE deposits. The Wabassi and Wabassi North properties were staked by Northern Shield Resources Inc. in 2007 based on the geophysical pattern observed on the magnetic survey published by the Ontario Geological Survey (OGS) in the Fort Hope area, which suggests a layered intrusion. The anomalous values of Pt and Pd (130 ppb Pt+Pd) found in one of the 3 samples analysed from the first sample collection in 2007 also confirms the potential for PGE and/or Ni-Cu-(PGE) deposits in the intrusive complex. In 2008, Northern Shield optioned the neighbouring Max Property from East West Resource Corp. Subsequently, drilling confirmed the distinct magnetic anomaly in the northern portion of the property to be a nickel, copper and PGE-enriched ultramafic (peridotite) intrusion.

The Northern Shield geology map of the project area, based on the regional aeromagnetic data is seen in Figure 2, with the 22 historical drill holes plotted (Appendix F). Past-identified Wabassi conductive plate responses were associated with sulphides for seven holes. Plate conductivities associated with the massive sulphides were up to 5000 mS/m.

The geology of the grid area is described by Northern Shield as follows:

WABASSI LAYERED INTRUSION

This is a layered mafic-ultramafic intrusion composed of olivine-gabbronorites and norites in the upper (northern) portion. To date, very little exploration has been conducted on the southern portion but it is now believed to represent the lower, and most prospective, levels of the intrusion. The Wabassi intrusion is a well-layered mafic-ultramafic complex with similarities to the Stillwater Complex in Montana, where PGEs are mined from the J-M reef. Rock-types so far identified include, olivine gabbronorites, olivine norites and norites; these are all ideal lithologies in nickel and PGE bearing systems. The intrusion is being explored for Ni-Cu-PGE massive sulphides along the contacts and in feeders, and for disseminated mineralization hosted in "reefs.

WABASSI NORTH INTRUSION

Other than one drill hole, no other exploration has been conducted to date on the Wabassi North Property. Drilling intersected a variety of gabbroic rocks which may, or may not be related to the main Wabassi layered intrusion or the Max peridotite intrusion. The geophysics suggests that this body may consist of composite phases of gabbroic and other mafic/ultramafic phases.

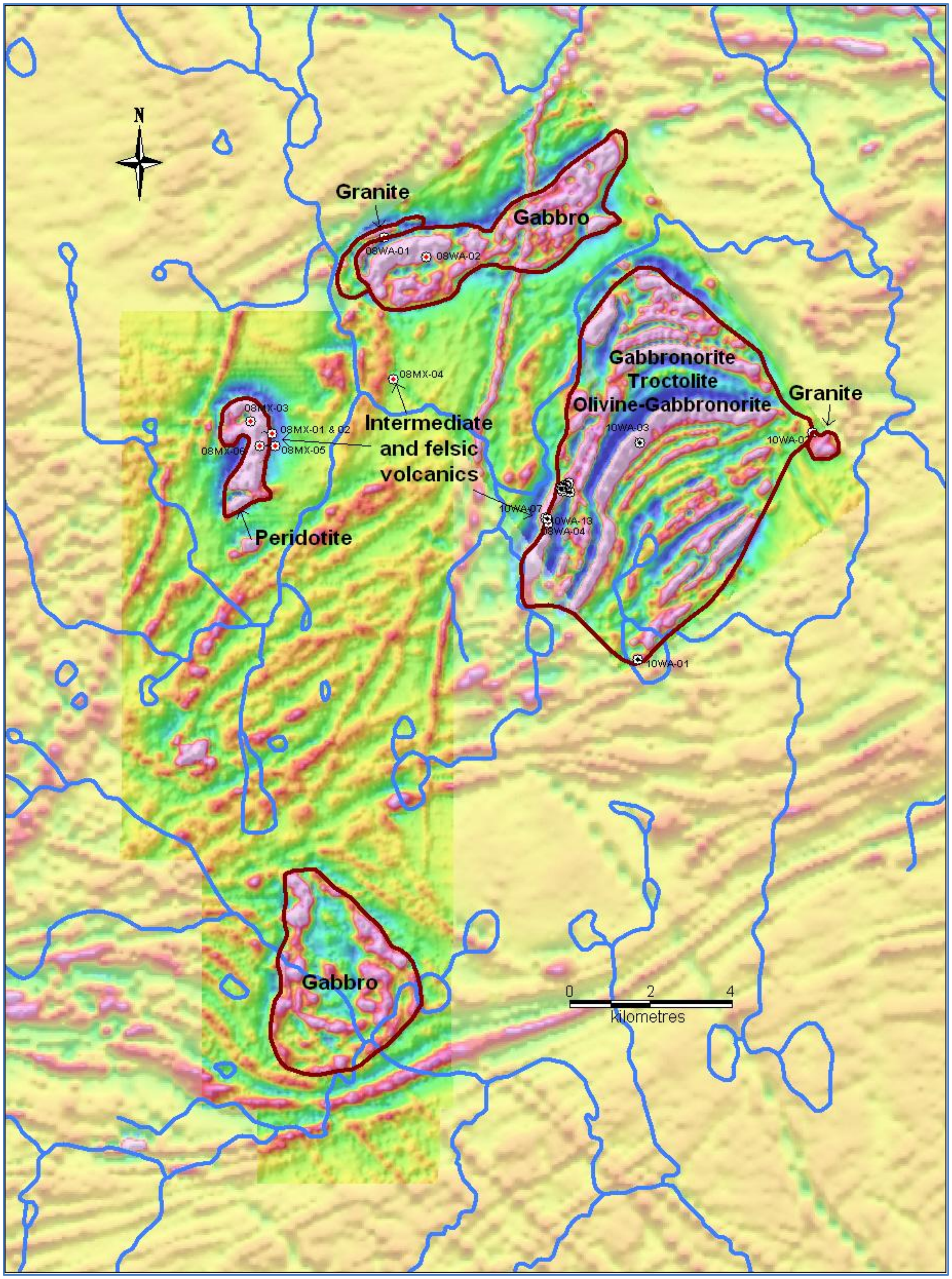

Figure 2: Northern Shield geology map of the merged grid area.

MAX PERIDOTITE INTRUSION

Five drill-holes were completed on this target by Northern Shield in 2007 as part of an option agreement to earn a 50% interest in the property. The body is composed mostly of peridotite (harzburgite) and comprises the most primitive rocks intersected to date within the two properties. The body has high background levels of Ni-Cu-PGE. Geophysics suggests a possible feeder conduit between the Max peridotite and Wabassi North gabbro.

GABBROIC INTRUSION

An intrusion in the southern portion of the Max property has been mapped by the OGS as a gabbroic body, but no exploration has taken place to date on this portion of the Property.

Deposit Model

Northern Shield's website description of the deposit model has been parsed below:

"Feeder conduits are ideal hosts for Ni-Cu-(PGE) mineralization. Fragments of nickel-bearing pyrrhotite and blebs of primary nickel-copper mineralization were observed in core from a drill-hole completed in 2008 adjacent to one of the VTEM conductors….

….Because the sulphide minerals and PGEs are dense, they tend to sink to the bottom of their host body or accumulate in traps. The sulphur has acted as a filter removing nickel, copper and PGEs from the magma as it flows along the conduit and hence the magma downstream from the filter contains very little PGEs and is said to be depleted….

…Thus if one can find two mafic-ultramafic bodies formed from the same magma with one being enriched and the other one being depleted, then there is a good chance that somewhere in between, PGE mineralization may have formed….

….In the case of Max/Wabassi, the Max peridotite is enriched in PGEs (average 45 ppb Pt+Pd). The Wabassi Intrusion shows signs of being depleted in PGEs (average <3 ppb Pt+Pd), which suggests that PGE mineralization may have formed between the two bodies."

A few examples of conduit-associated magmatic nickel sulphide occurrences are Voisey's Bay, Kennecott's Eagle, N'orilsk, and Jinchuan. These occurrences can sometimes be associated with serpentinized peridotite that can have varying conductivity. These ore occurrences can present elevated EM and magnetic responses due to both elevated sulphide and/or associated magnetite content.

In the present situation, blobby-style mineralization could be challenging to locate and target for drilling, even if the zones are quite conductive. PGE-rich mineralization typically is not massive sulfide-rich and can be very difficult to map geophysically. Condor has some familiarity with projects in the general region by Magma Metals and HTX. In both cases, the mineralized zones lack large size and high conductance.

4. Processing, Analysis Techniques and Products

Processing

The following processing steps were carried out on the VTEM EM and magnetic data.

EM Data Processing

Layered-Earth Inversion

The layered-earth inversion (LEI) algorithm models the EM data with a 28-layered earth model (Farquharson and Oldenburg, 1993, Ellis 1998) increasing in thickness from the surface to depth in an approximately logarithmic fashion. A starting model of 10,000 ohm-m (0.1 mS/m) was used, with a reference model of 10,000 ohm-m (0.1 mS/m). The reference model resistivity is what the program defaults to at depth when there is no longer enough information to further refine the inversion outcome. The results of the inversion are presented in the form of a conductivity depth section (CDS).

Time Constant: AdTau

The AdTau program calculates the time constant (tau) from time domain decay data. The program is termed ***AdTau*** since rather than using a fixed suite of channels as commonly done, the user sets a noise level and depending on the local characteristics of the data, the program will then select the set of five channels above this noise level. In resistive areas, this means the calculation will favor earlier channels, whereas in conductive terrains the latest channels will more likely be above the noise floor. A typical decay fit; in this case, the last five channels are shown to the right in Figure 3.

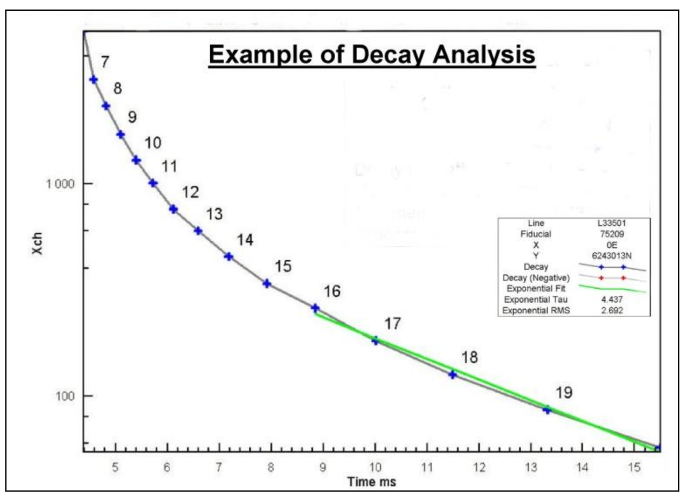

Figure 3: Example of AdTau decay.

Maxwell Modeling

Maxwell is an EM modeling program developed by EMIT (Electro Magnetic Imaging Technology) of Perth, Australia. Maxwell is designed for the analysis of ground, borehole and airborne surveys. A brief description of Maxwell is provided in Appendix B.

The *Fly to Drill* template was done using encom pa software and is used to present the Maxwell modeling outcomes; these are provided in Appendix C.

Magnetic Data Processing

Geosoft was used to filter the magnetic data. In addition to the normal filters available in the Geosoft application, additional processing was done using encom pa software and algorithms described by Shi and Butt 2004 – this paper is included in Appendix D.

Magnetic Data Modeling

The magnetic data for the survey block has been modeled using the code Mag3D; this is a voxel-style inversion program developed at the University of British Colombia-GIF (Li and Oldenburg 1996). Information on this program is provided in Appendix C. Encom's ModelVision Pro was used to model the observed magnetic response against plate-derived model responses. This is briefly described in Appendix E.

Analysis

EM

Anomaly Shapes

For discrete plate-like targets, the VTEM system produces two main types of responses; those termed inductively thin or double-peaked responses (DPR) and those termed inductively thick or single-peak responses (SPR). These basic shapes are shown in profile form in Figure 4.

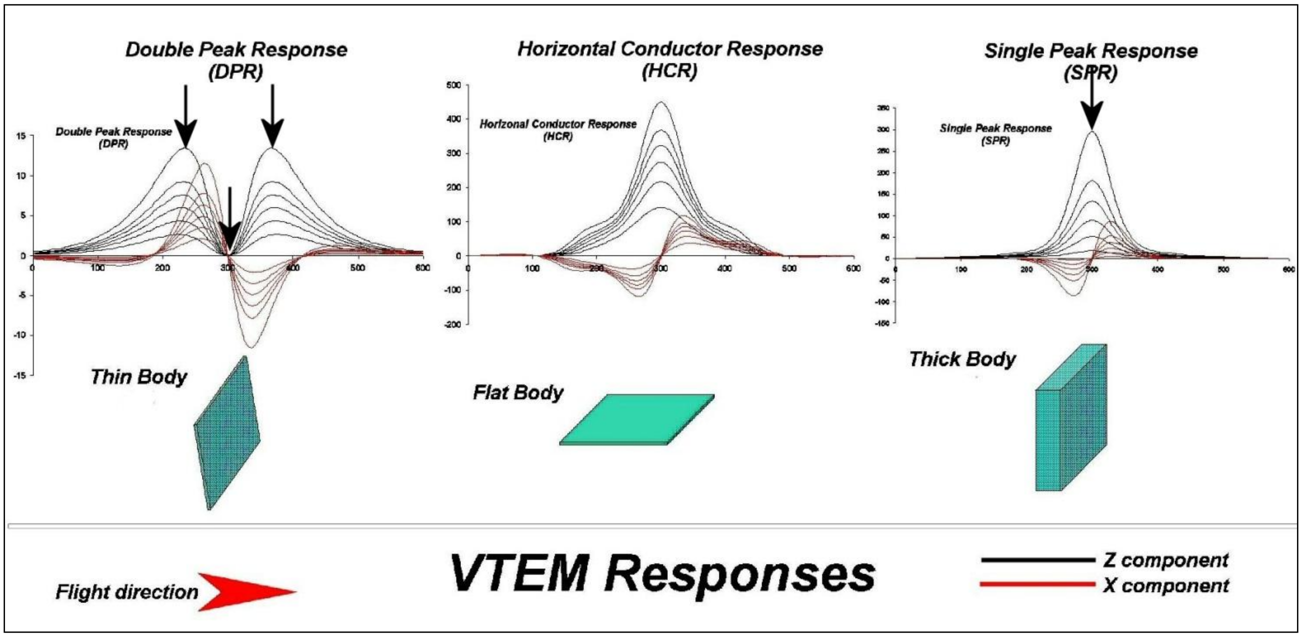

Figure 4: Examples of VTEM responses.

Picking

The MultiPlot™ display was the primary means to examine, identify and then rank the anomalies. This overall process is termed anomaly picking and was performed on a line-by-line basis, with several passes being required to finalize the process.

The discrete EM responses were picked and ranked based on their profile response and character in the 1D inversions. They are plotted on the various provided products. These are listed in Appendix A.

Magnetics

The magnetic results were examined in section (profile and cross-section through the 3D voxel models as well as 3D perspective voxel models.

Target Zones

Target Zones are groupings of conductors (either discrete picks or wide zones) that are deemed to be a geophysically-logical feature. The Target Zones (or TZs) are prioritized based on their degree of correlation with the expected response from the target models.

Products

Table 4-1 lists the maps and products that are provided. Other products can be prepared from the existing dataset, if required.

Base Maps: All maps are created using the following NAD83 UTM 16 N parameters:

Projection Description:
Datum: NAD83
Ellipsoid: GRS 1980
Projection: Transverse Mercator
Central Meridian: 87ºW
False Northing: 0
False Easting: 500000
Scale factor: 0.9996
Latitude of origin: 0ºN
Longitude of origin: 87ºW

Table 4-1 Survey Products

For this assessment three versions of the MultiPlots were prepared. One set covered each of the two separate airborne surveys and a third set provided comparative plots of the VTEM results.

TargetMaps @ 1:30 000 (one copy of each)

All maps show the indicated themes as well as the Condor picks and Target Zones

- Total Magnetic Intensity (TMI)
- EM B-field Z Channel 14 (234 µsec)
- B-Field AdTau (threshold 0.003 or 0.002 ms) draped on 1VD magnetic, 7 target zones, EM and magnetic interpretation, and AdTau picks
- Magnetic tilt angle and contours with AdTau contours and EM picks. The merged magnetic 1VD grid interpretations with the 7 Target Zones, Maxwell Models and anomaly picks
- DTM (SRTM)

MultiPlots™ @ 1:20 000 (PDF only)

Mini-Plates™: TMI, TMI-Tilt, EM Bfield Ch [5] (234 usec), Bfield Ch [14] (1 151 usec), AdTau Bfield Z, DTM

- EM dB/dT Z Channels 1-24 (on Wabassi and Max) and Channels 1-32 on Wabassi West
- EM Bfield Z Channels 1-24 (on Wabassi and Max) and Channels 1-32 on Wabassi West
- Profiles-Magnetics: TMI, TMI-Tilt and TMI-1st vertical derivative
- Profiles-AdTau Bfield, dB/dT, power line monitor
- LEI Conductivity Depth Section (Z dB/dT) with EM System Height, Maxwell Plate Models and Proposed Drill Holes Section
- LEI Conductivity Depth Section (Z Bfield) with EM System Height, Maxwell Plate Models and Proposed Drill Holes Magnetic Susceptibility Model and Proposed Drill Holes
- Magnetic Susceptibility Model + Maxwell models + Proposed Drill Holes
- TrackMap: Magnetic Tilt Angle with Flight Path, Anomaly Picks and Maxwell models

Mag3D Modeling

The following products are provided as part of the Mag3D modeling. Some are stand-alone and some are imbedded with other products; the letters S and I are used to flag which; S= stand-alone and I = imbedded.

- UBC MAG3D mesh and sus files (S)
- 3D DXFs (S)
- Susceptibility Depth Sections (I- in MultiPlots)
- Notes on processing (S)-Appendix C

Processing and analysis report (PDF and 1 hardcopy)

On the archive DVD (Appendix I) the following files are provided:

-Digital archive in Geosoft format

-Profile Analyst session file (to create MultiPlots™)

-Digital files for LEI modeling (modcon dB and modcon Bf)

-Digital files for Mag3D modeling

-PDFs of MultiPlots™

-Processing and analysis report (PDF)

5. Geophysical Interpretation

Target Zones and Targeting

Summary

The review of the EM and magnetic data indentified seven Target Zones in the Wabassi-Max merged grid (red boxes in Figure 5). TZ 1, the Max peridotite; TZ 2, Wabassi A1-A2; TZ 3, Wabassi West; and TZ 4, the southern Max 1 and Max 2 grid areas are ranked high priority. In Figure 5 the green outlines trace the more obvious AdTau responses and

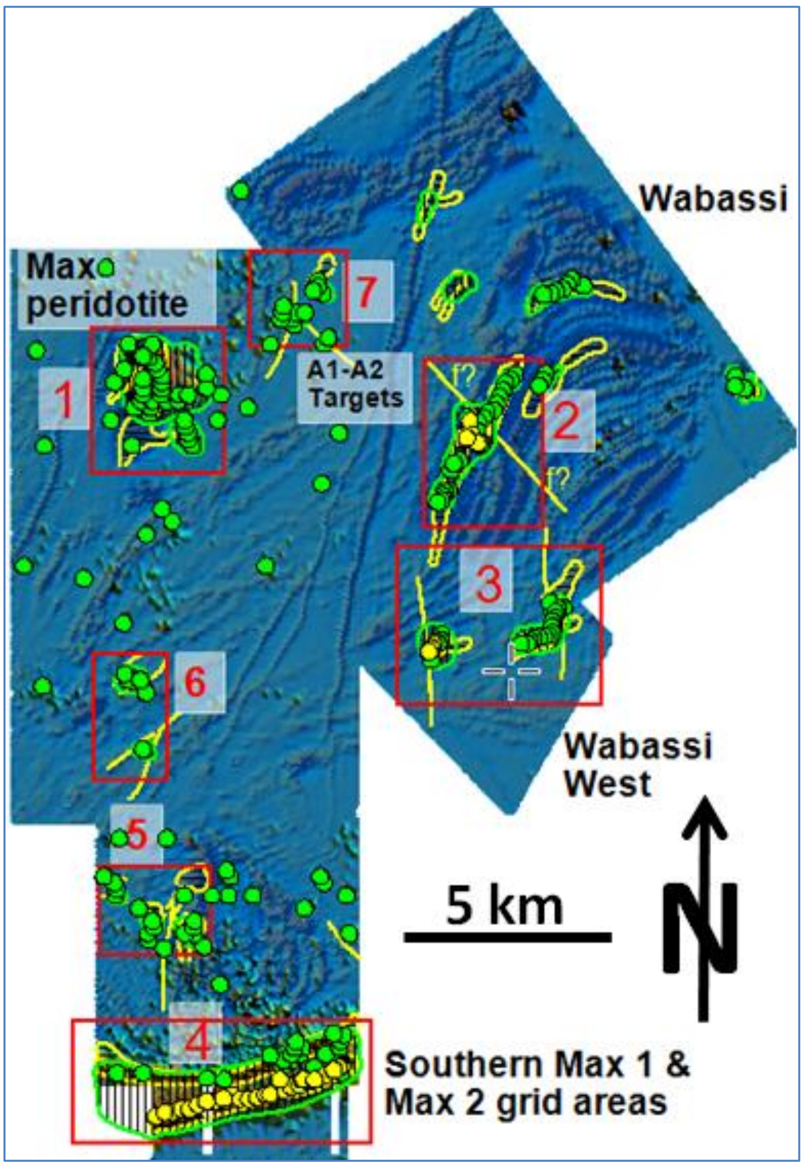

Figure 5. Merged Max, Wabassi and Wabassi West grids,
AdTau draped on TMI-tilt angle with the seven Target Zones highlighted.

the yellow lines trace in the magnetic signatures coincident with the flagged AdTau signatures. An assessment of the line-by-line EM profiles returned 218 anomalies, broken down into the green colored SPR picks and yellow colored DPR picks shown in Figure 5. A complete anomaly listing is provided in Appendix A.

Maxwell modeling of the VTEM and InfiniTEM responses of four TZ's returned a total of 41 target plates and 31 proposed drill holes; these outcomes are provided in Appendices G, H (VTEM) and I (InfiniTEM). For the client-drilled TZs 1 and 2, the plate and drill holes were located after reviewing the locations of the existing drill holes and rejecting plates that were already drilled.

There are 10 more plate solutions than proposed drill holes as some targets could be modeled with both a shallow and deep plate fits the observed responses. These tandem plates are typically intersected by one drill hole, allowing the client to determine if drilling to the deeper plate is warranted. The plate and drill hole "fly to drill" templates plates are in Appendix C, with brief note captions for each target.

Assessment

The data are assessed and interpreted using 2D plans and sections as well as 3D voxel models.

The summary review (Figure 5) shows the more obvious conductive responses on the grid to be associated with discrete magnetic horizons. The AdTau accentuates the more conductive zones, particularly in TZ 1 and TZ 3 (Figure 6). In TZ 1 a smaller satellite conductor located south of the main Max peridotite (Figure 6 right panel) returns an obvious AdTau signature in plan that is lost in background EM late-time noise (Figure 6 left panel). Likewise, the easternmost TZ 3 is enhanced from an indeterminate response in the late-time amplitude image (Figure 6 left panel) to being a clear response in the AdTau image (Figure 6 right panel).

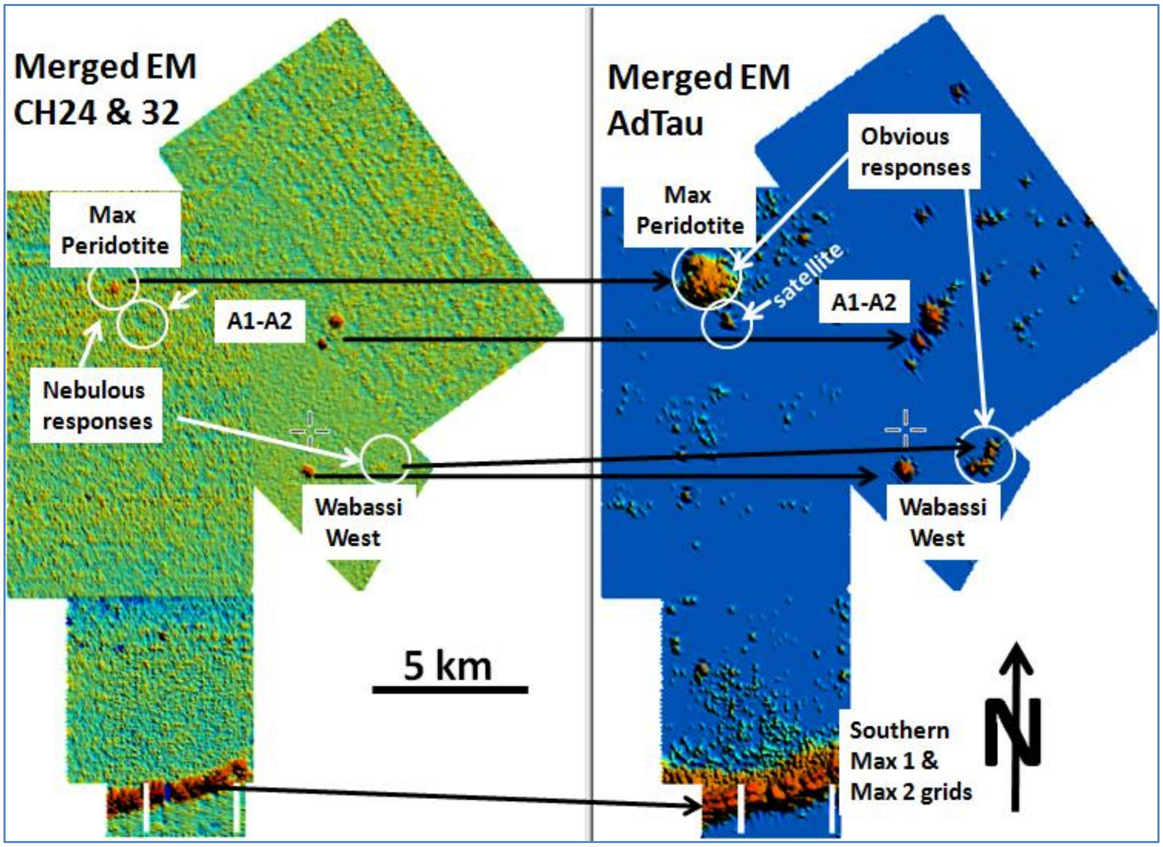

Figure 6: VTEM late-time plan left panel, AdTau plan right panel. The AdTau enhances the smaller and more subtle late-time EM responses.

The TMI-Tilt (Figure 7) provides greater detail of both the structure and lithologies. The TMI-Tilt response in the left panel was contoured as was the AdTau response (Figure 6) and the result merged and displayed in the right panel of Figure 7 along with the anomalous EM picks. The blue lines trace magnetic lineaments, some of which appear to be faults showing lateral offset.

An example of a magnetic structural break is seen to the north and east of the A1 EM anomaly (Figure 8), where a NE-SW striking magnetic horizon appears to be laterally E-W offset up to 500 m along a demagnetized magnetic linear. Though most of the Wabassi-Max region conductivity appears to be stratabound and concentrated in particular magnetic horizons in the layered mafic sequences, there may be a structural component to elevated conductivity at some sites, as indicated by the magnetic breaks that possibly track faults in the A1-A2 conductive horizon.

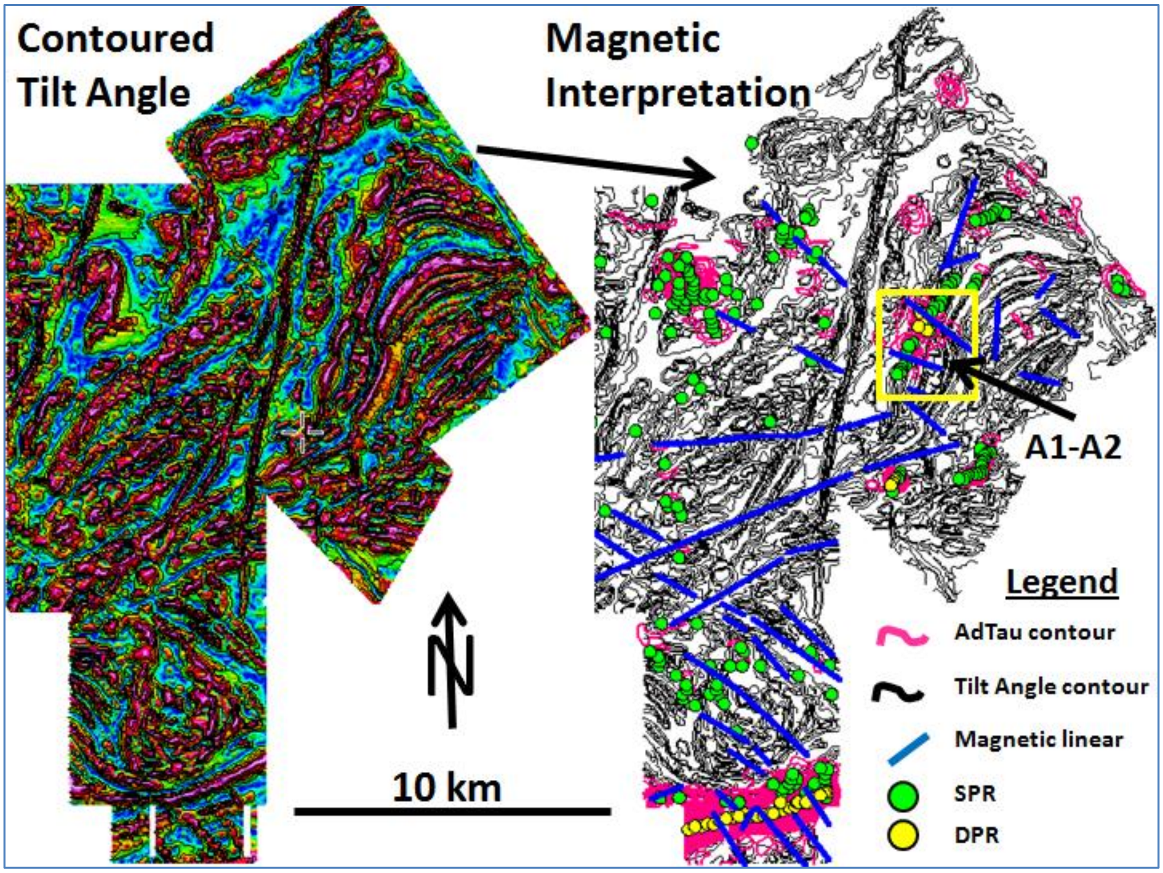

Figure 7: TMI-tilt grid left panel, with the TMI-tilt contours in black on the right panel. The right panel red contours are the AdTau. The green and yellow dots are the anomalous EM picks. Blue lines mark magnetic linears or breaks. The A1-A2 focus area is highlighted by the yellow square is zoomed in on in Figure 8.

Figure 9 shows a merged Mag3D and EM voxel model display. TZs 1-4 produce the most coherent voxel responses whereas much of the area north of TZ 4 (which includes TZs 5 and 6) show a quite broken up appearance in the voxel representation.

Unlike the spatially limited EM responses, higher susceptibility coherent 3D magnetic signatures can be traced for tens of kilometers that map lithology and geologic structures. As noted from the plan analysis, most of the larger conductors appear stratabound within discrete higher susceptibility magnetic surfaces, though these may possibly be disrupted by cross-cutting magnetic breaks in certain locations like at A1.

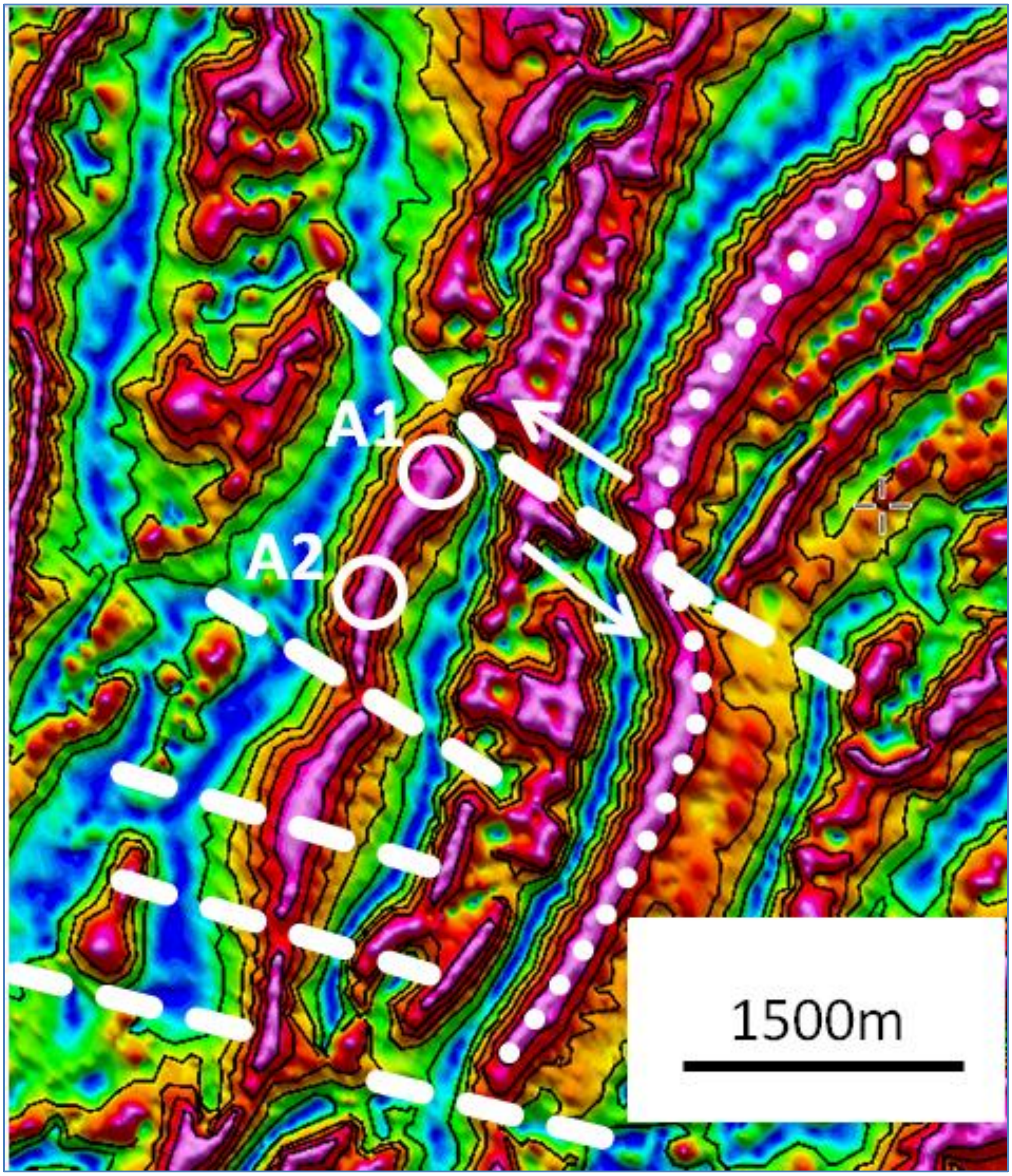

Figure 8: Zoom-in on the tilt angle grid over the A1-A2 conductors. The dashed lines trace inferred magnetic breaks that bisect the magnetic horizon carrying the A1-A2 conductivity. A 500 m lateral offset is indicated at the arrows if indeed the horizon "bend" is structural in origin and not a primary intrusive layering effect.

The final assessment confirms the four higher priority TZs. Whereas TZs 1 and 2 are previously explored, TZ 3 was unknown; returning two new conductors one at least 1 400 m long and TZ 4 is untested.

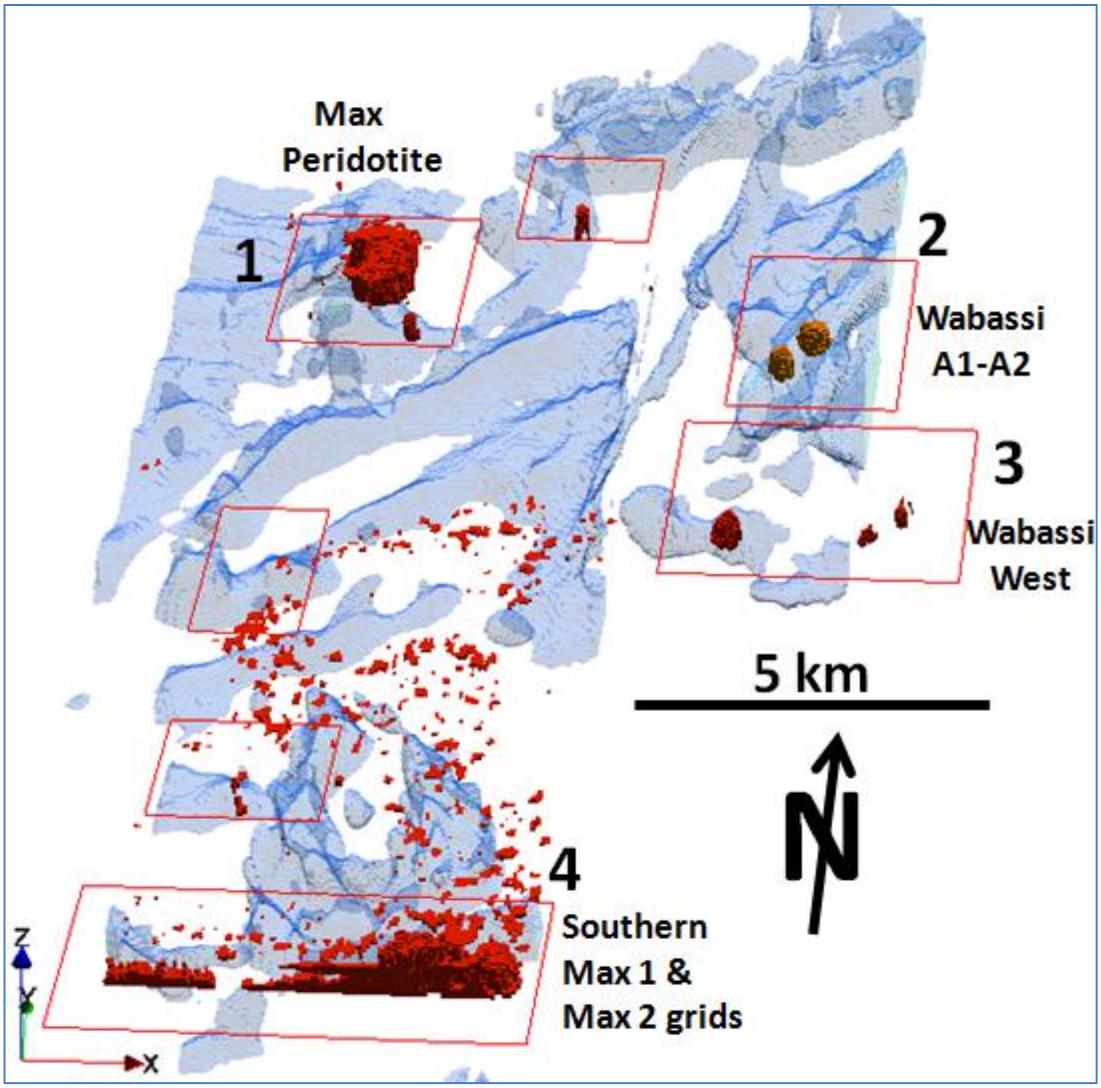

Figure 9: Perspective 3D view looking northward of the threshold Mag3D surface (blue) and the 3D voxel gridded 1D EM surfaces (red). The most significant conductive responses are identified in TZs 1, 2, 3 and 4,

Plate Modeling and Drill Targeting

Following the identification of the priority TZs, Maxwell modeling was undertaken on targets approved by Northern Shield for TZs 1, 2, 3, and 4 (Figure 10). In previously drilled TZs 1 and 2, the new plates were compared with drilling information provided by Northern Shield. Conductors which did not appear to have been previously drilled are provided to the client for possible drill testing. Figure 10 shows that most of the EM target plates are enclosed within magnetic horizons, the exceptions are the TZ 1 satellite conductor, the TZ 2 deeper A1 plates, one of the TZ 3 conductive subzones, and one of the TZ 4 plates.

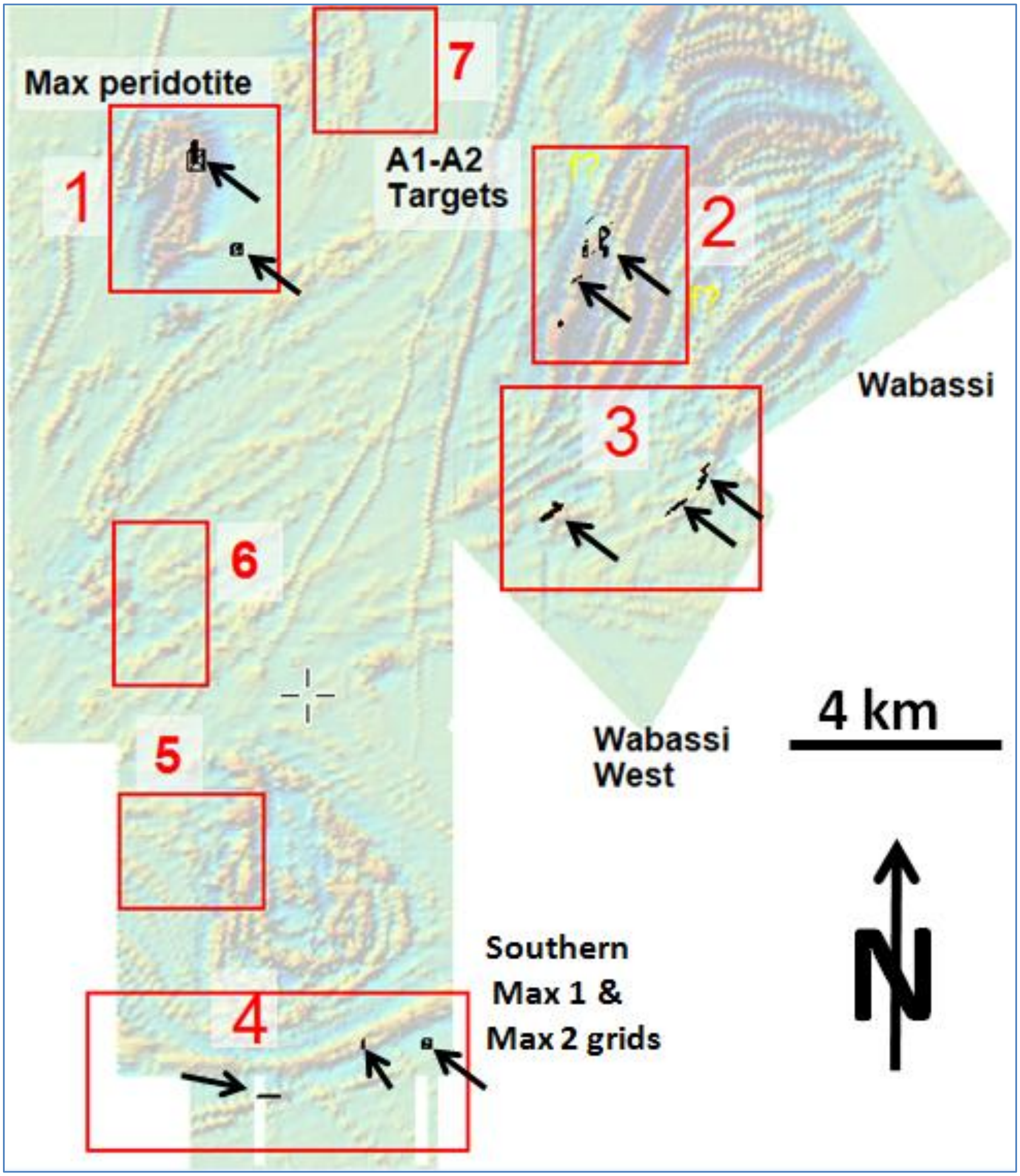

Figure 10: The 41 Maxwell plates on the 1VD magnetic plan. Arrows point out the plate locations. The plates are located in the four priority TZs.

6. Priority Target Zone Discussion

Target Zone 1 includes the Max peridotite and satellite conductor and is comprised of three plate models for lines L2180, L2190, and L2300.

Target Zone 2 encloses the Wabassi A1 and A2 conductors, returning 12 plates in total with two higher priority focus plates; L500 and L4390.

Target Zone 3 on the Wabassi West grid is comprised of two conductive sub areas separated by 2 km. The eastern conductor, continuous for 1 400 m, is split into two more-conductive subzones, subzone 1 and subzone 2, that return plate models for lines L1040, L1050, L1060 L1070; and L1120, L1130, L1140 and L1150 respectively. The third feature is called subzone 3. It shows the highest TZ 3 EM response amplitude and is coincident with a higher magnetic susceptibility zone; plate models for lines L1290, L1300, L1310 and L1320 were defined.

Target Zone 4 on the far south of the Max 1 and Max 2 merged grid has a 6 km long E-W striking conductive signature, identified by a string of DPR EM picks, that is coincident with a magnetic horizon. This appears to be a formational conductor with one plate model for L4080 thought to be representative of the 6 km long conductor. Two SW-NE and N-S striking deeper conductive responses that span 5-6 flight lines are also identified. These conductors are discordant to the generally E-W striking parallel magnetic horizons that characterize TZ 4. As Northern Shield advised the modeling of two TZ 4 lines, L3280 was chosen as the second line as it is typical of the two 500 m long conductors. L3280 returns two plate models, one for the more eastern NS striking conductor, and a second plate for the more western SW-NE striking conductor.

The lower priority ***Target Zones 5, 6 and 7*** are characterized by smaller conductive responses of generally lower EM response amplitude. These lesser conductive responses will not be discussed in this paper but can be reviewed in detail and targeted in future if required.

TZ 1

The Max peridotite is located on the north of the larger Max survey grid. Six holes were drilled into the peridotite (08MX-01 to 08MX-06), including a hole into a smaller satellite conductor to the northeast. Northern Shield's report for the Max peridotite that- *"Magnetite/serpentine veins were common and were noticed to be conductive on the drill core scale. No massive sulphides were intersected and thus it was concluded that the magnetite veins may have caused the VTEM anomalies. However, a few blebs of chalcopyrite, pentlandite and millerite were seen in all drill-holes and the background levels of Ni and PGE in the peridotite is high and hence the need to re-evaluate the VTEM".*

Figure 11 is the plan view of the main Max peridotite AdTau response with the proposed three new plates and drill holes, and five existing 08MX drill holes. The drilled holes, except perhaps 08MX-03, appear to have intersected higher AdTau responses. The satellite conductor returns an obvious AdTau response.

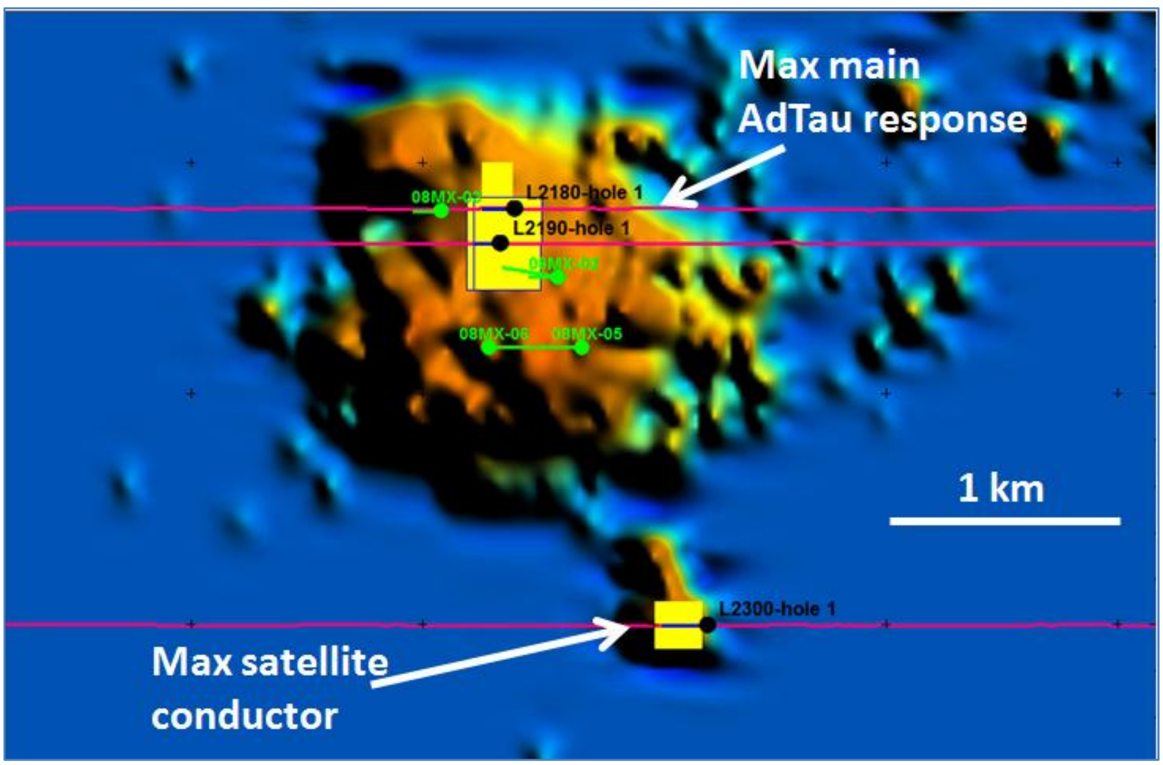

Figure 11: AdTau image Max peridotite with three proposed plates (yellow) and drill holes, and the five historical drill holes in green.

The 3D surface views in Figures 12 and 13 show that the historical holes (except 08MX-01) appear to miss the more-magnetic lithology with a threshold above 0.14 SI. The N-S striking plate models parallel the conductive and magnetic isosurfaces inferring that holes 08MX-03 and 08MX-05 may have also missed the more conductive bulk of the peridotite. The three other MX holes do appear to have tested the more conductive surfaces. The isosurfaces indicate that the higher conductivities may be offset toward the eastern top edge of the more magnetic peridotite; magnetic plate modeling would help better resolve this observation. New holes L2180 and L2190 as sited intersect the tops of both the more conductive and more magnetic isosurfaces that surround the target plates. The higher conductivity surface plunges to the south, whereas the magnetic surface plunges to the north and northwest.

Figure 14 shows the satellite conductor's 0.37 mS/m surface returning a conduit-like shape that encloses the Maxwell plate response for L2300. A portion of the northward trending "conductive bridge" that strikes toward the larger Max peridotite is also seen.

When the higher susceptibility Max 1 magnetic surface is threshold to 0.035 SI, the curvilinear magnetic horizon south of the Max peridotite, that strikes eastward toward the satellite conductor, is seen to terminate several tens of meters to the west of the satellite conductor as shown below in Figure 15.

TZ 2

Twelve new Wabassi plates were modeled. Four InfiniTEM[1] and six VTEM plates were completed around the A1 anomaly. One VTEM and InfiniTEM plate each were modeled for the A2 anomaly and are not discussed here.

The Figure 16 ground TMI image shows the six VTEM plates plotted up with the one thicker and deeper L500 InfiniTEM plate model. The deeper, thicker, higher-priority L500 and L4390 target plates are plotted up in yellow with their boreholes, to distinguish them from the lesser priority shallower VTEM plates in black.

[1] Refer to Cunion and Witherly 2010 for a detailed outline of the original assessment of the Abitibi ground and borehole EM data.

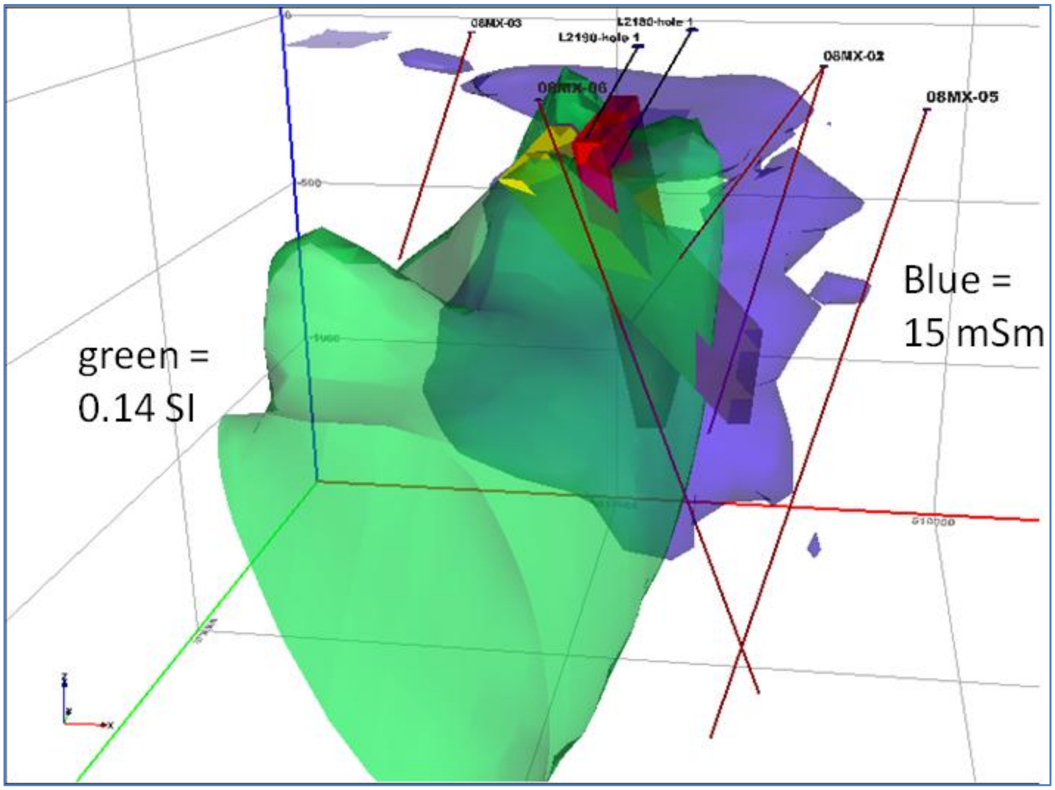

Figure 12: North-looking view of the TZ 1 Max peridotite; green magnetic surface, blue conductivity surface, two proposed drill holes, and five historical holes.

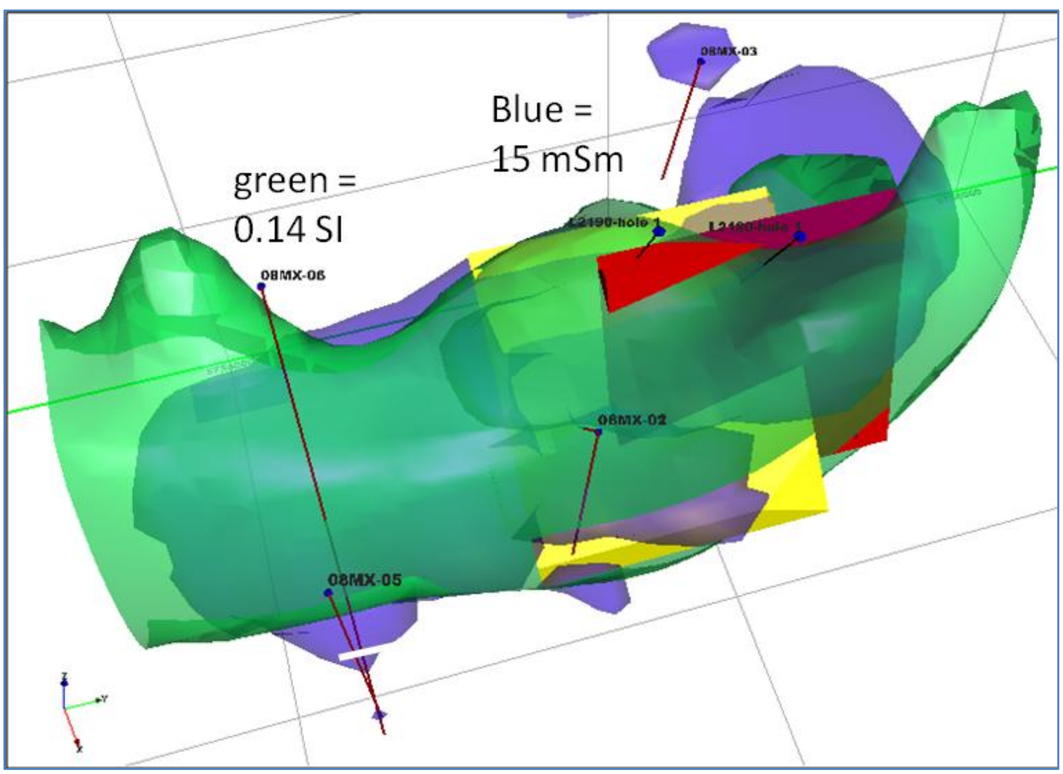

Figure 13: WNW looking view Max peridotite; green magnetic surface, blue conductivity surface, two proposed drill holes, and five historical holes.

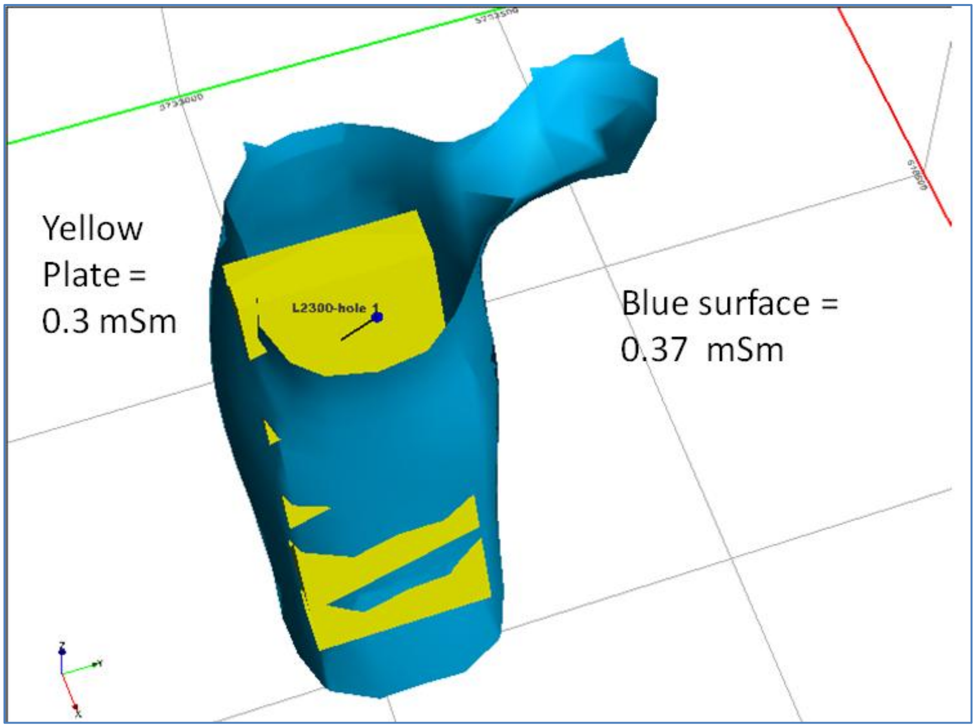

Figure 14: Elevated eastern view of the TZ 1 satellite conductor, 0.37 mS/m surface enclosing 0.30 mS/m plate.

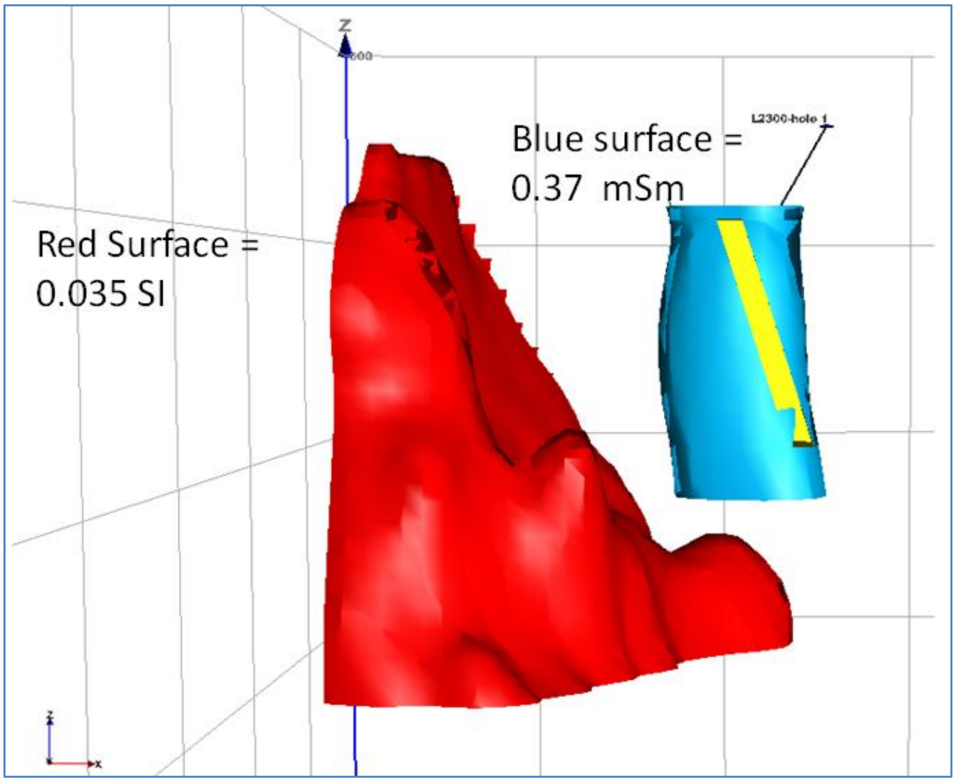

Figure 15: North-looking view of the TZ 1 satellite conductor situated NE 0.035 SI surface that represents a magnetic horizon striking toward the satellite conductor from the SW.

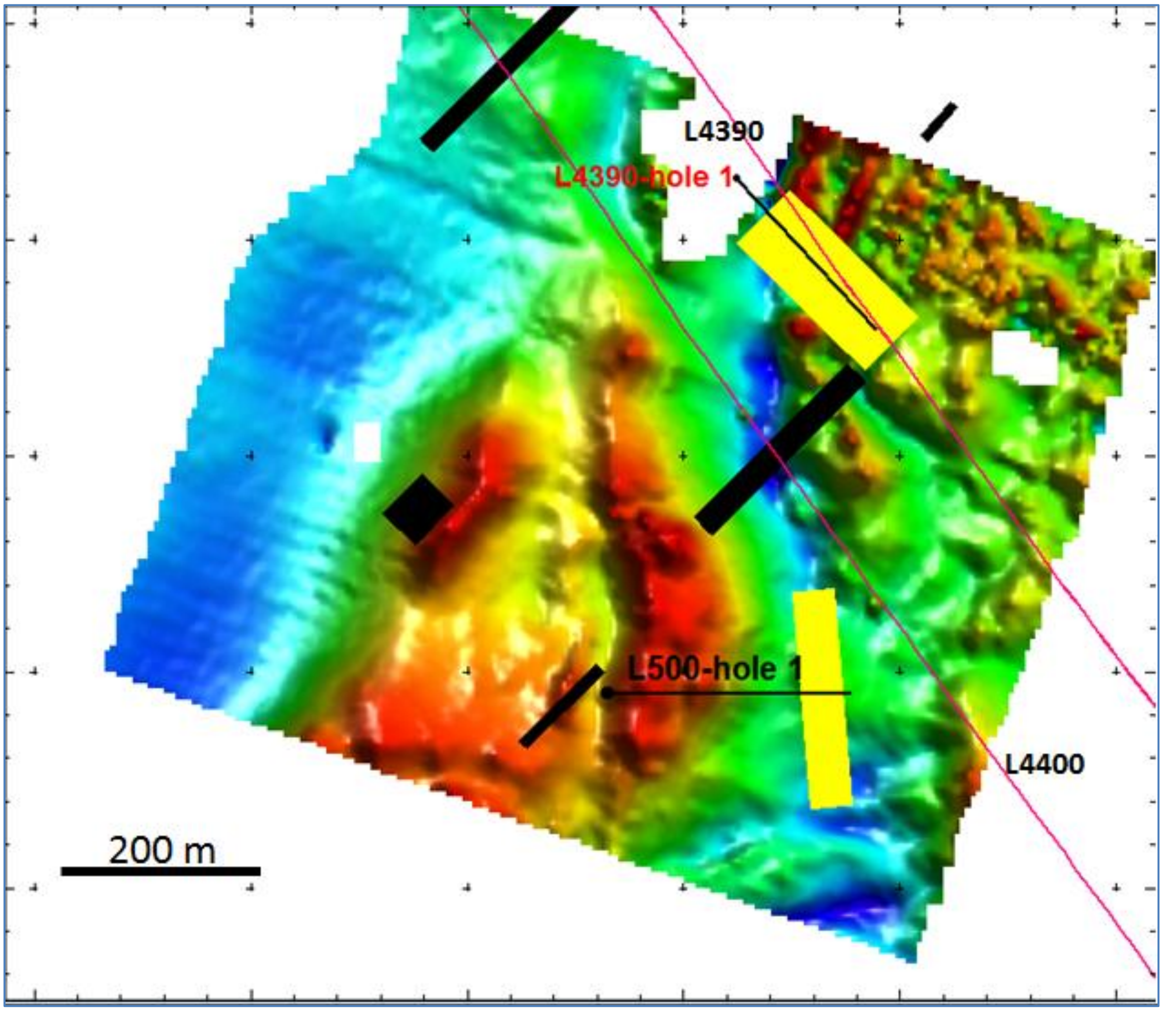

Figure 16: TZ 2, the Wabassi A1 anomaly ground TMI grid with the six new VTEM plates and one of four new InfiniTEM plates shown, the L500 plate. The two yellow plates, L500 and L4390 are the proposed drill targets, both plates are deeper, thicker and less conductive than the shallower plates shown in black.

Plate L500 is coincident with a subtle ground magnetic signature, located about 200 m to the east of the main Wabassi magnetic horizon that carries most of the observed Wabassi conductivity. L500 is aligned parallel and coincident with a N-S striking magnetic low to the east of the main Wabassi magnetic horizon. The plate is 31 m thick, is located 283 m below surface, and has a lower conductivity of 27 mS/m. Plate L4390 is located about 250 m to the north of plate L500, in a magnetic break of the main A1-A2 magnetic horizon, just to the north of the main A1 EM and magnetic responses. It has a depth of -227 m, is 41 m thick, and also has a low conductivity of 11 mS/m.

Figure 17 shows the relationship of the two deeper plates with the A1 conductivity and magnetic surfaces. The magnetic break in the blue susceptibility surface, just north of

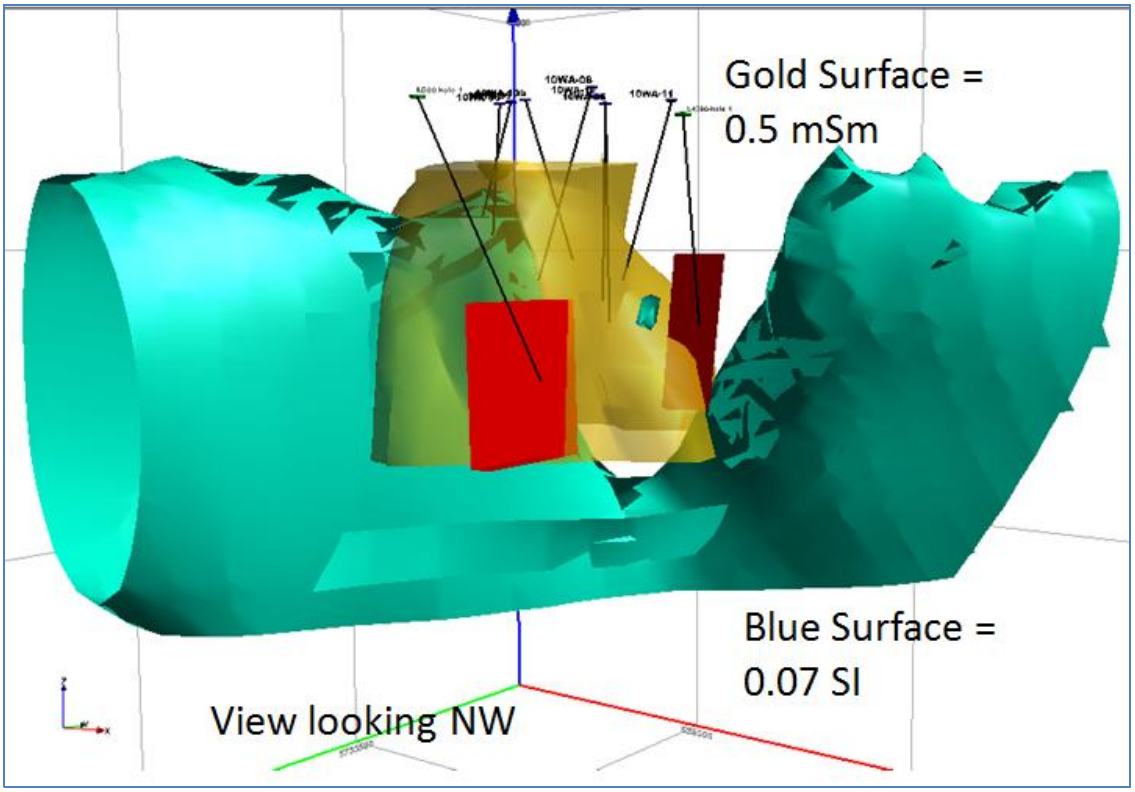

Figure 17: Threshold A1 magnetic signature (blue) shows a magnetic break just north of the A1 conductor. Plate L500 is enclosed by the conductive surface (gold), Plate L4390 is located on the northern edge of the conductive surface.

the main A1 EM response (brown surface), is evident. Though the L500m plate is partially enclosed by the brown conductivity surface, this may be a LEI inversion artifact as the smaller plates nearer surface are much more conductive, being in the thousands to tens of thousands of mS/m; these shallower conductors likely produce the downward projecting EM surface.

Figure 18 provides an alternate view of the deeper plates and conductivity surface. It is possible that these two deeper plate results were not returned in the past due to a masking effect of the shallower, much more conductive plate results nearer surface. Though the two deeper, thicker, undrilled plates are considered to be higher priority as they are repeatable larger plate models, it's advised that the two deeper plate's lower conductivities be considered as to their representing viable geologic targets to chase or not, prior to drilling them.

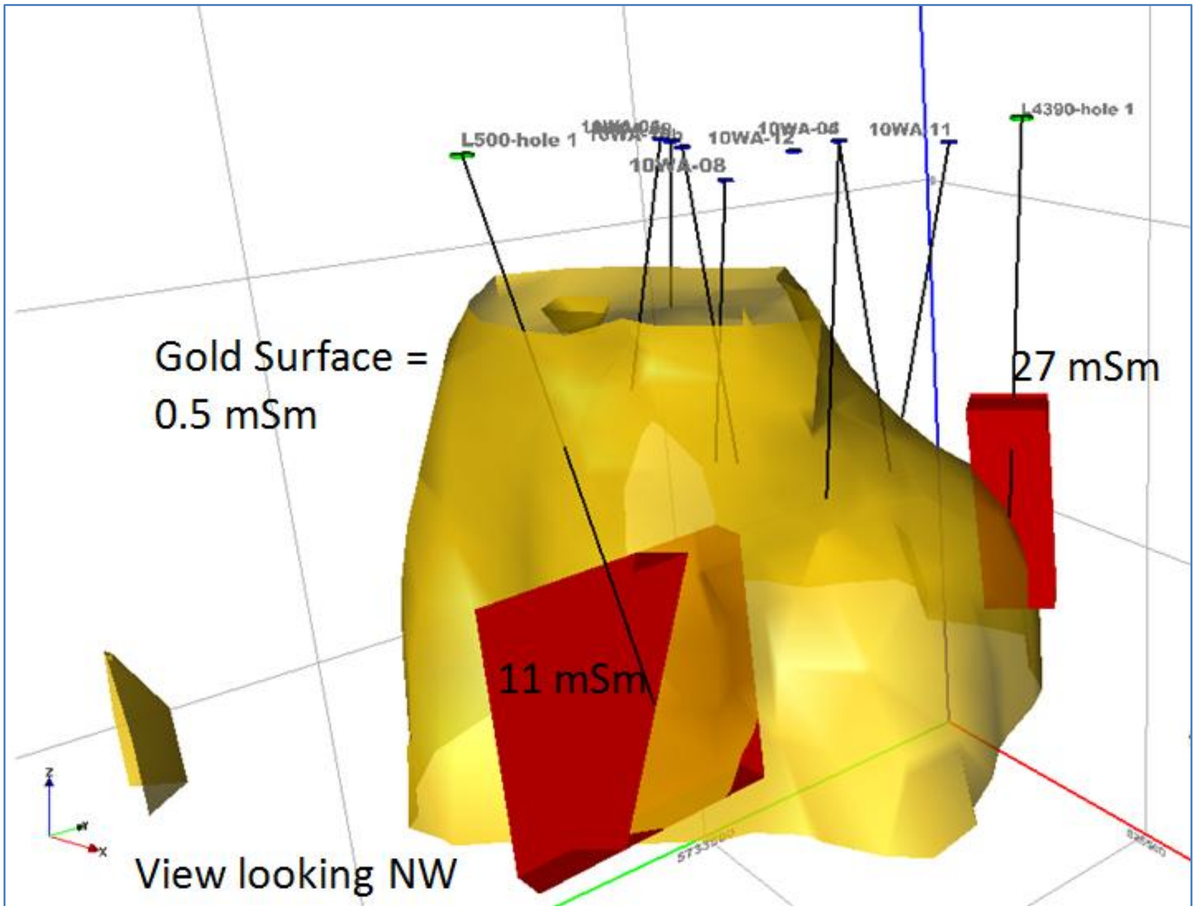

Figure 18: 3D view of the A1 anomaly conductive surface and the two deeper plate models with the historical and proposed drill holes.

TZ 3

Two priority conductors are identified on the Wabassi West grid. The 1 400m long eastern conductor spans 15 flight lines. This eastern conductor breaks up into the two more-conductive subzones 1 and 2 seen in Figure 19. Subzone 3 is located 2 kms to the west of subzone 2.

Subzone 1

Subzone 1 is the easternmost coherent conductive signature. This NS striking conductor is coincident, but sub-perpendicular to a NE-SW striking magnetic horizon on its north. The conductor strikes southward out of the magnetic unit. The plate strikes for the subzone 1 models were kept perpendicular to the flight line directions, though the conductive horizon appears to trace the plate centers as seen in Figure 20. This is better seen in Figure 21, where the green conductive surface is seen striking southward out of the red magnetic surface with the plate centers tracking the conductive surface. Figure 22

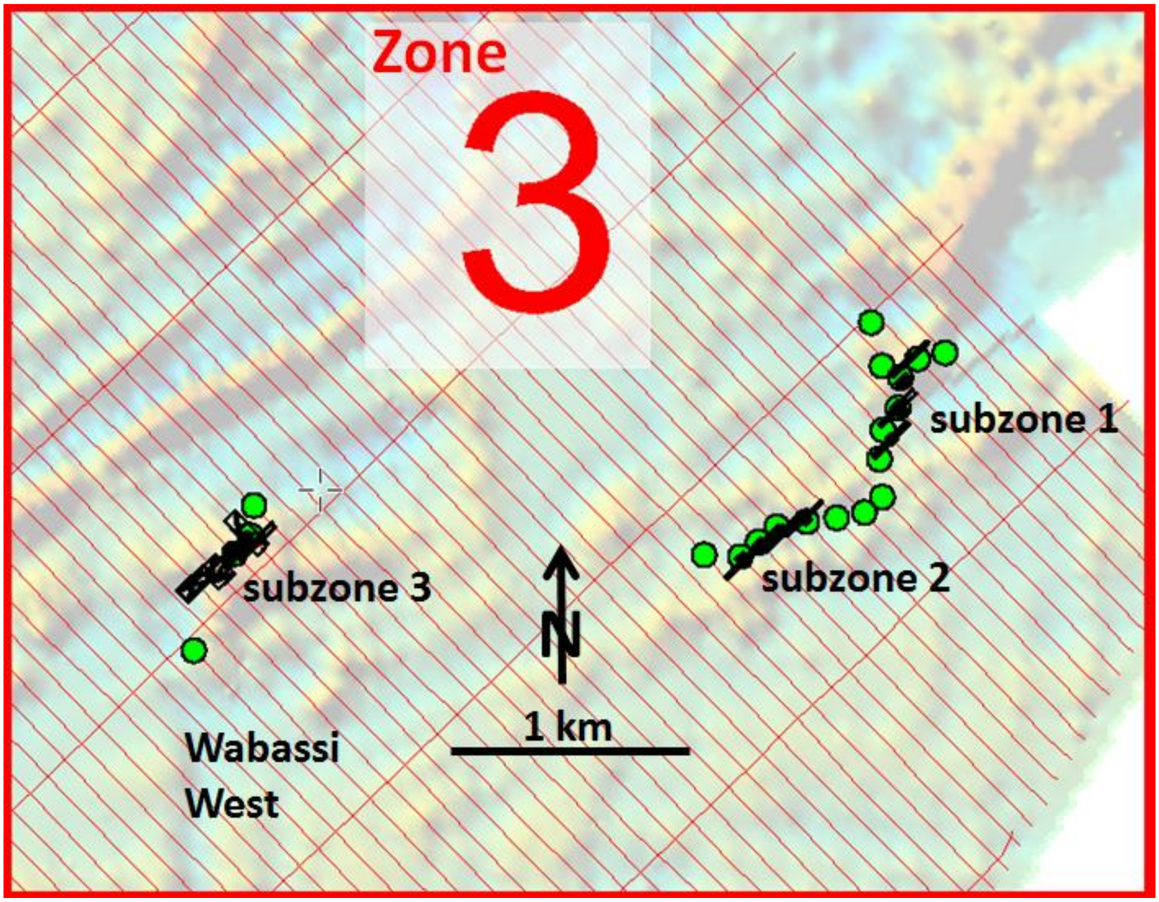

Figure 19: Plan view of the three conductive subzones in Zone 3, on the Wabassi West grid. The background image is the magnetic 1VD.

shows that the 0.014 SI magnetic surfaces (red) fully encloses the two more northern plates, with the third and fourth more southerly plates being located fully outside the magnetic surface. This corroborates the conductor as being a continuous N-S striking body that is sub-perpendicular to the magnetic signature on the north. Existing drill hole 10WA-01 misses the new plates as modeled, but does appear to intersect the larger NS striking conductive subzone 1.

L1060 and L1070 provide two plates that are each intersected by one drill hole. The shallower shorter strike length plates return lower conductivities than the longer deeper plates. The vertical offset between the plates are about 20 m.

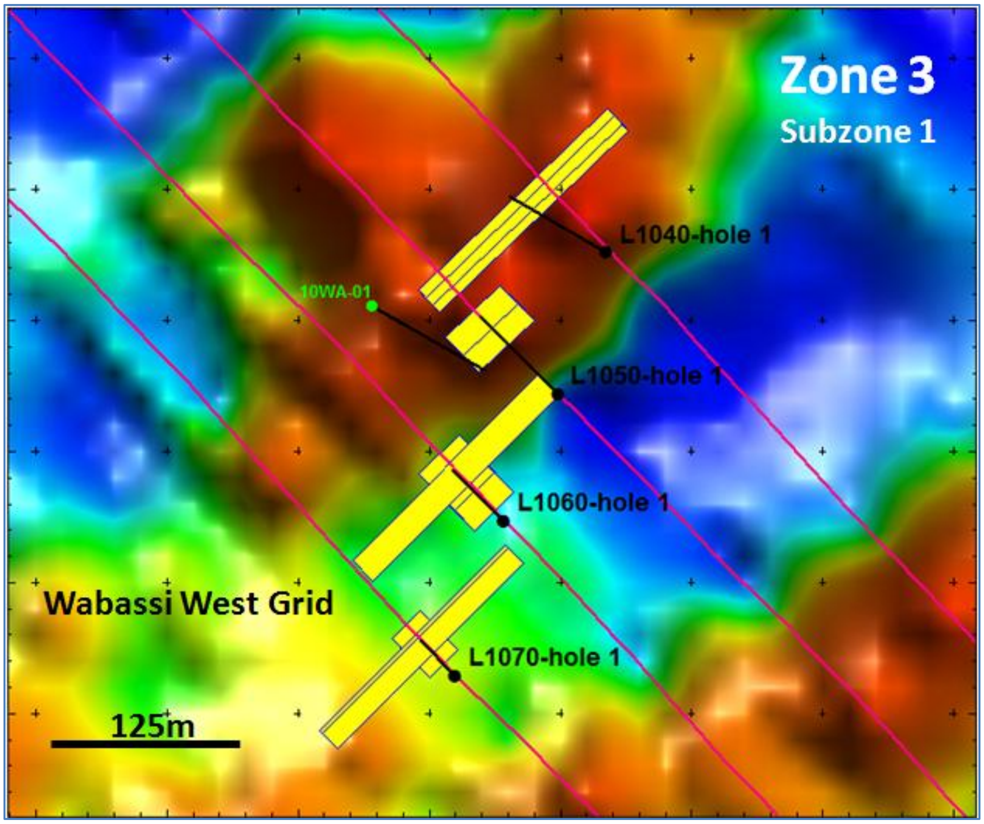

Figure 20: Plan view of the TZ 3 subzone 1 with plate models.
Background image is the magnetic 1VD.

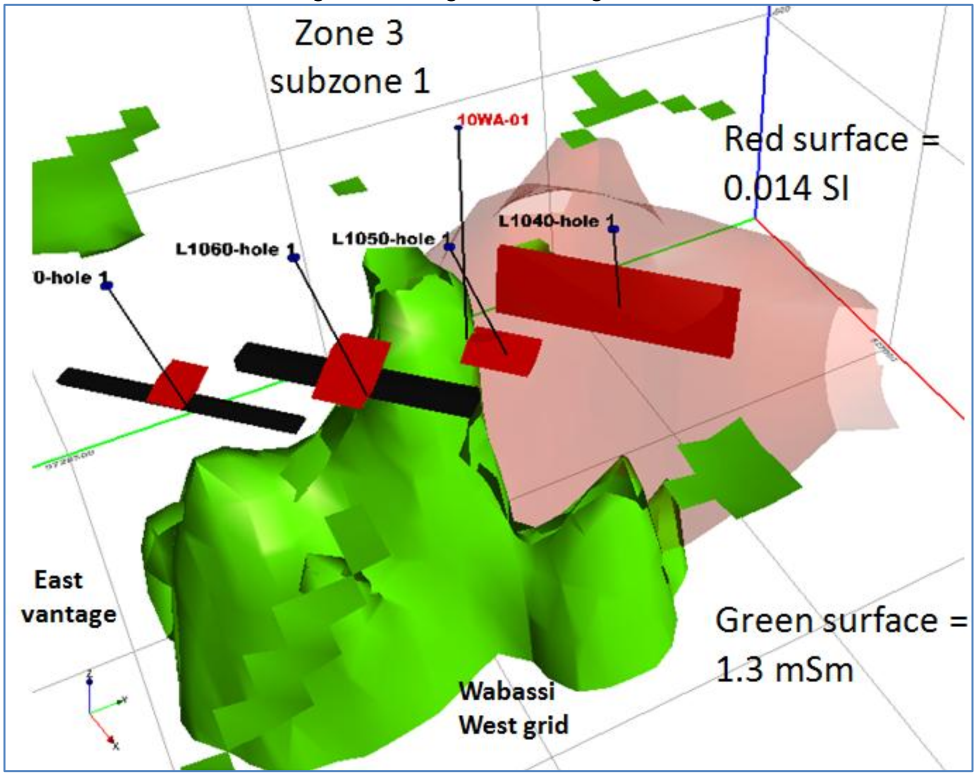

Figure 21: West-looking 3D view of the TZ 3 subzone 1 threshold; conductivity (green) and magnetic (red) surfaces, with plate models.

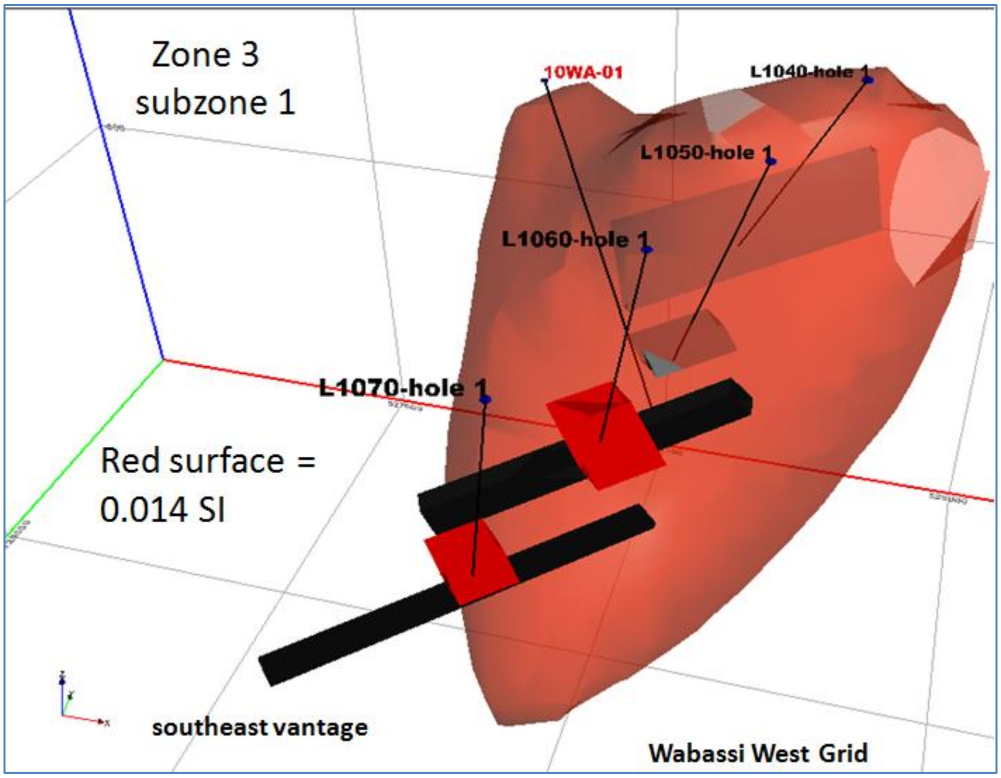

Figure 22: Northwest-looking view of the TZ3 subzone 1 magnetic surface with conductive plate models.

Subzone 2

Wabassi West subzone 2 (Figure 23) is located about 500 m southwest of subzone 1. The strike of the subzone 2 conductor has flattened out from subzone 1, from N-S to a NE-SW strike, perhaps indicating a structural jog between the two. As seen for subzone 1 the conductive strike of the plate models is not fully coincident with a magnetic signature, the subzone 2 conductor appears to be sub-parallel and in-between two adjacent magnetic horizons. This is evident in Figure 24, where the conductive surface (green) is seen sandwiched between two more-magnetic surfaces (blue).

All four plate model sets for subzone 2 are double plate sets, with vertically adjacent shallower and deeper plates. In two cases the vertical plate separations are 20 m, the third is 5 m offset, the fourth is 10 m offset. In all cases the deeper plates are the longer and more conductive plates.

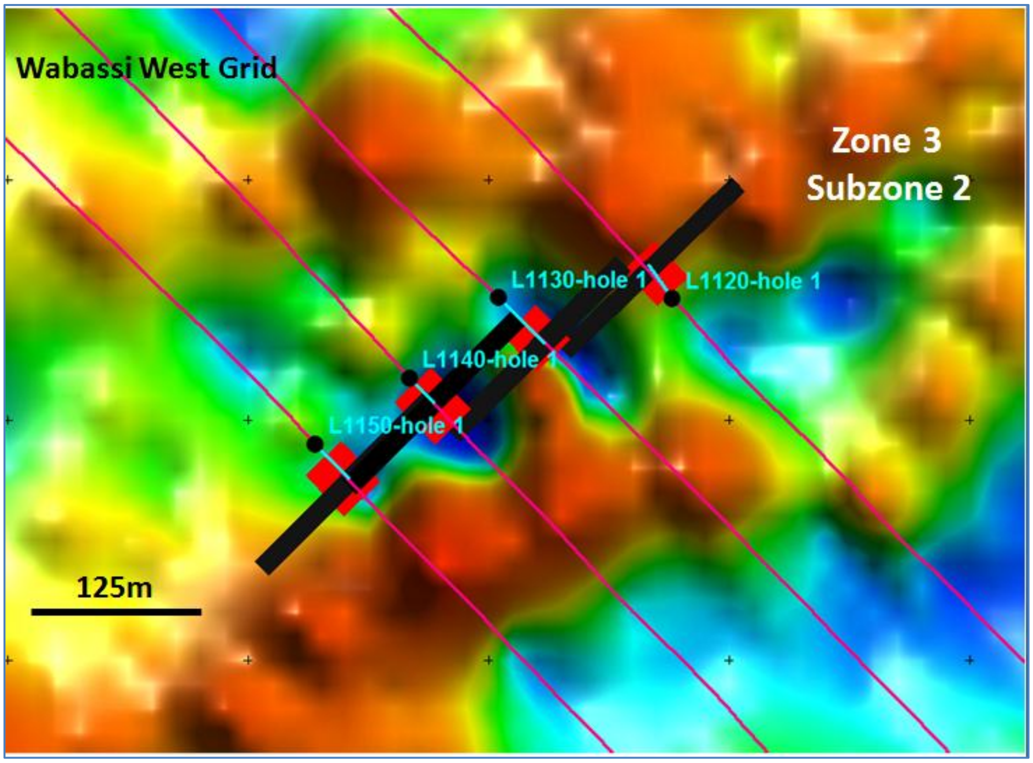

Figure 23: Plan view of TZ 3 subzone 2 with plate models.
Background image is the magnetic 1VD.

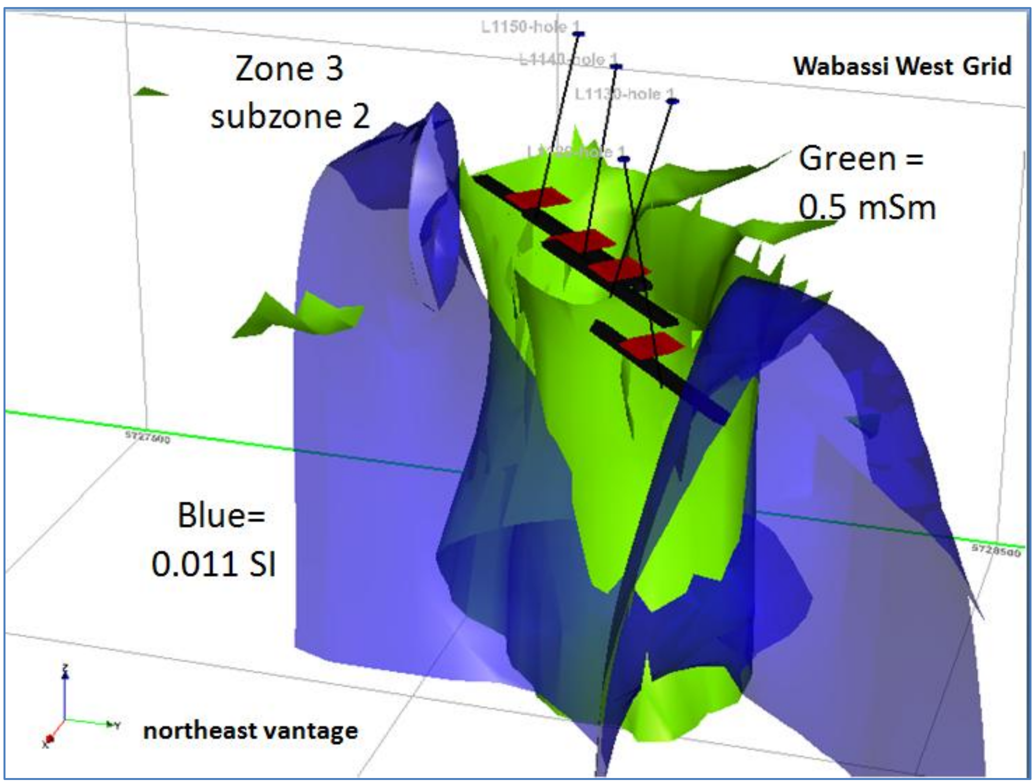

Figure 24: Southwest-looking view of TZ 3 subzone 2 conductivity (green) and magnetic (blue) surfaces and conductive plate models.

Subzone 3

The TZ 3 subzone 3 conductor is the highest amplitude Wabassi West grid EM response and is coincident with a significant higher amplitude magnetic signature, unlike subzones 1 and 2. The subzone 3 conductor appears to bisect the center of two north-verging magnetic horizons (Figure 25).

The subzone 3 conductor, like the prior two Wabassi West subzones, returns a shallow and deeper set of plates with similar calculated fit errors. The plate geometry variability is greater though in subzone 3 than it was in the prior mentioned two subzones. Like the prior two subzones, the TZ 3 plate sets taken together are approximately 300 m long and span four lines (Figure 25). The shallower plates locate above the northwestern top edge of a higher susceptibility (0.024 SI) discrete magnetic surface seen in Figures 26 and 27. The deeper plate set is partially imbedded in the northwestern top of the magnetic surface. The shallower plate set in subzone 3 is comprised of the longer and more conductive plates, whereas the shorter strike length thicker plates are deeper and less conductive. This plate-conductivity structure counters the dual-plate model sets obtained for subzones 1 and 2. Though Wabassi West subzone 3 returns the higher amplitude EM responses, it does not return the highest conductivity Wabassi West modeled mS/m numbers.

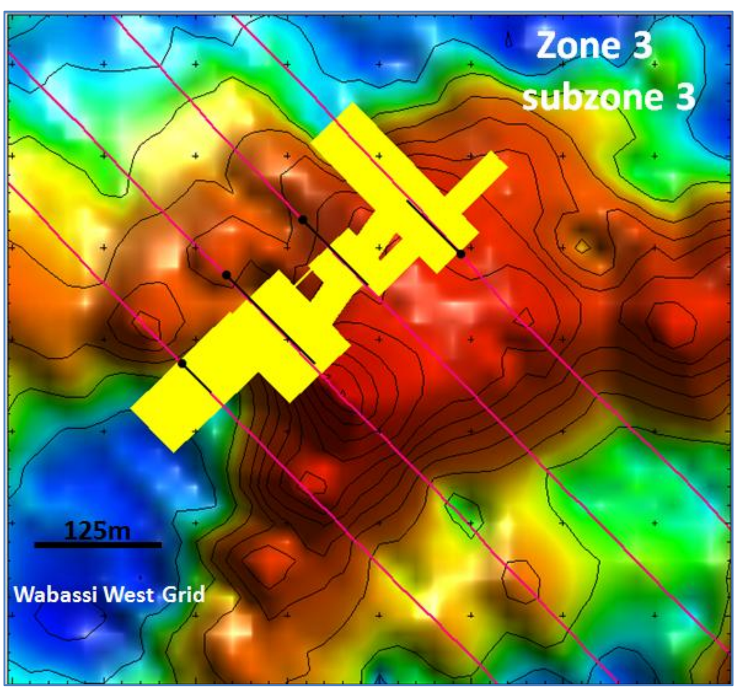

Figure 25: Plan view of the TZ 3 subzone 3 on the Wabassi West grid, with plate models. Background image is the magnetic 1VD.

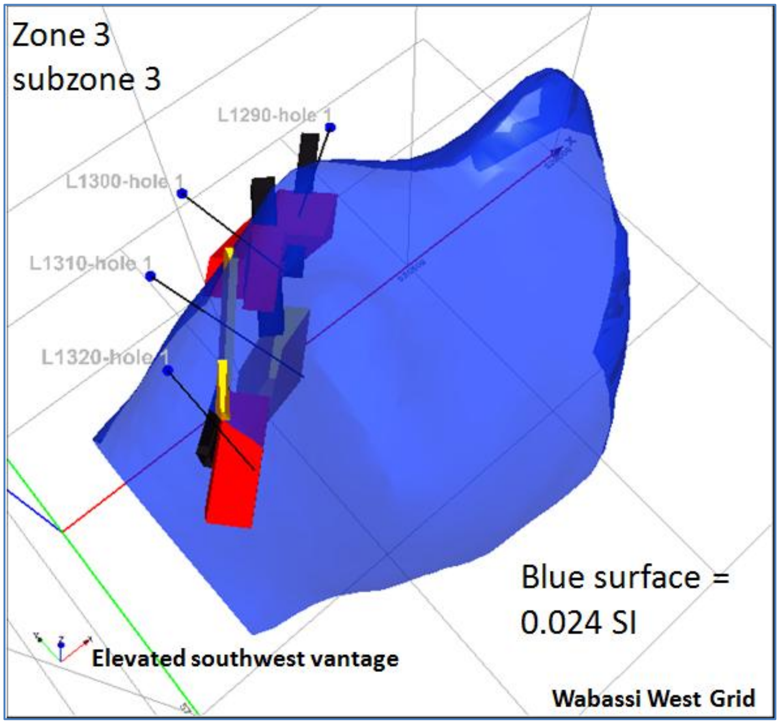

Figure 26: Northeast-looking view of the TZ 3 subzone 3 magnetic surface with Maxwell conductive plate models.

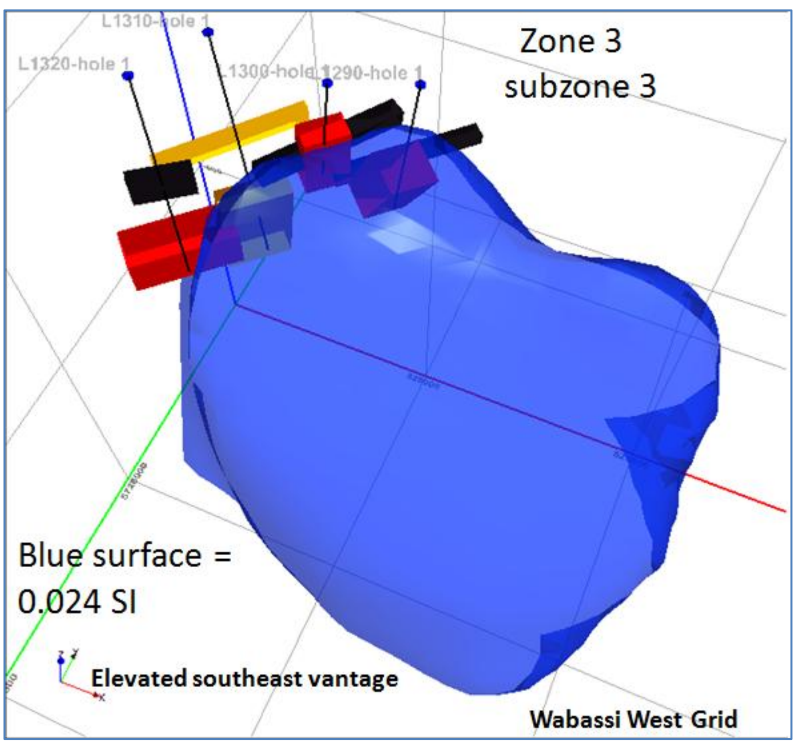

Figure 27: Northwest looking view of the TZ 3 subzone 3 magnetic surface with Maxwell conductive plate models.

TZ 4

On the far south of the Max merged grid, two parallel ENW-WSW striking magnetic signatures parallel a 6 km long prominent conductor. The conductor is coincident with the thinner, more southern magnetic signature and returns a series of DPRs. Plate L4080 models this response (Figures 28 and 29). The detailed EM profile review and picking revealed two less-obvious conductive trends on the south beside the main formational conductor. The first is a trend of SPRs striking more steeply NE-SW that is sub-parallel to the more northern of the two nearby magnetic horizons, and located at L3280-1 (Figures 28 and 29). The 2nd is a trend of SPRs striking NS that is sub-perpendicular to the northern magnetic horizon and located at L3280-2 (Figures 28 and 31).

In Figure 30, it's seen that the shallower thin plate model for L4080 is enclosed within the green magnetic threshold surface that maps a more magnetic and conductive geologic formation. The L4080 plate model is thought to be representative of the 6 km long magnetic horizon of elevated conductivity that contains it. The conductivity in this magnetic horizon appears moderate at 250 mS/m.

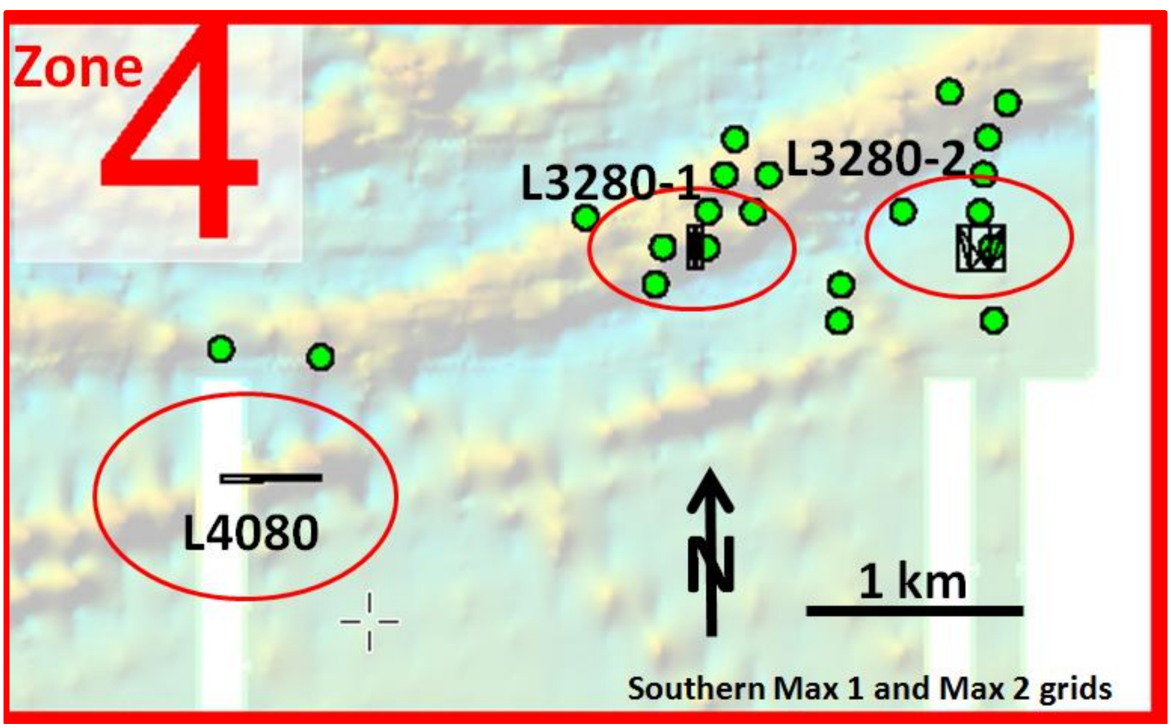

Figure 28: Plan view of TZ 4 on the south of the merged Max 1 and Max 2 grids. The three Maxwell plate models and SPR picks are shown. The SPRs appear to define two NNE-SSW striking deeper more subtle conductors of limited strike length.

Figure 31 is a plan view of the two L3280 plates on the local 1VD magnetic grid. The western plate is located on an ENE-WSW striking magnetic horizon, while the eastern plate appears in a non-magnetic gap between two magnetic horizons. The 3D representation of the two plate models returned from L3280 is seen in Figure 32. These two plates are from one E-W line segment, the western SPR conductor has a strike length of at least 400 m, and could be modeled on at least five lines. The eastern SPR conductor has a strike length of at least 500 m and could be modeled on six lines.

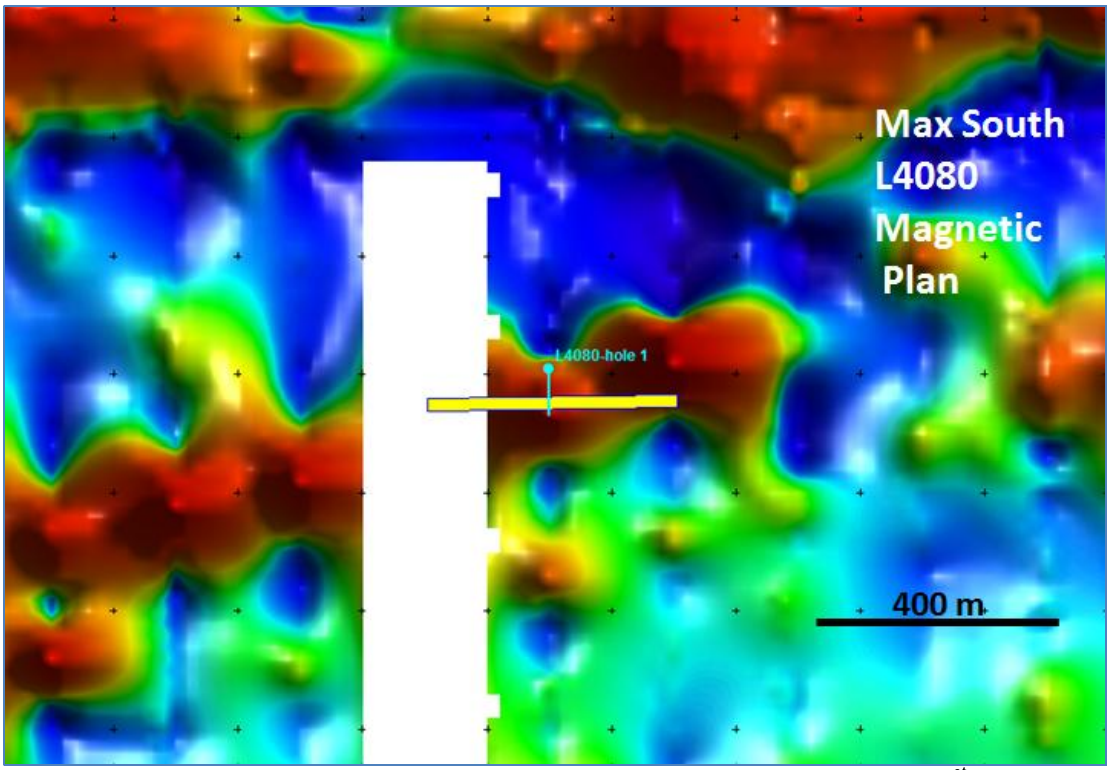

Figure 29: Plan view of the TZ 4 plate L4080, background image is TMI 1st VD.

Figure 32 shows that the two NS striking plates are not tightly, but loosely, enclosed by coincident 1.25 mS/m conductive surfaces. The deeper conductive surface is seen situated between and parallel to the two magnetic horizons that sandwich it. This deeper conductive surface could be a 1D EM voxel gridding artifact beneath the shallower DPR conductor that is coincident with the southern magnetic horizon, if it is not truly representative of a deeper SPR conductivity. As the conductivity surface thresholding does convincingly corroborate the two SPR conductive profile signatures, whereas the Maxwell modeling does resolve the profile signatures, further Maxwell plate modeling of the SPR conductors is recommended if there is interest in them.

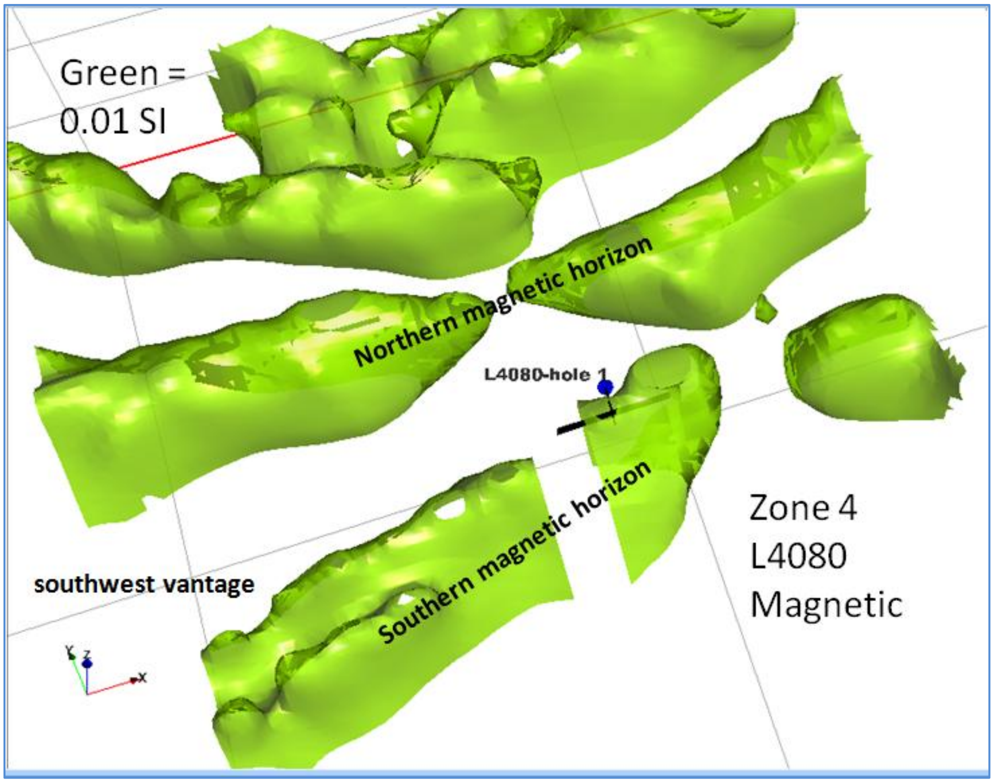

Figure 30: Northeast-looking view of the L4080 Maxwell plate model imbedded in the TZ 4 southern magnetic horizon, surface threshold 0.01 SI.

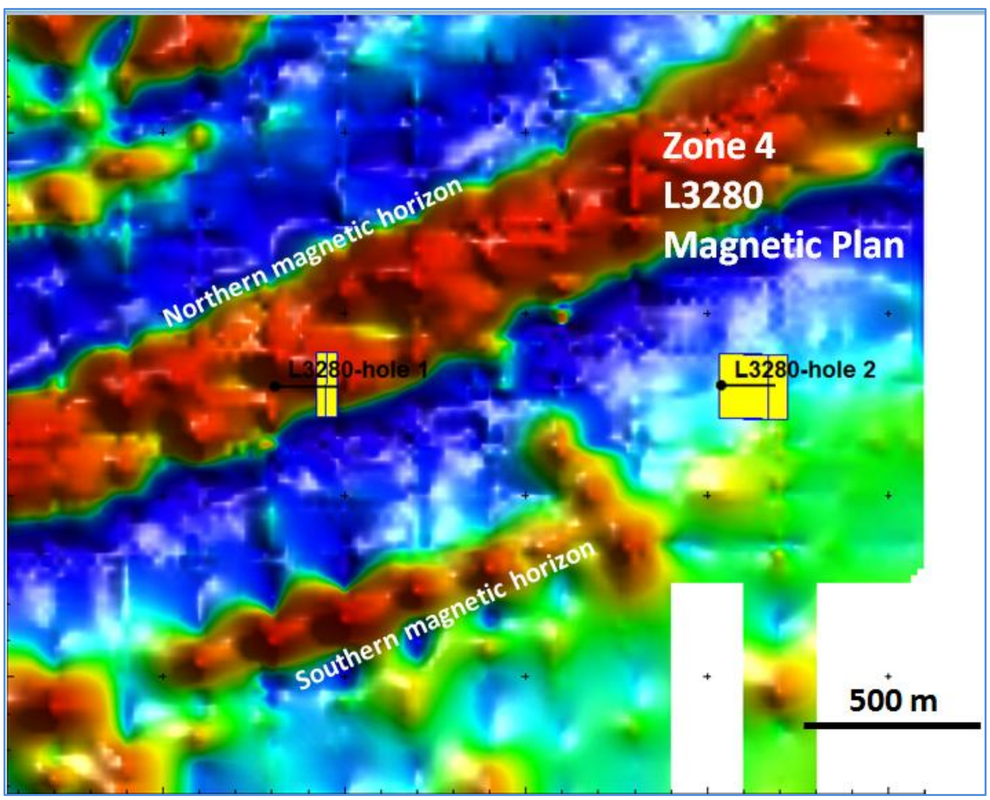

Figure 31: Plan view of the TZ 4 L3280 area Maxwell plates, background image is magnetic 1VD.

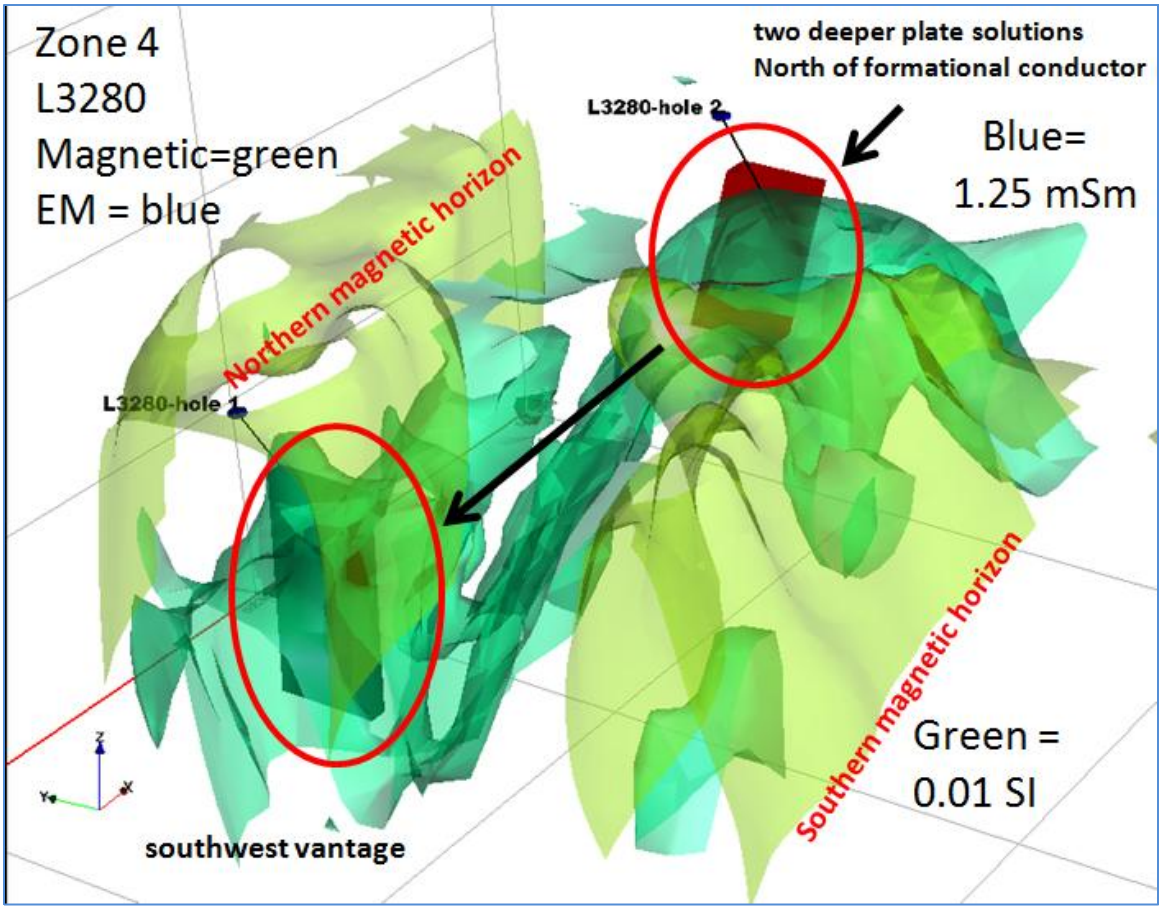

Figure 32: Northeast-looking view of TZ 4 L3280 SPR plate models. The plates are discrete and north of the formational conductor that is coincident at shallower depths with the southern magnetic horizon.

7. Conclusions

The processing and assessment of the merged VTEM EM and magnetic surveys returns the higher priority Target Zones 1-4 comprised of 41 conductive plates targeted by 31 drill holes. There are 10 fewer drill holes than plates, as the TZ 3 modeling was undertaken with two plate geometries, shorter strike-length-limited plates and longer flight line-perpendicular plates. In most cases, the Wabassi West TZ 3 two-plate model sets locate the tandem plates within 20 m of each other vertically, and are intersected by one drill hole. The two prominent TZ 3 conductors are split up into three conductive subzones. The eastern conductor is a 1400 m long continuous NNE-SSW striking band defined by the two more-conductive subzones 1 and 2 that are separated by 500 m. The more western subzone 3 conductor, located 2 km to the west of subzone 2, returns the highest amplitude TZ 3 VTEM response. The subzone 3 conductor is also coincident with a significant magnetic signature of higher amplitude and susceptibility.

New plate models were generated in TZs 1 and 2 in undrilled sites in the Max peridotite and Wabassi A1-A2 areas. Two plates are in the main Max peridotite body. The satellite conductor, the third Max peridotite plate, is well-identified by the AdTau plan response. It also returns a larger plate model that is enclosed by a threshold conductivity surface of similar mS/m amplitude. Twelve new plate models are proposed for TZ 2, at undrilled sites in the Wabassi A1-A2 anomalies. Ten of the plates are small and higher conductivity, with modeled conductivity values often in the thousands and in two cases tens of thousands of mS/m. These plates have limited spatial extent and would be easy to miss with a drill hole if the drill site topography differs by more than a few meters from the VTEM or InfiniTEM derived DEM elevations.

Differential GPS surveying of drill hole sites is recommended for smaller or thinner plates as the subsequent elevations could be used to adjust the drill hole trajectories prior to drilling. The two new L500 and L4390 A1 anomaly plate models are thicker, of lower conductivity, and deeper than the average Wabassi plate model. These two plates appear to be coincident with more-subtle magnetic signatures and not with the formational magnetic signature that contains most of the A1-A2 conductive response. Their novelty, i.e. their depth, size, lower conductivity, and thickness increases their priority to high in this report, though an argument could be made that they are not characteristic of the typical A1-A2 conductor, and therefore makes them higher risk.

Three target plates are provided for TZ 4. The most obvious conductor identified is a 6 km long ENE-WSW striking DPR conductive horizon coincident with the southernmost prominent ENE-WSW striking magnetic horizon. Though plate L4080 is thought to model a formational conductor, it's born in mind that mineralized layered mafic systems can be formational in character. To the NNE, two more subtle and deeper conductors were identified from the profile responses and mapped as 500 m long and 600 m long SPR strings. Both SPR strings are readily Maxwell modeled, and the two L3280 plates provided fit the two separate SPR responses on one of the lines traversed by both SPR strings. Up to 10 more Maxwell plates could be fit to the two SPR strings. More Maxwell modeling is recommended if there is interest in these SPR responses. The preliminary indications are that the two SPR conductors plunge to the NNE.

Respectfully submitted,

Ken Witherly
Condor Consulting, Inc.

Ed Cunion
Consultant

October 25, 2010

8. References

Acorn, W., Legault, J., Venter, N., Smith, G., 2010, Report on a Helicopter-borne Versatile Time Domain Electromagnetic (VTEM) Geophysical Survey, Wabassi West, High Bank Camp, Ontario; for Northern Shield Resources Inc. by Geotech Ltd., Project 10047, June 2010.

Au, K., Fiset, N and Legault, J. 2009, Report on a Helicopter-borne Versatile Time Domain Electromagnetic (VTEM) Geophysical Survey, Hale Lake Property and Wabassi Property, Ogoki Post Area, Ontario; report for Northern Shield Resources Inc. by Geotech Ltd., Project 8012 January 2009.

Cunion, E. and Witherly, K. 2010, Wabassi TEM Review; for Northern Shield Resources Inc. report by Condor Consulting, Inc. July 19, 2010.

Ellis, R.G., 1998, Inversion of airborne electromagnetic data: Exploration Geophysics, 29, 121-127.

Li, Y., and Oldenburg, D. W. 1996, 3-D inversion of magnetic data: Geophysics, 61, no.2, 394-408.

Prikhodko, A., 2008, Report on a Versatile Time Domain Electromagnetic Survey (VTEM), Thunder Bay Mining Division Project, Northern Ontario, Canada for East-West Resources; by Geotech Ltd., Project 8027 May 2008.

Shi, Z., and Butt, G. 2004, New enhancement filters for geological mapping Preview, 111, 87-88

9. Appendixes

Appendix A-List of Picked EM Anomalies

Pick_ID	Line	grid	X	Y	SF	BF	Ad-Tau_B	TMI	pick-type	rank	
Maxspr1	L3310	Max	519910	5717851	0.000601	0.00074	2.6164	58210	spr	2	in southern mafic complex but small 3D response, perhaps noise
Maxspr2	L3300	Max	522045	5717998	0.006434	0.035453	4.5185	57987	spr	2	shallower Maxwell plate (-83m) fit
Maxspr3	L3300	Max	522682	5718002	0.003049	0.014158	4.4206	57961	spr	2	deeper Maxwell Plate fit (-163m)
Maxspr4	L3300	Max	517385	5717997	0.000379	-0.0015	2.0033	58140	spr	2	deep Maxwell plate fit (-298m)
Maxspr5	L3290	Max	521288	5718151	0.000275	0.000717	2.1426	58166	spr	1	deep Maxwell plate fit -352m
Maxspr6	L3290	Max	522053	5718147	0.001299	0.007176	4.9512	58008	spr	1	deeper Maxwell plate fit -220m
Maxspr7	L3280	Max	522674	5718302	0.004289	0.026311	5.0088	57931	spr	1	deeper Maxwell plate fit -174 meters
Maxspr8	L3280	Max	521499	5718300	0.000133	-0.00103	1.0283	58327	spr	1	deeper Maxwell plate fit -192 meters
Maxspr9	L3280	Max	521319	5718303	0.000086	-0.00089	1.3411	58307	spr	2	more subtle EM response, difficult to model
Maxspr10	L3270	Max	522625	5718447	0.001441	0.007272	4.4800	57941	spr	1	prominent broad response Maxwell plate -198
Maxspr11	L3270	Max	521691	5718450	-0.000051	-0.00163	1.0658	58309	spr	1	prominent broad response Maxwell plate -207
Maxspr12	L3270	Max	521505	5718450	0.000314	0.000557	1.0464	58288	spr	3	smaller sub-response to adjacent larger response
Maxspr13	L3270	Max	522307	5718450	0.000172	0.00136	2.2943	57980	spr	3	smaller to adjacent larger response
Maxspr14	L3260	Max	522639	5718603	0.000474	0.000644	2.0607	57997	spr	1	deeper Maxwell plate at -206m
Maxspr15	L3260	Max	521754	5718600	0.000263	0.000586	0.8871	58370	spr	1	deeper Maxwell plate at -215m
Maxspr16	L3250	Max	522659	5718754	0.000067	-0.00058	1.1393	58153	spr	1	deeper Maxwell plate at -217m
Maxspr17	L3240	Max	522738	5718896	0.000586	-7.1E-05	0.2583	58285	spr	2	more subtle response, difficult to Maxwell model
Maxspr18	L3160	Max	519824	5720099	0.000433	0.002002	0.1650	58272	spr	3	in southern Max grid mafic complex but lesser 3D voxel response
Maxspr19	L3090	Max	518130	5721151	0.00041	0.001225	0.2254	57988	spr	3	in southern Max grid mafic complex but lesser 3D voxel response
Maxspr20	L3100	Max	519430	5720998	0.000772	0.002296	0.2169	58331	spr	3	in southern Max grid mafic complex but lesser 3D voxel response
Maxspr21	L3080	Max	518108	5721301	0.000083	-0.00057	0.3424	58015	spr	3	in southern Max grid mafic complex but lesser 3D voxel response
Maxspr22	L3080	Max	519214	5721301	-0.000011	0.002004	0.0066	58774	spr	3	in southern Max grid mafic complex but lesser 3D voxel response
Maxspr23	L3080	Max	518979	5721304	0.000394	0.000762	0.1242	58753	spr	3	in southern Max grid mafic complex but lesser 3D voxel response
Maxspr24	L3080	Max	522864	5721298	-0.000151	-0.0006	0.3356	57927	spr	3	in southern Max grid mafic complex but lesser 3D voxel response
Maxspr25	L3070	Max	519187	5721451	0.000091	0.000411	0.9817	58542	spr	3	in southern Max grid mafic complex but lesser 3D voxel response
Maxspr26	L3070	Max	518251	5721453	0.000098	0.002727	1.0417	58038	spr	3	in southern Max grid mafic complex but lesser 3D voxel response

Maxspr27	L3060	Max	518223	5721599	0.000011	0.000364	1.4577	58101	spr	3	in southern Max grid mafic complex but lesser 3D voxel response
Maxspr28	L3060	Max	519210	5721603	0.000472	0.001135	0.0597	58396	spr	3	in southern Max grid mafic complex but lesser 3D voxel response
Maxspr29	L3060	Max	518223	5721599	0.000011	0.000364	1.4577	58101	spr	3	in southern Max grid mafic complex but lesser 3D voxel response
Maxspr30	L3040	Max	517902	5721902	0.001182	-0.00261	0.0000	58104	spr	3	in southern Max grid mafic complex but lesser 3D voxel response
Maxspr31	L3040	Max	521806	5721902	0.000113	0.006533	0.0000	58034	spr	3	in southern Max grid mafic complex but lesser 3D voxel response
Maxspr32	L3020	Max	522794	5722207	0.000556	0.008396	0.4420	57922	spr	3	in southern Max grid mafic complex but lesser 3D voxel response
Maxspr33	L3020	Max	520590	5722201	0.000506	0.004481	0.0000	58027	spr	3	in southern Max grid mafic complex but lesser 3D voxel response
Maxspr34	L3020	Max	520009	5722202	-0.000158	0.002578	0.0000	57861	spr	3	in southern Max grid mafic complex but lesser 3D voxel response
Maxspr35	L3020	Max	519622	5722203	0.001759	0.002943	0.1317	58006	spr	3	in southern Max grid mafic complex but lesser 3D voxel response
Maxspr36	L3020	Max	518969	5722207	0.000396	0.000726	0.0222	58164	spr	3	in southern Max grid mafic complex but lesser 3D voxel response
Maxspr37	L3020	Max	517349	5722206	0.000268	-0.00101	0.5917	58112	spr	3	in southern Max grid mafic complex but lesser 3D voxel response
Maxspr38	L3010	Max	517376	5722350	0.000234	-0.0057	0.0132	58069	spr	3	in southern Max grid mafic complex but lesser 3D voxel response
Maxspr39	L3000	Max	522267	5722500	0.000747	0.012671	0.0000	57965	spr	3	in southern Max grid mafic complex but lesser 3D voxel response
Maxspr40	L3000	Max	517320	5722499	0.000929	0.002574	0.5152	58058	spr	3	in southern Max grid mafic complex but lesser 3D voxel response
Maxspr41	L2990	Max	517074	5722654	-0.002363	-0.00208	0.0067	58163	spr	3	in southern Max grid mafic complex but lesser 3D voxel response
Maxspr42	L2990	Max	520060	5722651	-0.002023	0.06348	0.0000	57945	spr	3	in southern Max grid mafic complex but lesser 3D voxel response
Maxspr43	L2990	Max	522181	5722650	0.000286	0.002323	0.0000	57960	spr	3	in southern Max grid mafic complex but lesser 3D voxel response
Maxspr44	L2980	Max	519967	5722798	-0.000135	0.000391	0.0000	57954	spr	3	in southern Max grid mafic complex but lesser 3D voxel response
Maxspr45	L2930	Max	518565	5723551	0.000065	0.006367	0.0000	58141	spr	3	isolated small EM response
Maxspr46	L2930	Max	517440	5723553	0.000954	0.002102	0.0000	57997	spr	3	isolated small EM response
Maxspr47	L2790	Max	518015	5725647	0.000376	-0.00079	0.1102	58227	spr	3	isolated small EM response
Maxspr48	L2700	Max	518073	5727004	0.000093	0.003323	0.0471	58263	spr	3	isolated small EM response
Maxspr49	L2690	Max	515629	5727151	-0.001385	0.009744	0.0151	57912	spr	3	isolated small EM response
Maxspr50	L2680	Max	517650	5727302	0.000187	0.008907	2.4362	58130	spr	3	small cluster of lesser EM responses
Maxspr51	L2680	Max	517944	5727299	0.000343	0.003425	0.0028	58160	spr	3	small cluster of lesser EM responses
Maxspr52	L2670	Max	517567	5727449	0.000061	0.000439	0.0000	58096	spr	3	small cluster of lesser EM responses
Maxspr53	L2590	Max	517535	5728650	0.000269	0.002741	0.8569	58067	spr	3	isolated small EM response

Maxspr54	L25 20	Max	516 601	5729 701	- 0.000 708	0.005 02	0.000 0	580 00	spr	3	isolated small EM response
Maxspr55	L25 00	Max	515 187	5729 998	- 0.000 345	0.006 307	0.000 0	580 67	spr	3	isolated small EM response
Maxspr56	L25 00	Max	520 900	5729 999	- 0.000 364	0.004 15	0.000 0	580 75	spr	3	isolated small EM response
Maxspr57	L24 50	Max	518 079	5730 751	- 0.000 09	0.004 383	0.000 0	581 79	spr	3	isolated small EM response
Maxspr58	L24 30	Max	518 689	5731 050	0.000 123	0.004 254	0.000 0	580 86	spr	3	isolated small EM response
Maxspr59	L24 10	Max	518 442	5731 349	0.000 171	0.003 149	0.000 0	581 73	spr	3	isolated small EM response
Maxspr60	L23 70	Max	522 217	5731 948	0.000 267	0.002 568	0.000 0	579 47	spr	3	isolated small EM response
Maxspr61	L23 10	Max	515 668	5732 848	0.000 518	0.003 724	0.006 9	580 18	spr	3	isolated small EM response
Maxspr62	L23 10	Max	517 737	5732 849	0.000 06	0.004 126	0.000 0	596 97	spr	1	Possible IP drop-out effect over a 3000 nT magmetic signature
Maxspr63	L23 10	Max	519 163	5732 849	0.000 557	0.003 2	0.000 0	580 31	spr	1	Max southern satellite conductor
Maxspr64	L23 00	Max	519 061	5732 997	0.000 548	0.001 537	1.141 5	580 52	spr	1	Max southern satellite conductor
Maxspr65	L22 90	Max	519 052	5733 147	0.000 09	0.000 205	0.607 8	580 64	spr	1	Max southern satellite conductor
Maxspr66	L22 90	Max	522 630	5733 148	0.000 195	0.012 118	0.313 8	580 46	spr	3	isolated small EM response
Maxspr67	L22 80	Max	519 004	5733 300	0.000 262	- 0.001 12	0.824 4	580 70	spr	1	Max southern satellite conductor
Maxspr68	L22 70	Max	518 976	5733 448	0.000 178	- 0.000 17	0.000 0	580 52	spr	1	Max southern satellite conductor
Maxspr69	L22 70	Max	517 239	5733 451	0.000 062	0.003 786	0.025 0	578 95	spr	3	smaller EM response west of Max peridotite
Maxspr70	L22 60	Max	518 150	5733 602	0.000 419	- 0.000 32	0.153 1	598 04	spr	2	undrilled stronger broad EM response in center of Max peridotite, a drilled horizon though
Maxspr71	L22 50	Max	518 170	5733 746	0.000 059	0.001 135	0.507 7	599 68	spr	2	undrilled stronger broad EM response in center of Max peridotite, a drilled horizon though
Maxspr72	L22 70	Max	519 760	5733 452	0.000 364	0.002 128	0.000 0	579 69	spr	3	isolated small EM response east of Max peridotite
Maxspr73	L22 50	Max	520 475	5733 747	0.000 23	0.004 452	0.000 0	579 76	spr	3	isolated small EM response east of Max peridotite
Maxspr74	L22 50	Max	517 785	5733 749	0.000 402	0.002 658	0.079 8	580 99	spr	2	subtle conductive shoulder on western edge of larger Max peridotite main signature, Maxwell model?
Maxspr75	L22 40	Max	517 954	5733 902	- 0.000 141	0.001 369	1.585 1	592 39	spr	2	subtle conductive shoulder on western edge of larger Max peridotite main signature, Maxwell model?
Maxspr76	L22 40	Max	518 229	5733 901	0	0.001 606	1.381 8	597 70	spr	2	undrilled stronger broad EM response in center of Max peridotite, a drilled horizon though
Maxspr77	L22 40	Max	518 543	5733 900	0.000 305	0.001 824	1.500 6	584 37	spr	2	undrilled stronger broad EM response in center of Max peridotite, a drilled horizon though
Maxspr78	L22 40	Max	518 818	5733 907	0.000 437	0.002 071	0.436 2	580 44	spr	3	lesser EM response to east of main Max peridotite
Maxspr79	L22 30	Max	517 994	5734 052	0.000 679	0.004 209	1.429 7	593 59	spr	2	subtle conductive shoulder on western edge of larger Max peridotite main signature, Maxwell model?
Maxspr80	L22 30	Max	518 423	5734 049	0.001 334	0.003 046	2.132 6	592 38	spr	2	Main Max Peridotite stronger broad EM response

Maxspr81	L22 30	Max	518 848	5734 047	0.000 091	0.003 03	0.463 0	579 88	spr	3	lesser EM response to east of main Max peridotite
Maxspr82	L22 30	Max	519 070	5734 046	0.000 127	0.003 686	0.147 4	579 21	spr	3	lesser EM response to east of main Max peridotite
Maxspr83	L22 30	Max	519 851	5734 052	0.000 797	0.001 992	0.020 4	579 38	spr	3	lesser EM response to east of main Max peridotite
Maxspr84	L22 20	Max	518 441	5734 198	0.002 555	0.008 482	2.440 6	592 71	spr	3	drilled main Max Peridotite stronger broad EM response
Maxspr85	L22 20	Max	518 002	5734 200	0.000 98	0.000 955	1.856 7	590 58	spr	2	subtle conductive shoulder on western edge of larger Max peridotite main signature, Maxwell model?
Maxspr86	L22 10	Max	518 445	5734 348	0.002 195	0.004 172	1.679 9	595 02	spr	3	drilled main Max Peridotite stronger broad EM response
Maxspr87	L22 10	Max	517 324	5734 347	0.000 367	0.004 225	0.362 3	584 63	spr	2	more subtle EM response on northern Max peridotote "magnet-ic hook"
Maxspr88	L22 00	Max	518 449	5734 497	0.002 599	0.003 999	1.296 0	594 18	spr	3	drilled main Max Peridotite stronger broad EM response
Maxspr89	L21 90	Max	518 331	5734 650	0.000 384	- 0.000 95	0.862 4	600 96	spr	1	new proposed Maxwell plate main Max conductor
Maxspr90	L21 90	Max	517 558	5734 650	- 0.000 091	0.002 484	0.000 0	587 17	spr	2	more subtle EM response on northern Max peridotote "magnet-ic hook"
Maxspr91	L21 90	Max	518 331	5734 650	0.000 384	- 0.000 95	0.862 4	600 96	spr	1	new proposed Maxwell plate main Max conductor
Maxspr92	L21 80	Max	518 289	5734 802	- 0.000 548	0.000 019	0.542 0	601 28	spr	1	new proposed Maxwell plate main Max conductor
Maxspr93	L21 70	Max	518 148	5734 947	- 0.000 615	- 0.002 02	0.452 8	594 54	spr	2	Main Max Peridotite stronger broad EM response at north of signature
Maxspr94	L21 60	Max	518 104	5735 099	- 0.000 468	0.002 225	0.486 0	595 98	spr	2	Main Max Peridotite stronger broad EM response at north of signature
Maxspr95	L21 50	Max	518 225	5735 247	0.000 002	0.001 96	0.281 9	589 01	spr	2	Main Max Peridotite stronger broad EM response at north of signature
Maxspr96	L21 50	Max	521 008	5735 250	0.000 11	0.002 763	0.000 0	581 16	spr	3	standalone smaller EM response east of max peridotite
Maxspr97	L21 50	Max	522 266	5735 251	- 0.000 255	0.003 385	0.072 7	578 75	spr	3	small EM response
Maxspr98	L21 50	Max	517 653	5735 249	- 0.000 25	0.002 354	0.000 0	585 33	spr	3	smaller EM response
Maxspr99	L21 40	Max	522 376	5735 400	0.000 12	0.000 202	0.491 3	579 23	spr	3	smaller EM response
Maxspr10 0	L21 60	Max	515 482	5735 098	- 0.000 285	0.002 589	0.000 0	580 29	spr	3	smaller EM response
Maxspr10 1	L21 20	Max	521 562	5735 700	0.000 313	0.001 262	0.456 6	580 13	spr	3	small group of EM responses drilled by hole 08MX-04
Maxspr10 2	L21 10	Max	521 519	5735 849	- 0.000 192	0.001 971	1.705 8	581 20	spr	3	small group of EM responses drilled by hole 08MX-04
Maxspr10 3	L21 10	Max	521 247	5735 849	- 0.000 428	0.002 271	0.048 1	582 24	spr	3	small group of EM responses drilled by hole 08MX-04
Maxspr10 4	L21 00	Max	521 588	5735 995	- 0.000 345	- 0.002 44	0.138 1	580 02	spr	3	small group of EM responses drilled by hole 08MX-04
Maxspr10 5	L21 00	Max	521 824	5735 994	0.000 431	- 0.000 45	0.000 0	579 61	spr	3	small group of EM responses drilled by hole 08MX-04
Maxspr10 6	L21 00	Max	521 295	5735 997	0.000 212	- 0.002 11	0.000 0	582 03	spr	3	small group of EM responses drilled by hole 08MX-04
Maxspr10 7	L20 90	Max	521 316	5736 151	0.000 15	0.002 111	0.000 0	582 08	spr	3	small group of EM responses drilled by hole 08MX-04

Maxspr108	L2070	Max	522237	5736450	0.000237	0.000614	0.4694	57966	spr	2	small group of EM responses NE of 08MX-04
Maxspr109	L2060	Max	522046	5736601	-0.0001	-0.00074	0.4061	58024	spr	3	small group of EM responses NE of 08MX-04
Maxspr110	L2050	Max	522124	5736751	-0.000099	0.001991	0.0000	58003	spr	3	small group of EM responses NE of 08MX-04
Maxspr111	L2030	Max	517127	5737048	0.00031	0.004153	0.3428	57938	spr	3	small isolated EM response
Wabassispr112	L4020	Wabassi	532193	5734193	-0.000282	-0.0013	0.0444	58387	spr	3	moderate EM response near hole 10WA-05
Wabassispr113	L4020	Wabassi	531985	5734488	-0.00024	0.000323	0.4451	58262	spr	3	moderate EM response near hole 10WA-05
Wabassispr114	L4030	Wabassi	531964	5734262	-0.000026	0.000893	0.0000	58206	spr	2	moderate EM response near hole 10WA-05
Wabassispr115	L4130	Wabassi	528398	5736638	-0.000049	-0.00123	0.0000	59441	spr	3	subtle EM response on prominent magnetic horizon
Wabassispr116	L4140	Wabassi	528114	5736781	-0.000011	-0.00055	0.0157	58784	spr	3	subtle EM response on prominent magnetic horizon
Wabassispr117	L4150	Wabassi	528012	5736659	-0.000204	0.000701	0.2787	59006	spr	3	subtle EM response on prominent magnetic horizon
Wabassispr118	L4160	Wabassi	527907	5736552	-0.00016	0.001877	0.0000	59500	spr	3	subtle EM response on prominent magnetic horizon
Wabassispr119	L4170	Wabassi	527744	5736517	0.000068	0.002438	0.0299	59302	spr	3	subtle EM response on prominent magnetic horizon
Wabassispr120	L4180	Wabassi	527623	5736439	0.00026	0.000196	0.0000	59308	spr	3	subtle EM response on prominent magnetic horizon
Wabassispr121	L4190	Wabassi	527444	5736421	0.000091	0.001037	2.3692	59284	spr	2	subtle EM response on prominent magnetic horizon
Wabassispr122	L4260	Wabassi	527500	5734549	0.000168	-0.00058	0.2096	58068	spr	3	subtle EM response on prominent magnetic horizon
Wabassispr123	L4270	Wabassi	527434	5734387	-0.000153	0.001886	0.0000	59308	spr	3	subtle EM response on prominent magnetic horizon
Wabassispr124	L4280	Wabassi	527342	5734267	0.000031	0.001599	0.0279	59670	spr	3	subtle EM response on prominent magnetic horizon
Wabassispr125	L4300	Wabassi	526779	5734528	0.000302	-0.00123	0.0000	58557	spr	2	subtle EM response on prominent the north of the A1-A2 magnetic horizon
Wabassispr126	L4310	Wabassi	526681	5734407	0.000223	-0.00125	0.0000	58514	spr	2	subtle EM response on prominent the north of the A1-A2 magnetic horizon
Wabassispr127	L4320	Wabassi	526553	5734324	0.000082	0.00094	0.2070	58648	spr	2	subtle EM response on prominent the north of the A1-A2 magnetic horizon
Wabassispr128	L4330	Wabassi	526493	5734152	-0.00046	-0.00153	0.0283	58675	spr	2	subtle EM response on prominent the north of the A1-A2 magnetic horizon
Wabassispr129	L4340	Wabassi	526418	5734005	-0.000127	-0.00039	0.0000	58718	spr	2	subtle EM response on prominent the north of the A1-A2 magnetic horizon
Wabassispr130	L4350	Wabassi	526353	5733831	0.000351	0.001329	0.0000	58719	spr	2	subtle EM response on prominent the north of the A1-A2 magnetic horizon
Wabassispr131	L4360	Wabassi	526277	5733686	0.000214	0.000311	0.1972	58779	spr	2	subtle EM response on prominent the north of the A1-A2 magnetic horizon
Wabassispr132	L4370	Wabassi	526121	5733647	0.000272	-0.00072	0.1427	58732	spr	2	subtle EM response on prominent the north of the A1-A2 magnetic horizon
Wabassispr133	L4380	Wabassi	526039	5733506	0.000007	-0.00034	0.0307	58655	spr	2	subtle EM response on prominent the north of the A1-A2 magnetic horizon
Wabassispr134	L4390	Wabassi	525904	5733425	0.00074	0.002623	4.3836	58536	spr	1	deeper undrilled VTEM plate on magnetic structure

Wabas-sispr135	L4400	Wabassi	525898	5733182	0.002361	0.015007	5.3199	58273	spr	2	on new undrilled Maxwell plate
Wabas-sispr136	L4400	Wabassi	525657	5733526	0.000221	0.000221	2.0509	58088	spr	2	near new Maxwell plate
Wabas-sispr137	L4450	Wabassi	525470	5732502	0.000867	-0.00081	0.2670	58695	spr	2	on new undrilled Maxwell plate
Wabas-sispr138	L4460	Wabassi	525348	5732411	0.006018	0.030244	4.5437	58776	spr	2	on new undrilled Maxwell plate
Wabas-sispr139	L4470	Wabassi	522122	5736609	0.000086	-0.00074	0.0000	57950	spr	3	smaller isolated EM response
Wabas-sispr140	L4470	Wabassi	525264	5732272	0.000174	0.000908	0.0000	58460	spr	2	on south of A2 anomaly
Wabas-sispr141	L4470	Wabassi	527658	5728957	-0.000066	0.000826	0.2678	58248	spr	1	in the Wabassi-West 1 conductive horizon
Wabas-sispr142	L4480	Wabassi	520311	5738882	-0.000229	-0.00087	0.0000	57889	spr	3	small isolated conductive response
Wabas-sispr143	L4480	Wabassi	522024	5736507	-0.000151	-7.6E-05	0.0000	57984	spr	3	small isolated conductive response
Wabas-sispr144	L4500	Wabassi	525113	5731709	-0.000024	-0.00081	0.8197	59504	spr	2	conductor in A1-A2 horizon
Wabas-sispr145	T4780	Wabassi	525329	5732427	0.005412	0.032748	4.8188	58835	spr	2	on new undrilled Maxwell plate
Wabas-sispr146	T4780	Wabassi	525983	5732900	0.000146	0.002314	0.5855	58144	spr	1	deeper undrilled VTEM plate on magnetic structure
Wabas-sispr147	T4820	Wabassi	527613	5729137	-0.000171	-0.0008	0.0000	58065	spr	1	in the Wabassi-West 1 conductive horizon
Wab-Westspr148	L1030	Wabassi West	525223	5731796	0.000221	0.000317	0.0000	59363	spr	2	south of A2 anomaly
Wab-Westspr149	L1040	Wabassi West	525123	5731760	0.000066	0.000216	0.0000	59072	spr	2	south of A2 anomaly
Wab-Westspr150	L1050	Wabassi West	525069	5731662	0.000091	0.001042	1.3555	59491	spr	2	on new undrilled Maxwell plate
Wab-Westspr151	L1060	Wabassi West	525043	5731558	-0.000099	0.000284	0.0000	59808	spr	2	on A1-A2 magnetic horizon
Wab-Westspr152	L1070	Wabassi West	524953	5731504	0.000232	0.000836	0.0000	59570	spr	2	on A1-A2 magnetic horizon
Wab-Westspr153	L1030	Wabassi West	527919	5729011	0.000187	-0.00024	0.0000	57984	spr	1	pick on
Wab-Westspr154	L1040	Wabassi West	527806	5728986	0.000138	-0.0004	1.2219	58103	spr	1	plate on new Wabassi-West conductor 1
Wab-Westspr155	L1050	Wabassi West	527734	5728909	0.000028	0.000595	0.7141	58080	spr	2	plate on new Wabassi-West conductor 1, near existing drillhole
Wab-Westspr156	L1060	Wabassi West	527724	5728782	0.000536	0.003093	3.1706	57933	spr	1	plate on new Wabassi-West conductor 1
Wab-Westspr157	L1070	Wabassi West	527661	5728691	-0.000304	0.002116	2.7499	57892	spr	1	plate on new Wabassi-West conductor 1
Wab-Westspr158	L1080	Wabassi West	527646	5728570	0.000001	-0.0002	0.4226	57910	spr	1	plate on new Wabassi-West conductor 1
Wab-Westspr159	L1090	Wabassi West	527658	5728413	0.000085	-0.00083	0.7444	57927	spr	2	conductive response in Wabassi-West A2 cluster
Wab-Westspr160	L1100	Wabassi West	527584	5728348	0.000257	0.000365	1.3138	57894	spr	2	conductive response in Wabassi-West A2 cluster
Wab-Westspr161	L1110	Wabassi West	527470	5728327	0.000243	0.000837	2.0673	57895	spr	2	conductive response in Wabassi-West A2 cluster

Wab- Westspr1 62	L11 20	Wabassi West	527 345	5728 311	0.000 341	0.001 523	2.901 4	579 08	spr	1	plate on new Wabassi-West conductor 2
Wab- Westspr1 63	L11 30	Wabassi West	527 220	5728 291	- 0.000 12	0.001 632	2.369 9	578 59	spr	1	plate on new Wabassi-West conductor 2
Wab- Westspr1 64	L11 40	Wabassi West	527 144	5728 225	0.000 236	- 0.000 19	1.543 1	578 39	spr	1	plate on new Wabassi-West conductor 2
Wab- Westspr1 65	L11 50	Wabassi West	527 070	5728 166	0.000 337	0.000 667	1.873 2	578 45	spr	1	plate on new Wabassi-West conductor 2
Wab- Westspr1 66	L11 60	Wabassi West	526 919	5728 172	- 0.000 113	- 0.000 16	0.000 0	578 46	spr	1	conductive response in Wabassi-West A2 cluster
Wab- Westspr1 67	L12 80	Wabassi West	525 050	5728 378	0.000 264	-8.9E- 05	0.357 8	577 85	spr	2	conductive response in Wabassi-West A3 cluster
Wab- Westspr1 68	L12 90	Wabassi West	525 032	5728 254	0.000 557	0.002 731	2.600 5	580 45	spr	1	conductive response in Wabassi-West A3 cluster
Wab- Westspr1 69	L13 00	Wabassi West	524 968	5728 177	0.003 122	0.011 056	3.415 2	581 30	spr	1	conductive response in Wabassi-West A3 cluster
Wab- Westspr1 70	L13 40	Wabassi West	524 800	5727 776	0.000 321	- 0.000 2	0.000 0	579 42	spr	2	conductive response in Wabassi-West A3 cluster
Maxspr17 1	L40 20	Max	518 501	5720 947	0.000 878	- 0.001 76	0.092 5	579 58	spr	3	smaller EM response
Maxspr17 2	L32 60	Max	521 573	5718 600	- 0.000 454	- 0.003 13	0.450 6	582 95	spr	1	near deeper Maxwell plate @ -215m
Maxspr17 3	T50 20	Max	518 000	5734 966	- 0.000 361	- 0.001 95	1.194 1	588 30	spr	2	on main Max peridotite conductor near existing drillhole
Maxspr17 4	T50 20	Max	517 998	5734 422	0.000 626	0.001 343	1.567 1	591 17	spr	1	on western edge of main Max peridotite conductor
Maxspr17 5	T50 20	Max	517 996	5725 662	0.000 605	0.000 343	0.423 0	582 76	spr	3	isolated small EM response
Maxspr17 6	T50 20	Max	518 005	5718 000	- 0.000 026	0.001 185	0.576 3	582 45	spr	2	response on west of larger east-west striking magnetic horizon, Maxwell model?
Maxspr17 7	T50 30	Max	519 498	5717 883	0.000 567	0.001 671	1.838 4	579 98	spr	2	response on west of larger east-west striking magnetic horizon, Maxwell model?
Maxspr17 8	T50 30	Max	519 498	5734 211	- 0.000 511	- 0.002 56	0.087 1	579 00	spr	3	smaller EM response to east of Max peridotite
Maxspr17 9	T50 30	Max	519 500	5734 547	- 0.000 374	0.001 798	0.125 4	579 04	spr	3	smaller EM response to east of Max peridotite
Maxspr18 0	T50 40	Max	521 002	5718 424	- 0.000 16	- 0.000 14	1.492 9	580 95	spr	2	response to north of the larger magnetic horizon
Maxspr18 1	T50 50	Max	522 500	5718 942	- 0.000 172	0.002 586	0.188 2	583 78	spr	2	near deeper Maxwell plates just to east
Maxspr18 2	L32 50	Max	521 617	5718 748	0.000 035	0.000 6	0.271 8	580 47	spr	1	Deeper Maxwell plate model nearby

Pick_ID	Line	grid	X	Y	SF	BF	AdTau_B	TMI	pick_type	Rank	Notes
Maxdpr1	L4010	Max	518297	5716978	0.004379	0.021666	5.274287	58097	dpr	2	located in the thinner southern magnetic horizon, appears to be a formational response
Maxdpr2	L4030	Max	518702	5717075	0.003621	0.021252	6.196445	58224	dpr	2	located in the thinner southern magnetic horizon, appears to be a formational response
Maxdpr3	L4020	Max	518503	5717074	0.001632	0.010897	5.986339	58105	dpr	2	located in the thinner southern magnetic horizon, appears to be a formational response
Maxdpr4	L4040	Max	518903	5717155	0.008476	0.046985	5.519978	58185	dpr	2	located in the thinner southern magnetic horizon, appears to be a formational response
Maxdpr5	L4050	Max	519094	5717151	0.011564	0.087261	6.538592	58301	dpr	2	located in the thinner southern magnetic horizon, appears to be a formational response
Maxdpr6	L4080	Max	519700	5717341	0.014516	0.058324	4.371406	58197	dpr	2	located in the thinner southern magnetic horizon, appears to be a formational response
Maxdpr7	L4100	Max	520102	5717468	0.001477	0.007368	4.188104	58016	dpr	2	located in the thinner southern magnetic horizon, appears to be a formational response
Maxdpr8	L4110	Max	520303	5717390	0.000151	0.001526	0.620384	57978	dpr	2	located in the thinner southern magnetic horizon, appears to be a formational response
Maxdpr9	L4120	Max	520502	5717384	0.002086	0.011168	4.039659	58070	dpr	2	located in the thinner southern magnetic horizon, appears to be a formational response
Maxdpr10	L4130	Max	520699	5717428	0.003116	0.017652	3.712779	58113	dpr	2	located in the thinner southern magnetic horizon, appears to be a formational response
Maxdpr11	L4090	Max	519902	5717401	0.046978	0.201819	4.177968	58348	dpr	2	located in the thinner southern magnetic horizon, appears to be a formational response
Maxdpr12	L4140	Max	520902	5717487	0.002667	0.009126	2.643374	57993	dpr	2	located in the thinner southern magnetic horizon, appears to be a formational response
Maxdpr13	L4060	Max	519302	5717250	0.001103	0.001456	2.096381	58194	dpr	2	located in the thinner southern magnetic horizon, appears to be a formational response
Maxdpr14	L4150	Max	521101	5717540	0.001619	0.004503	2.701415	58054	dpr	2	located in the thinner southern magnetic horizon, appears to be a formational response
Maxdpr15	L4160	Max	521300	5717593	0.003005	0.016022	3.809758	58152	dpr	2	located in the thinner southern magnetic horizon, appears to be a formational response
Maxdpr16	L4170	Max	521504	5717676	0.008816	0.037016	3.496566	58159	dpr	2	located in the thinner southern magnetic horizon, appears to be a formational response
Maxdpr17	L4180	Max	521697	5717720	0.026843	0.169166	5.333417	58092	dpr	2	located in the thinner southern magnetic horizon, appears to be a formational response
Maxdpr18	L4190	Max	521902	5717815	0.011482	0.057707	4.308468	58048	dpr	2	located in the thinner southern magnetic horizon, appears to be a formational response
Maxdpr19	L4200	Max	522100	5717838	0.002047	0.011613	3.312037	58035	dpr	2	located in the thinner southern magnetic horizon, appears to be a formational response
Maxdpr20	L4210	Max	522302	5717958	-0.0003	-0.00183	1.576498	58004	dpr	2	located in the thinner southern magnetic horizon, appears to be a formational response
Maxdpr21	L4230	Max	522698	5718170	0.000974	0.00629	3.400744	57949	dpr	1	located in the thinner southern magnetic horizon, appears to be a formational response
Maxdpr22	L3310	Max	521748	5717851	0.022044	0.125028	4.908394	57976	dpr	2	located in the thinner southern magnetic horizon, appears to be a formational response

Maxdpr23	L3310	Max	521236	5717847	0.0019	0.010181	3.954755	57947	dpr	1	just north of the main DPR horizon
Maxdpr24	L3310	Max	521790	5717852	0.032356	0.155227	4.206747	57984	dpr	2	located in the thinner southern magnetic horizon, appears to be a formational response
Maxdpr25	L3310	Max	522045	5717850	0.000599	0.003986	3.890086	58036	dpr	2	located in the thinner southern magnetic horizon, appears to be a formational response
Wabassidpr26	L4400	Wabassi	525718	5733438	0.000106	0.000686	1.12533	58167	dpr	2	located near anomaly A1
Wabassidpr27	L4410	Wabassi	525764	5733105	0.001362	0.009059	4.346874	58812	dpr	2	located near anomaly A1
Wabassidpr28	L4410	Wabassi	525906	5732907	0.000226	0.000489	1.5202	58169	dpr	2	located near anomaly A1
Wabassidpr29	L4420	Wabassi	525641	5733032	0.000008	-0.00015	0.656397	58803	dpr	2	located near anomaly A1
WabWestdpr30	L1310	Wabassi West	524866	5728136	0.001042	0.006328	5.276189	58062	dpr	1	Maxwell plate model on Wabassi-West 3
WabWestdpr31	L1320	Wabassi West	524810	5728049	0.000537	0.002125	4.921865	58020	dpr	1	Maxwell plate model on Wabassi-West 3
WabWestdpr32	L1330	Wabassi West	524751	5727970	-0.00033	-0.00091	0.244168	57938	dpr	1	Maxwell plate model on Wabassi-West 3
Maxdpr33	L3290	Max	522627	5718149	0.000322	0.000183	1.454792	57952	dpr	2	easternmost dpr on the Max South magnetic linear
Maxdpr34	T5050	Max	522503	5718072	-0.00038	0.001511	1.41289	57965	dpr	2	easternmost dpr on the Max South magnetic linear
Maxdpr35	T5040	Max	520997	5717496	0.000949	0.005384	3.719607	58035	dpr	2	located in the thinner southern magnetic horizon, appears to be a formational response
Maxdpr36	T5030	Max	519498	5717333	0.178703	1.17888	5.747471	58157	dpr	2	located in the thinner southern magnetic horizon, appears to be a formational response

Appendix B-Notes on Maxwell Modeling

The Geotech provided database was run through the Maxwell plate inversion program. The EM response is presented, and plate parameters are edited and inverted to better fit the observed EM response with the model EM response. The resulting deliverable products are Maxwell plate model PRJ, PTE, PTS, and DXF files are located within the delivered client CD.

Appendix C- "Fly to drill Templates"

Maxwell EM plate model and drill hole outcomes are presented in graphical plan and 3D format using Encom PA. The drill holes as sited are seen to intersect the top sections of the provided plate models. The drill hole collars and geometries are therefore thought to be accurate for the intersection of the modeled conductive plates out in the field, though there is always be some ambiguity in plate model results for any given observed EM response. It was noted for the TZ 2 and TZ 3 models in particular, where two plates of different geometries, either shallower or deeper, or of shorter or longer strike length, could fit the same response with a similar calculated fit error. For the smaller targets of limited spatial extent, accurate differential GPS sighting of drill holes is recommend to allow a drill hole's trajectory into a smaller conductor to be adjusted if necessary to reflect the more accurate XYZ collar coordinates out in the field. Conductors that are thin conductive ribbons or small blobs 100 m or more below surface can easily be missed by a drill hole if the proposed drill hole collar elevation deviates by more than a few meters from the real field topography elevation where a drill hole is sited.

Wabassi-Max Target Template Listing

Max Peridotite L2180 "Main conductor"

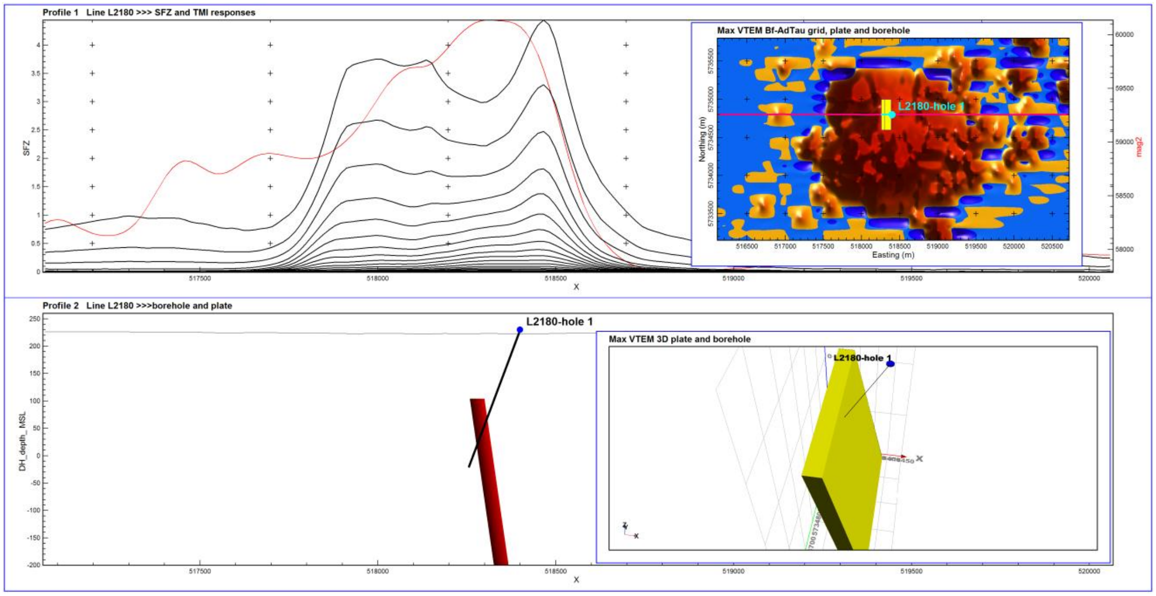

L2180 Larger thicker plate well fits the response, moderate conductivity, one drill hole proposed.

Max Peridotite L2190 "Main conductor"

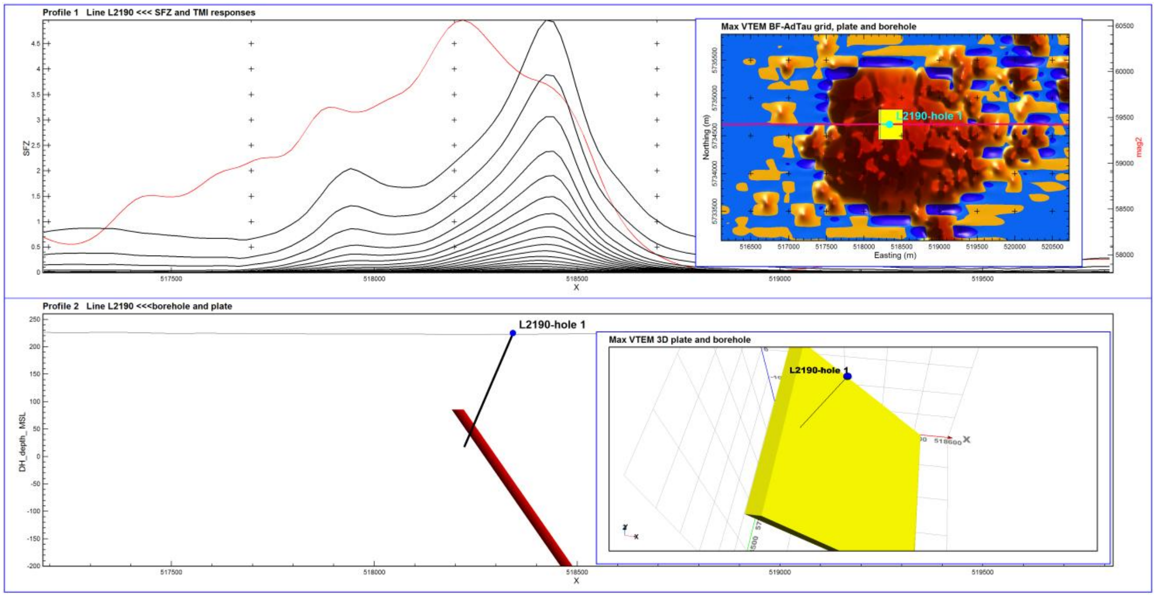

L2190 Larger thicker plate well fits the response, moderate conductivity, one drill hole proposed.

Max Peridotite L2300 "South satellite conductor"

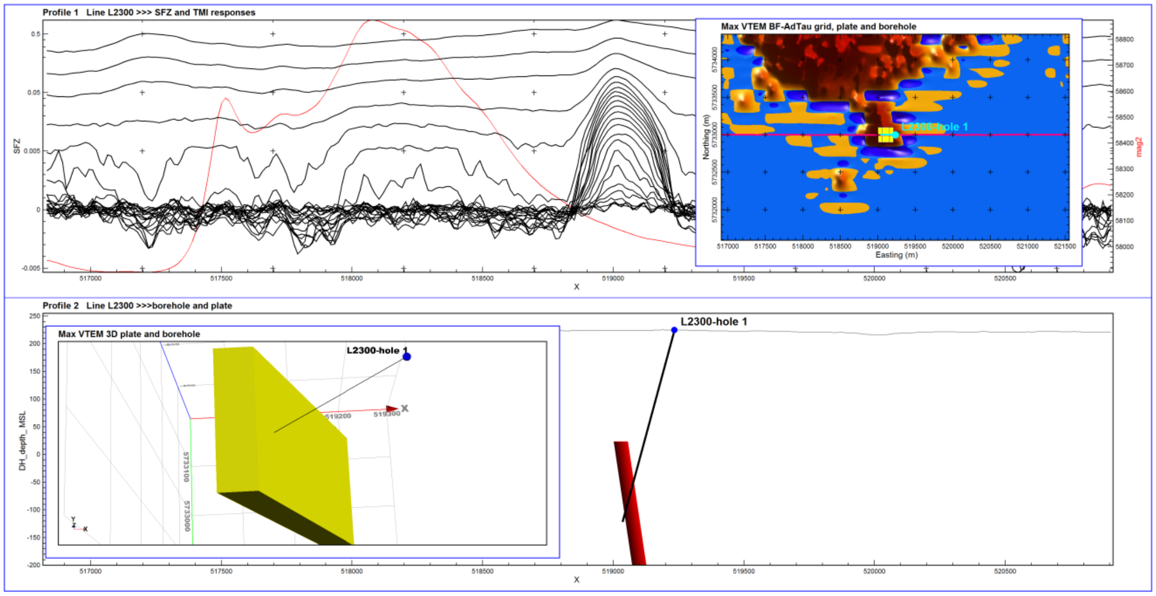

L2300 Larger thicker plate well fits the response, moderate conductivity, one drill hole, higher priority.

L3280 "deeper southern Max SPRs"

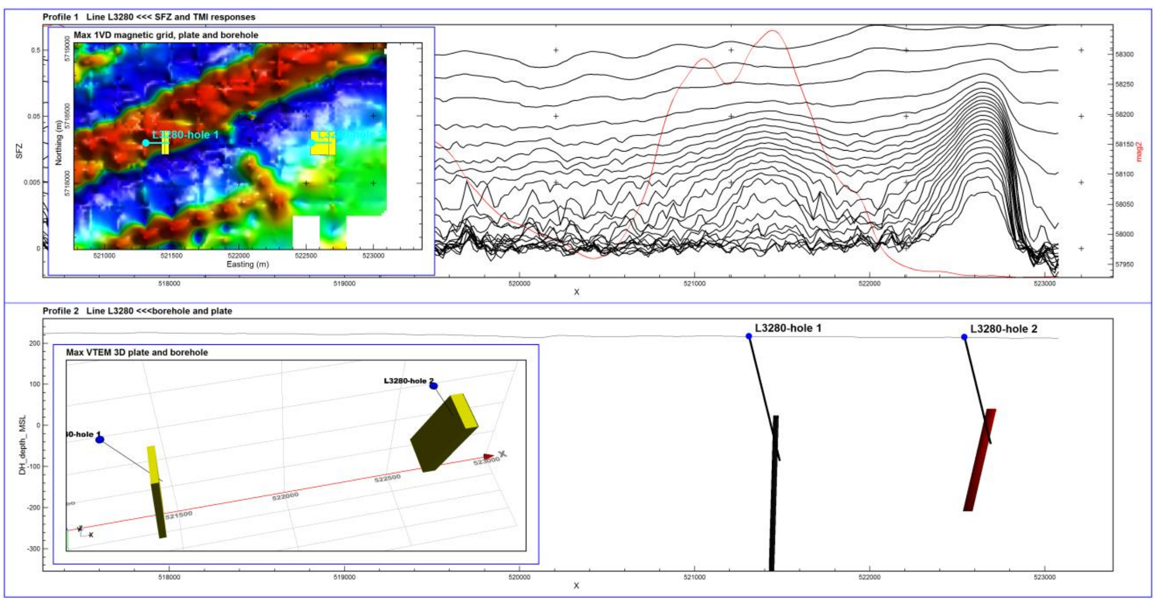

L3280 two plates fit the two along-line separated responses, lower conductivity, higher priority due the conductors being deeper and sub-parallel or sub-perpendicular from the NE-SW striking formational conductor just to the south.

L4080 Max grid far south “formational magnetic conductor”

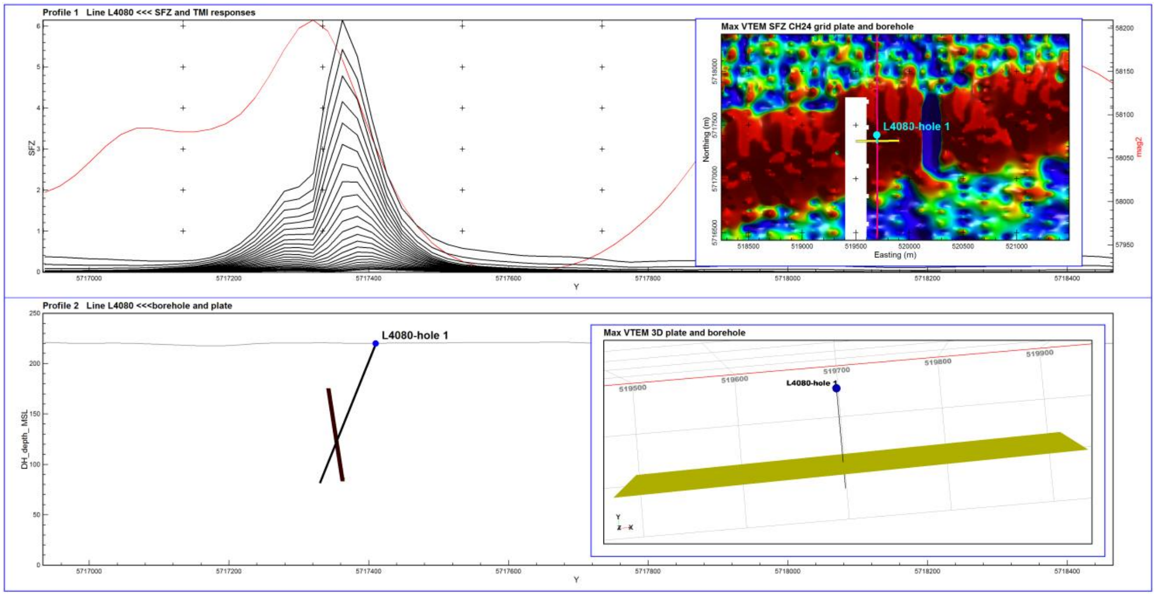

L4080 Max south thin plate well fits the response, moderate conductivity, higher priority.

Wabassi “A1 anomaly L4380”

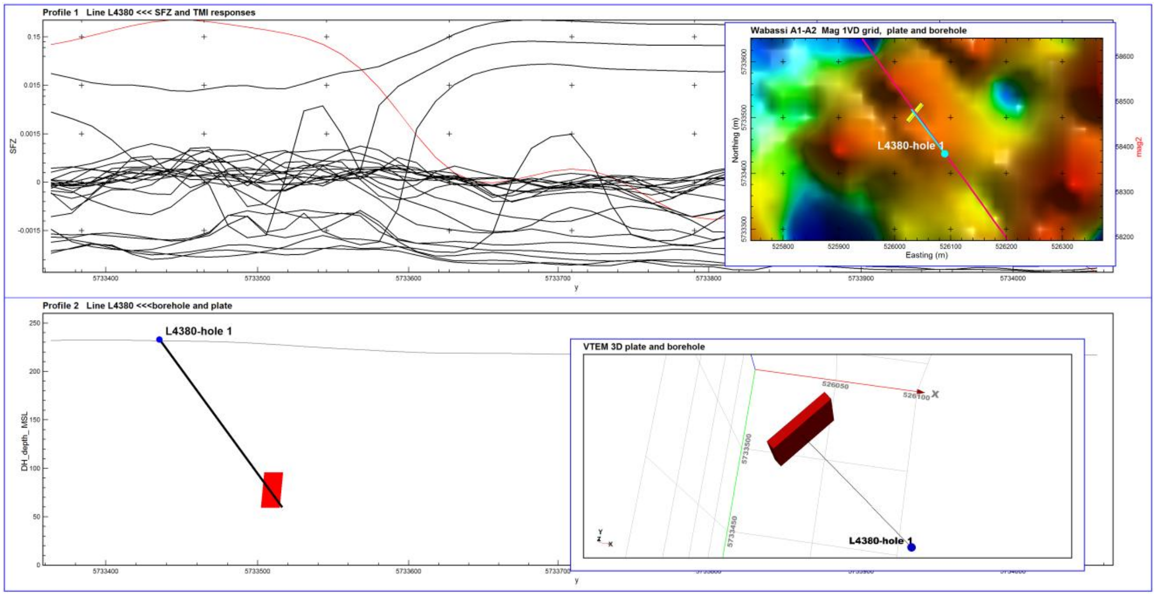

L4380- small conductive plate, accurate GPS positioning for the drill hole collar in the field is recommended, as the plate extents are limited in size. This model is fit to a noisier and more subtle response, lower priority target.

Wabassi "A1 anomaly L4390"

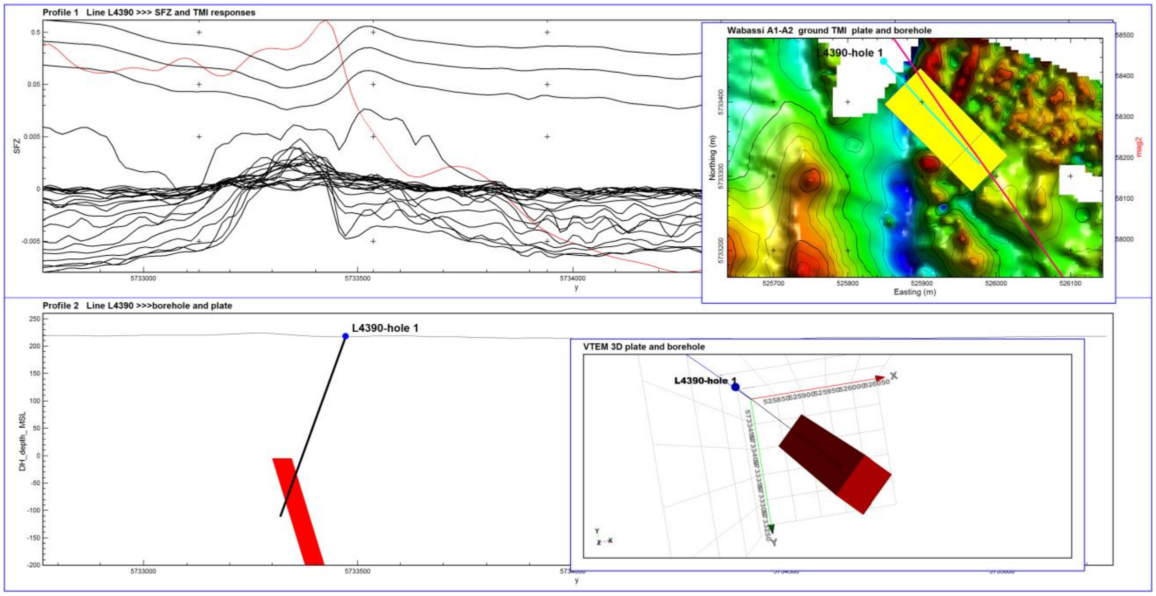

L4390- thicker deeper plate with a pipe-like morphology, of moderate conductivity. Higher priority target due to location in a magnetic structural break. but higher risk due to depth.

Wabassi "A1 anomaly L4400"

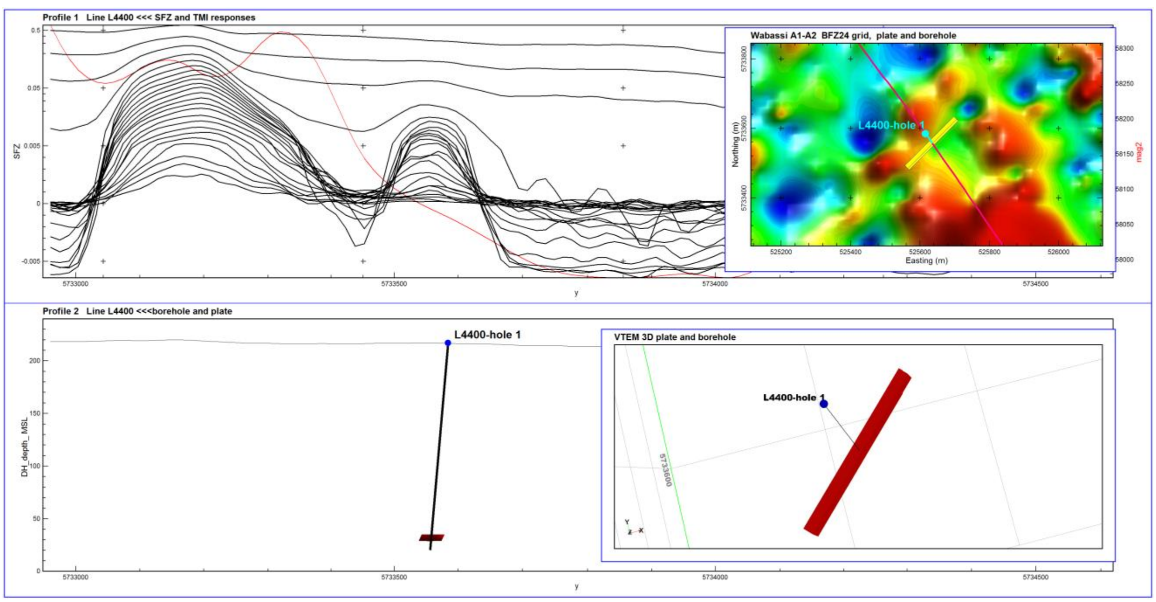

L4400- South plate was drilled by Northern Shield, the north plate target is a moderately conductive long thin plate. Lower priority, accurate GPS positioning for the drill hole collar in the field is recommended, as the plate extents are limited.

Wabassi "A1 anomaly L4420"

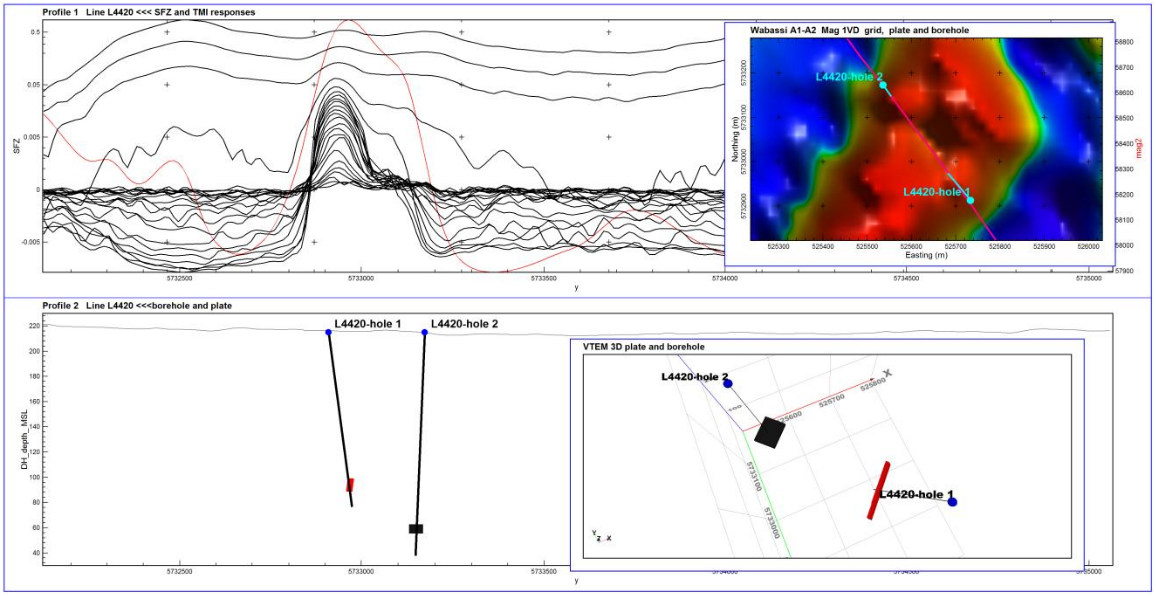

L4420- one highly conductive, one extremely conductive small plate separated by a few hundred meters along-flight line. Accurate GPS positioning of the drill hole collar in the field is recommended, as the plate extents are limited. Lower priority due to limited plate extents.

Wabassi "A1 anomaly L4450"

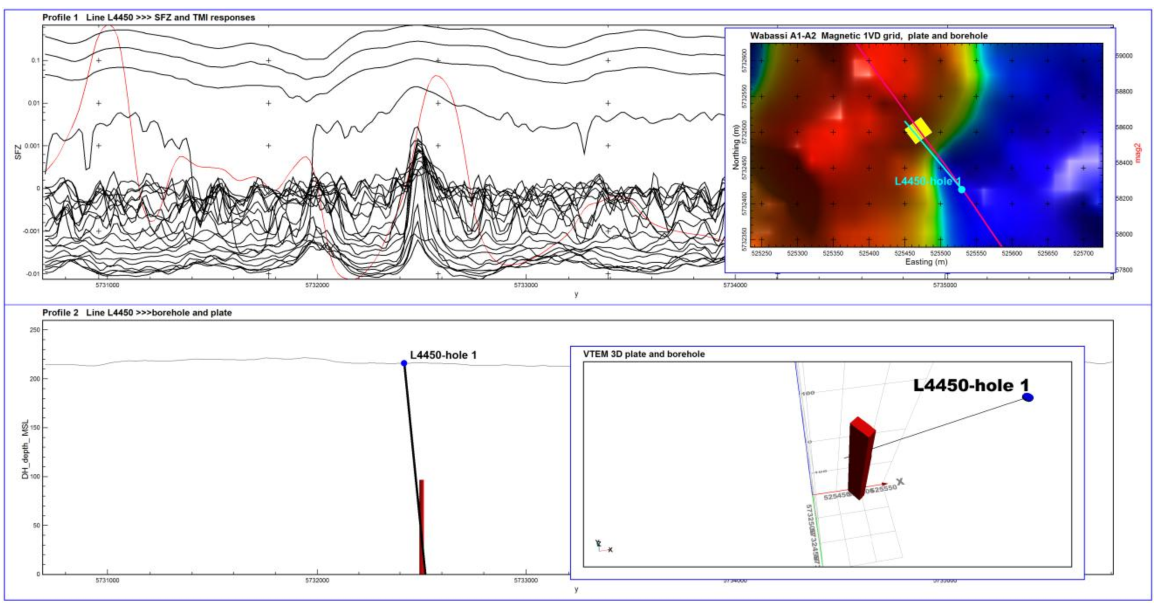

L4450- Thin vertical pipe-like plate of moderate conductivity. Accurate GPS positioning for the drill hole collar in the field is recommended, as the plate extents are limited. This is a noisier lower amplitude response, lower priority target.

Wabassi "A1 anomaly T4780"

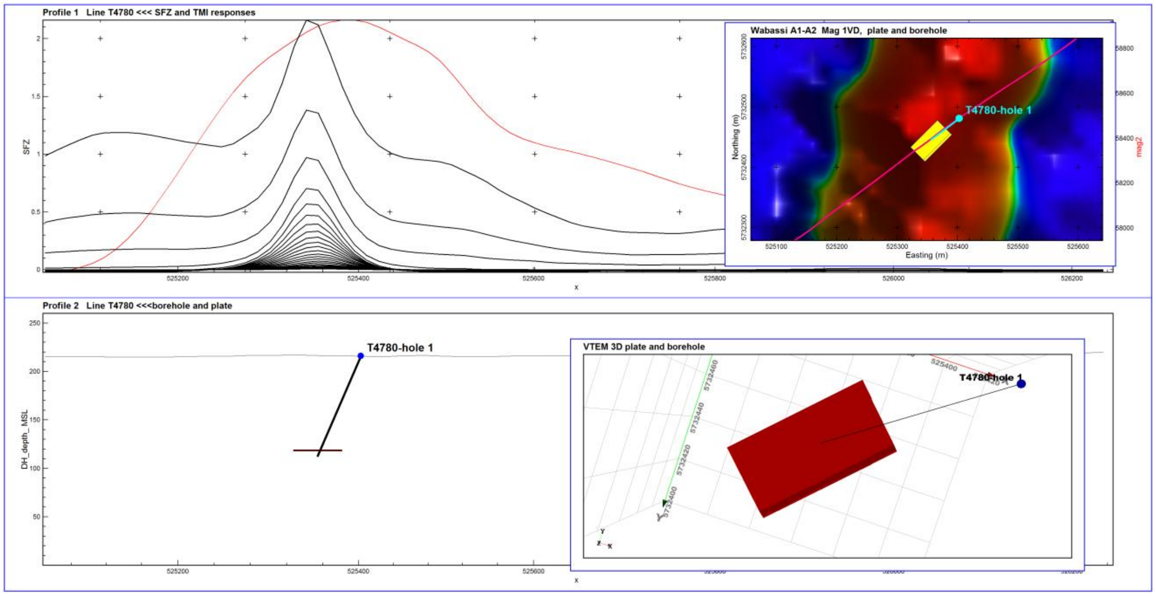

T4780- small flat-lying highly conductive plate in a magnetic dyke or other magnetic linear. Accurate GPS positioning of the drill hole collar in the field is recommended, as the plate extents are limited. Lower priority.

Wabassi "A1 anomaly InfiniTEM L300"

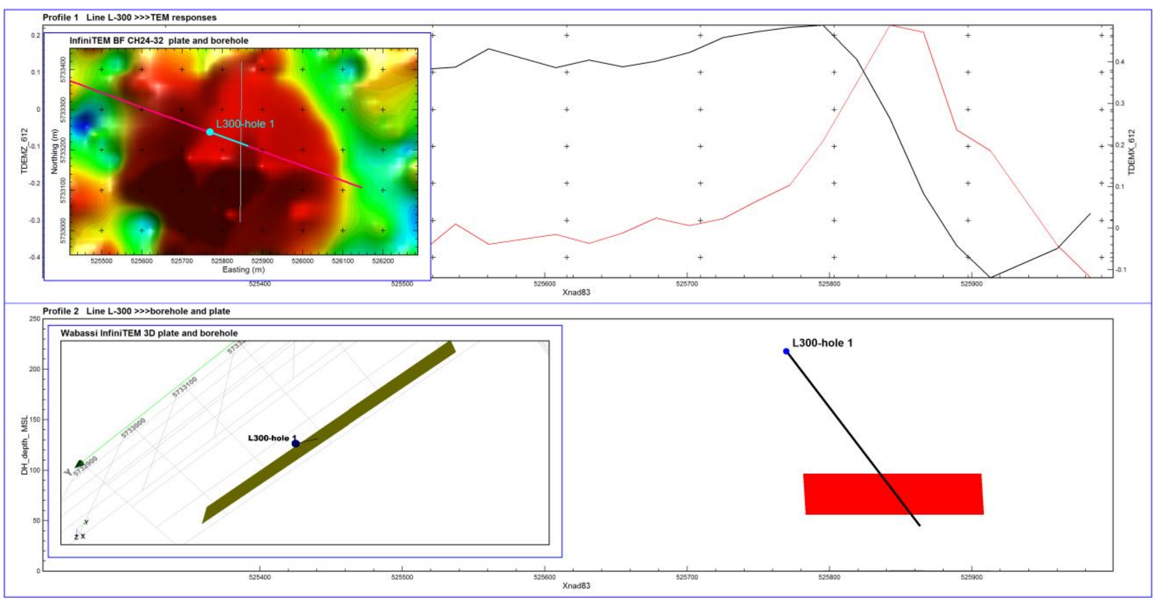

L300- Two plates fit this response; the NS striking thin plate was chosen as the model, though a sub-perpendicular thick plate also fits the response. The drill hole is sighted to intersect the center of both plates, both of which are high conductivity. These are lower priority targets due to the ribbon-like morphology. The profile traces in the top panel are the Abitibi-provided merged Z and X component InfiniTEM responses, there was not a located Z response database provided.

.

Wabassi “A1 anomaly InfiniTEM L400”

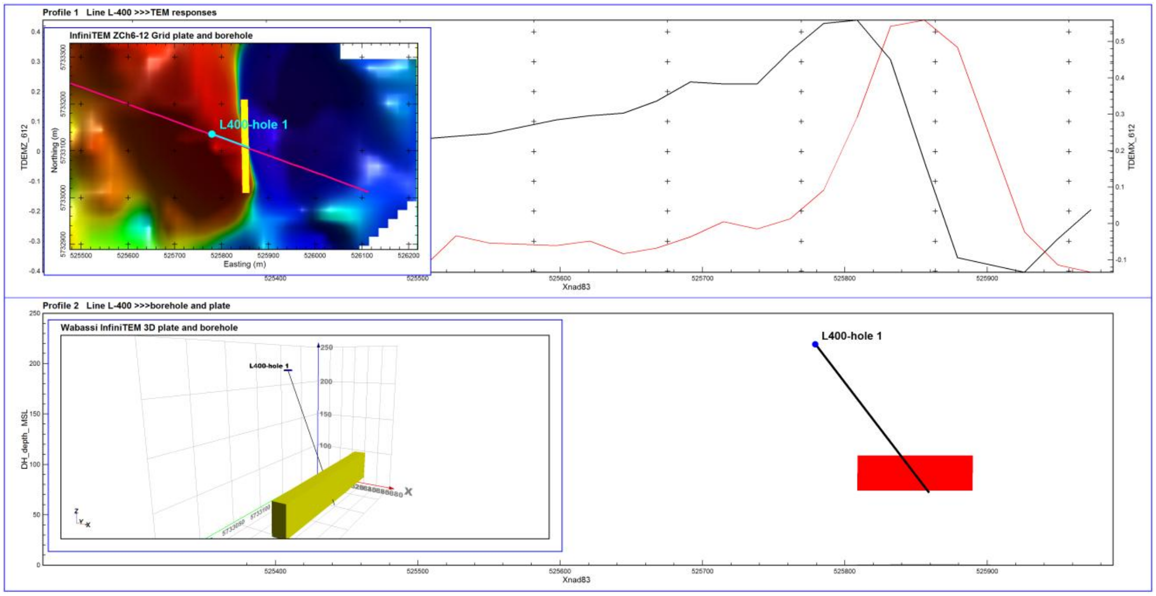

L400- A long rod-like plate model of higher conductivity fit the response. The model is ranked low priority as it has a limited spatial extent, is thin, rod-like. The profile traces in the top panel are the Abitibi-provided merged Z and X component InfiniTEM responses, there was not a located Z response database provided.

Wabassi “A1 anomaly InfiniTEM L500”

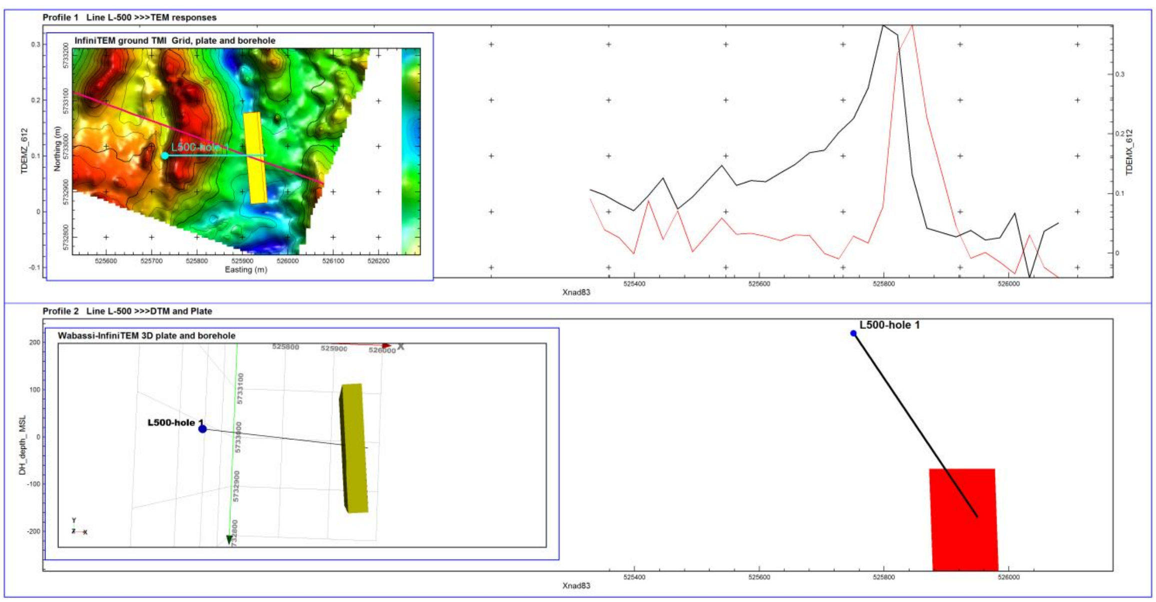

L500- A suite of deeper plates fit this response; the deepest plate was selected as the drill hole intersects the tops of the shallower plates on its trajectory to the deeper plate. Plate has lower to moderate conductivity and a coincident ground magnetic signature. The target is high priority for returning repeatable deeper model fits that may have been masked by shallower more conductive responses to the west, and also for being coincident with a subtle ground magnetic signature, though the depth makes it high risk.

Wabassi "A1 anomaly InfiniTEM L600"

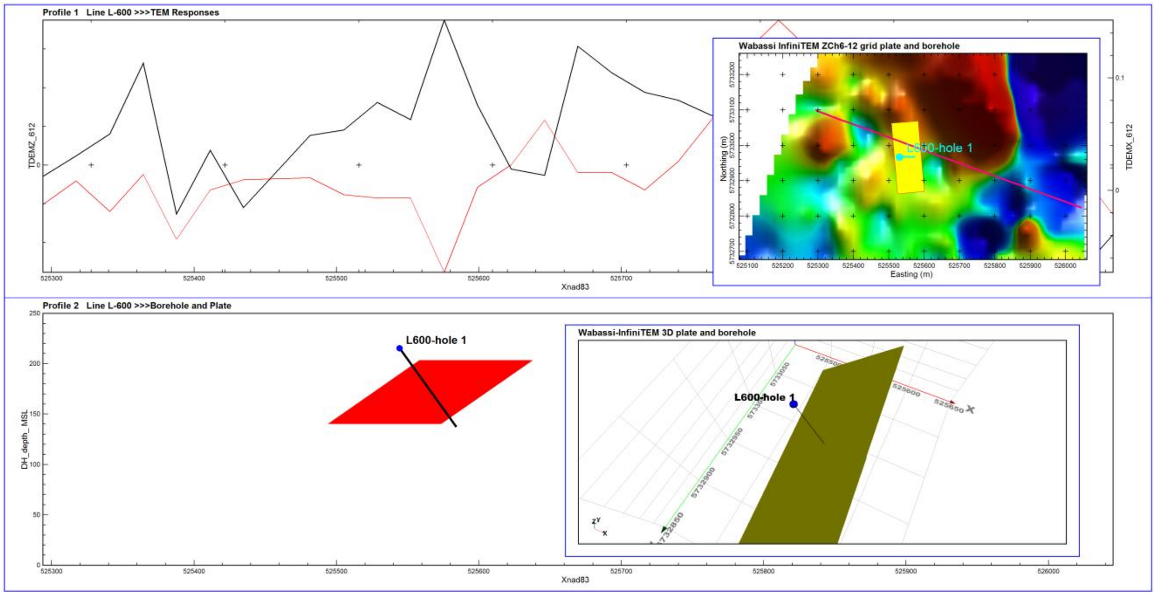

L600- shallow very conductive thin plate, a 2nd thick plate model with a perpendicular strike to the thin plate is also very conductive; the drill hole is sighted to intersect both plates piercing the center of the thin plate. Low priority due to limited plate extents. The profile traces in the top panel are the Abitibi-provided merged Z and X component InfiniTEM responses, there was not a located Z response database provided.

Wabassi "A2 anomaly InfiniTEM L1200"

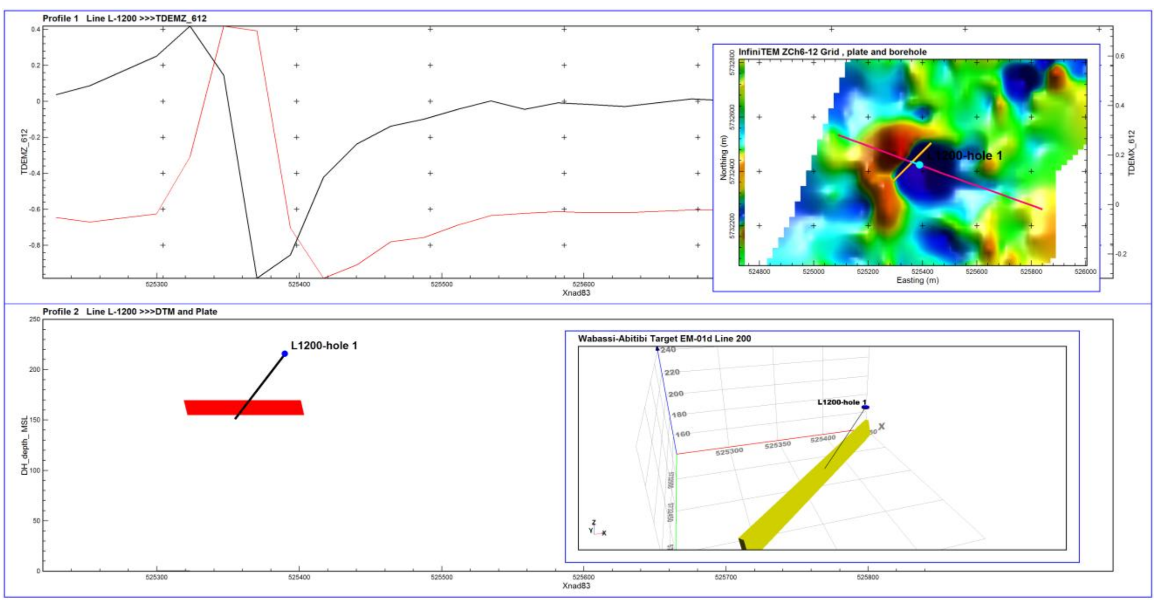

L1200- long thin shallow conductive plate model, low priority due to its being thin and rod-like. The profile traces in the top panel are the Abitibi-provided merged Z and X component InfiniTEM responses, there was not a located Z response database provided. The UTM conversion was internal in Maxwell to the modeled unlocated TEM files.

Wabassi West "Subzone 1 L1040"

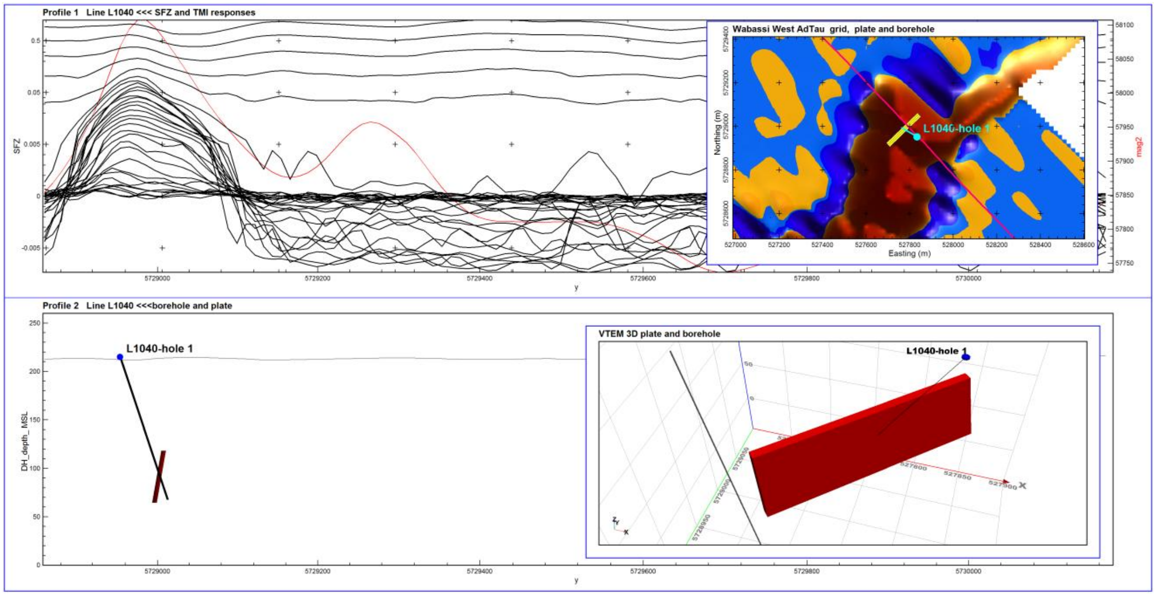

L1040- lower-moderate conductivity long thin plate. Higher priority for being part of a 1400m long conductive horizon. The existing drill hole 10WA-01 trace is seen to miss the southern plate edge just south of plate, on the right bottom panel.

Wabassi West "Subzone 1 L1050"

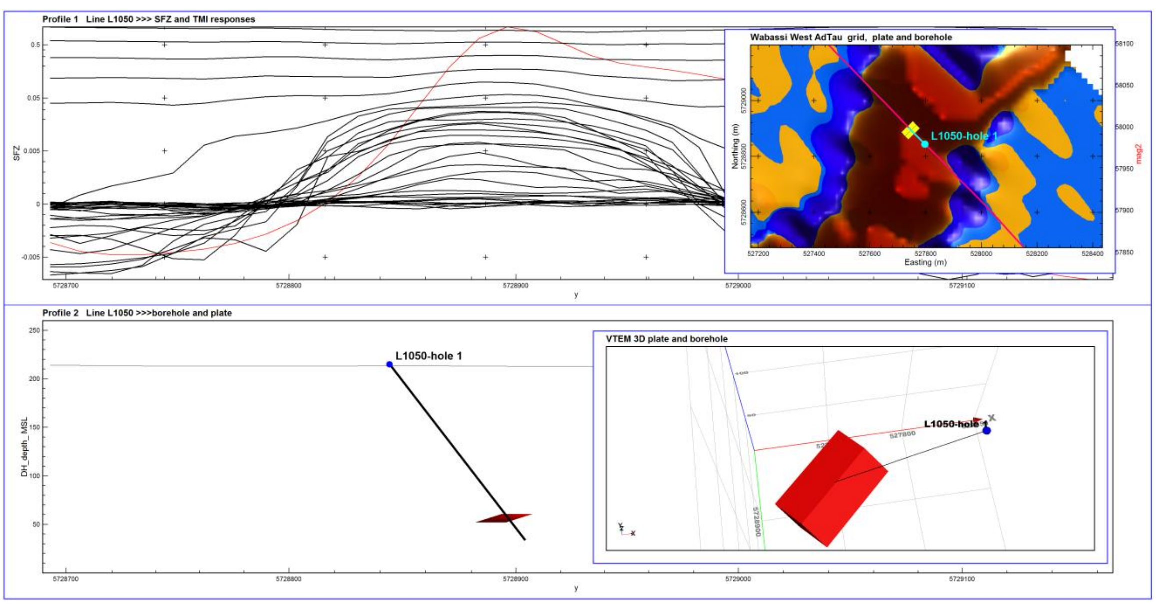

L1050- one of two small plates separated by 650m along the flight line. This is a lower conductivity plate. Ranked higher priority for being part of a 1400m long Wabassi West conductive horizon.

Wabassi West "Subzone 1 L1050 plate 2"

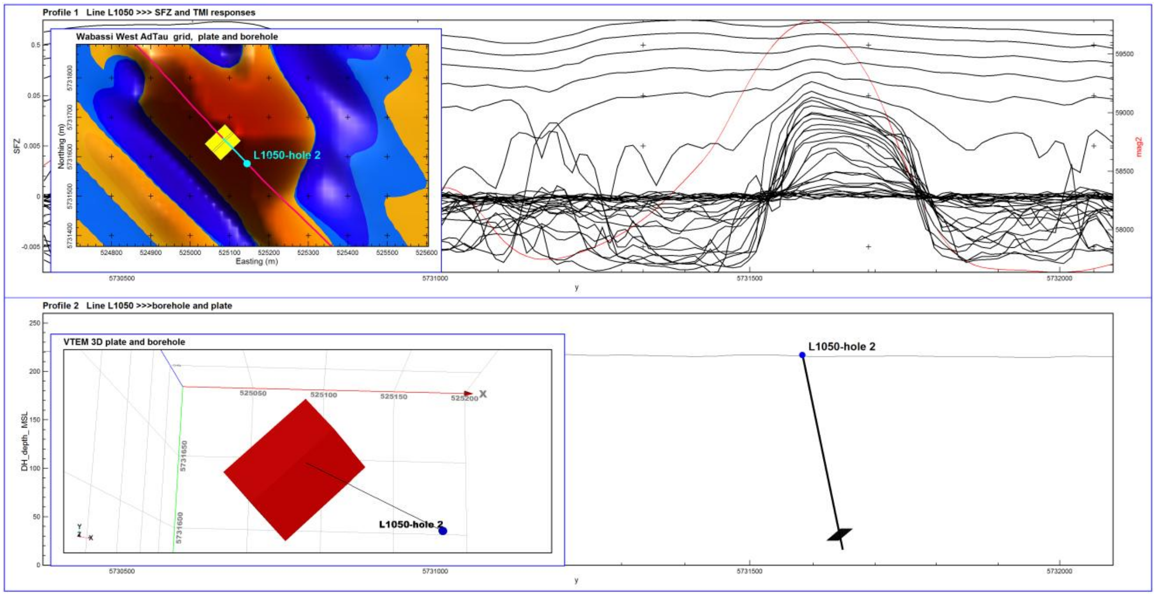

L1050 the 2nd of two widely separated small plates, this plate is part of A1-A2 conductive horizon. Low-moderate conductivity, low priority. Differential GPS hole sighting is rec-ommended as the plate is small, easy to miss.

Wabassi West "Subzone 1 L1060"

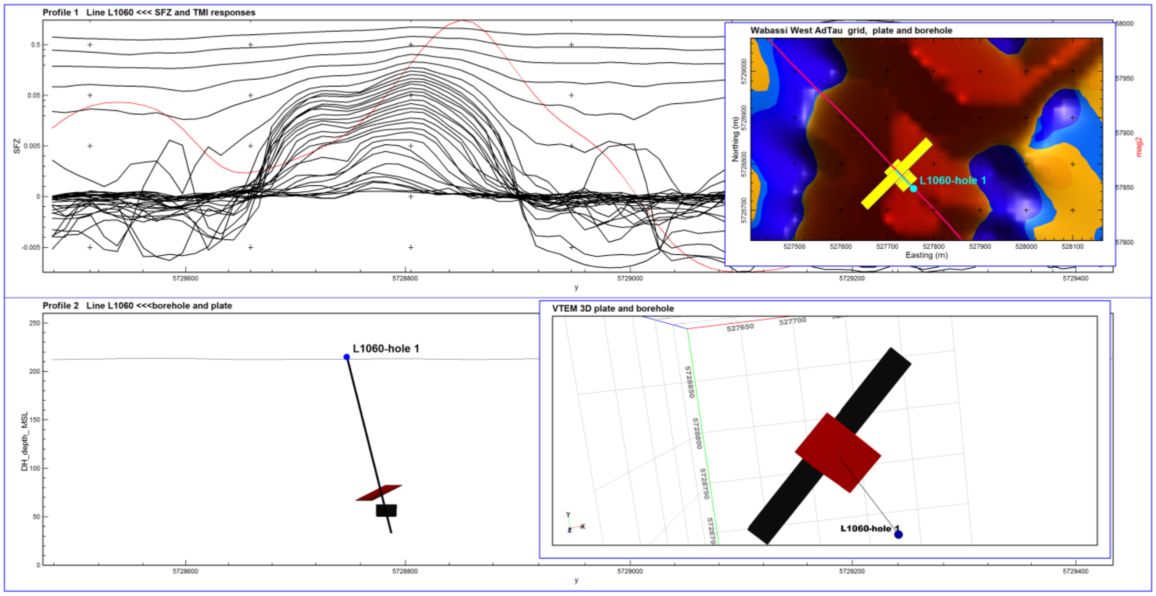

L1060- two thinner plates of moderate to high conductivity, one drill hole is sighted that intersects the center of both plates that are moderate-higher conductivity. High priority as part of a continuous 1400 m long Wabassi West conductive horizon.

.

Wabassi West "Subzone 1 L1070"

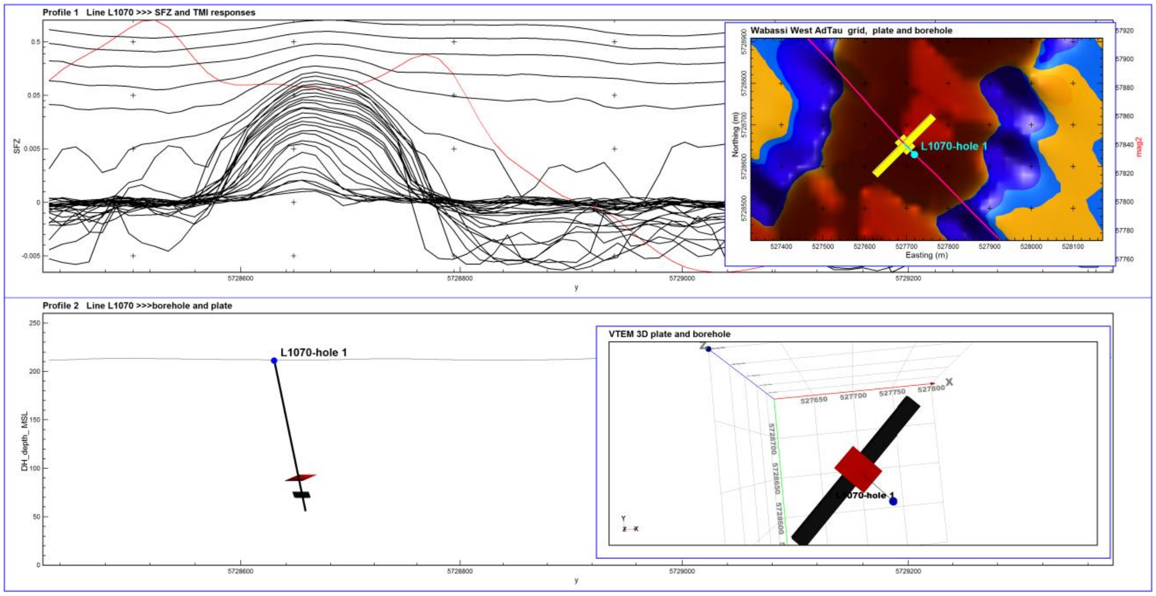

L1070- two thinner plates of moderate to high conductivity, one drill hole is sighted that intersects both plate centers, higher priority. Differential GPS Hole sighting recommended as both plates are small, easy to miss.

Wabassi West "Subzone 2 L1120"

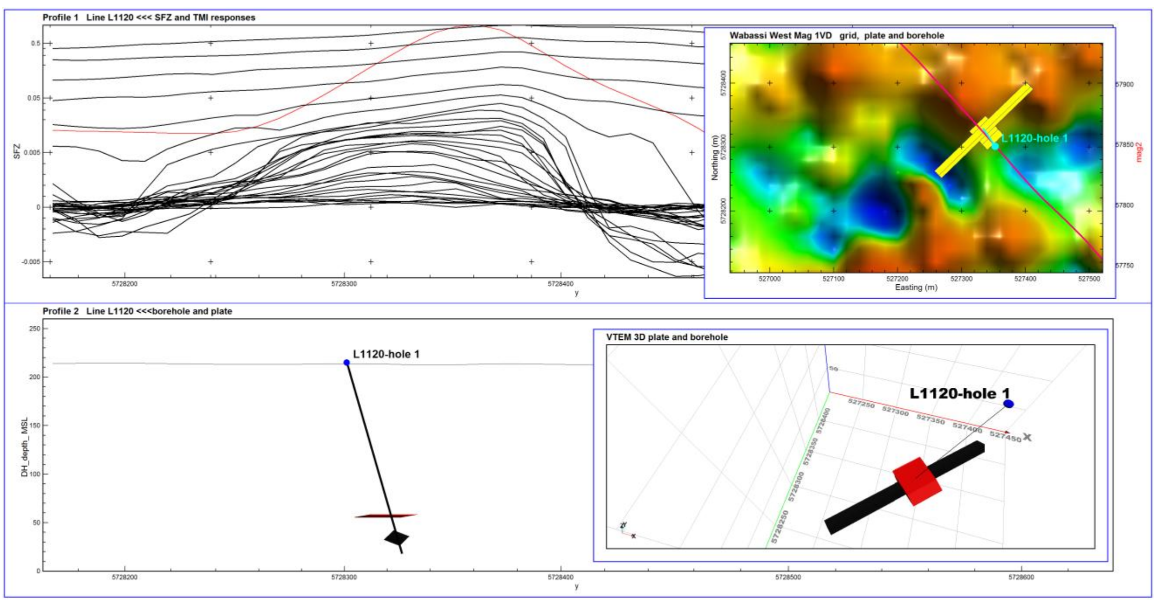

L1120 Two smaller plates, moderate to higher conductivity, higher priority due to being part of 1400 m long conductive horizon. One drill hole is sighted that intersects both plate centers, higher priority.

Wabassi West "Subzone 2 L1130"

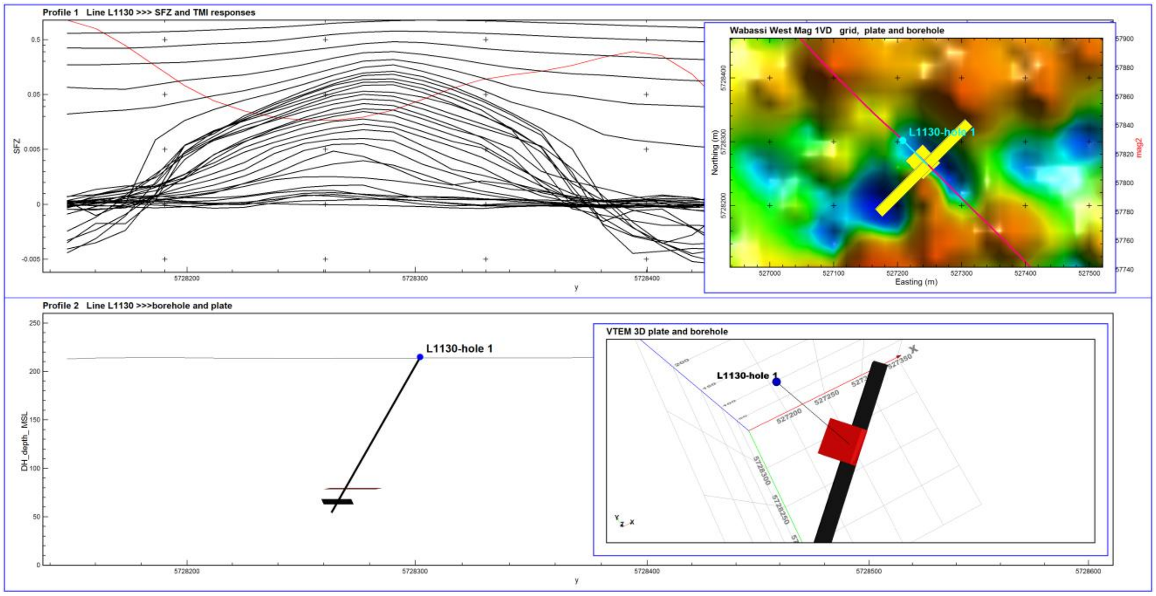

L1130- two thinner plates of moderate to high conductivity, one drill hole intersects both plates, higher priority as part of a 1400 m continuous conductive horizon.

Wabassi West "Subzone 2 L1140"

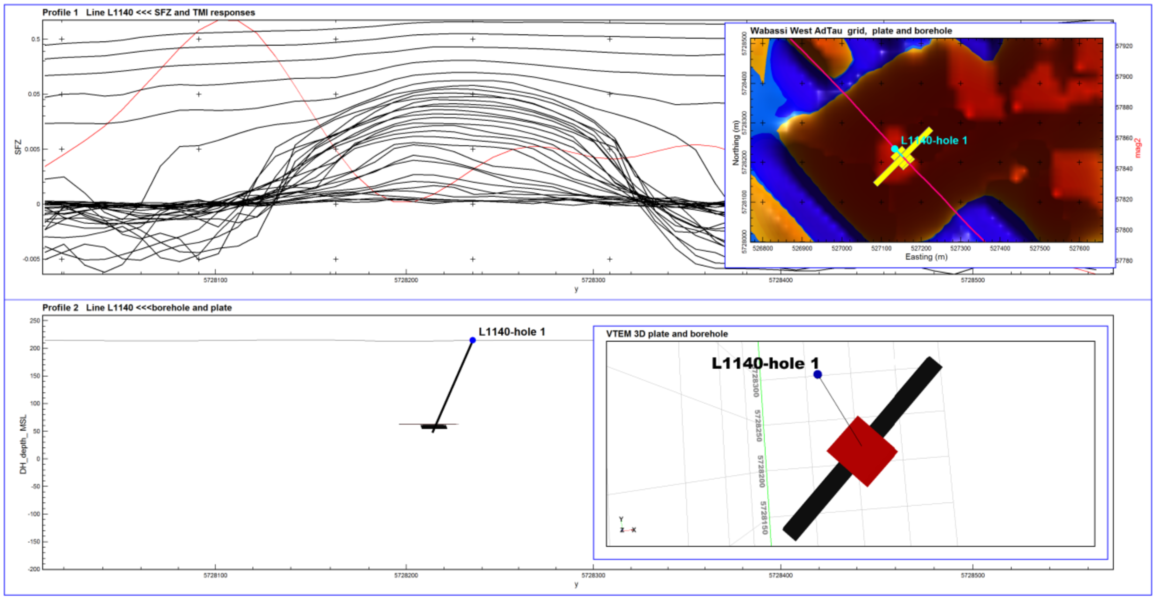

L1140- two thinner plates of moderate to high conductivity, drill hole intersects both plate centers, higher priority as part of a 1400 m long conductive horizon.

Wabassi West "Subzone 2 L1150"

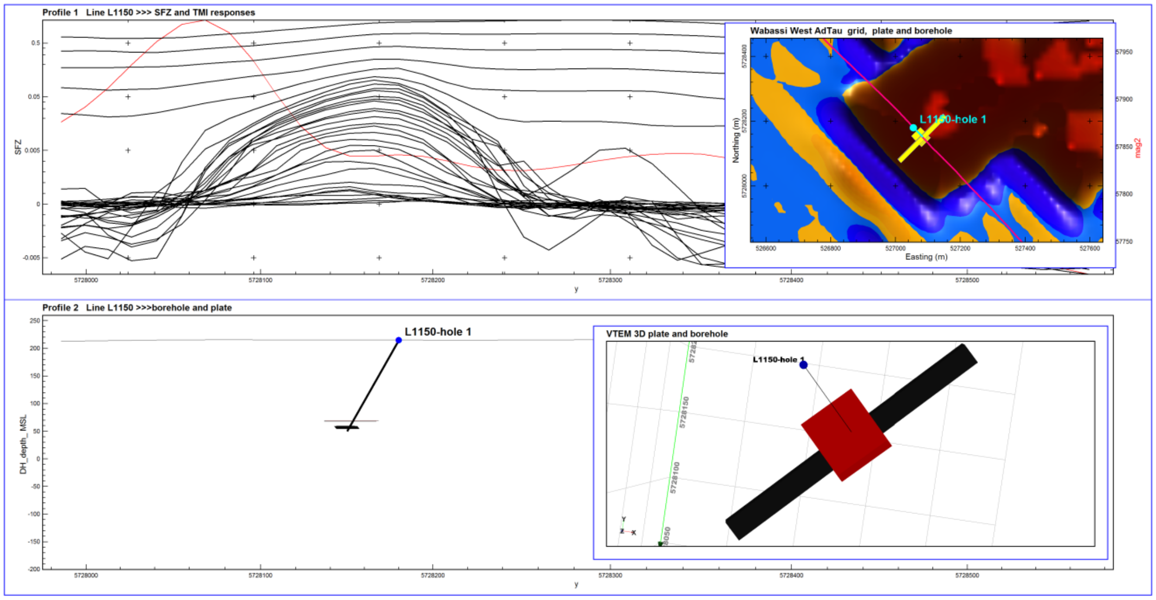

L1150 two vertically separated smaller plates of different strike lengths, higher conductivity, higher priority due to being part of a 1400m long conductive horizon. Hole intersects center of both deeper and shallower plates. Differential GPS Hole sighting important as plates are small, easy to miss.

Wabassi West "Subzone 3 L1290"

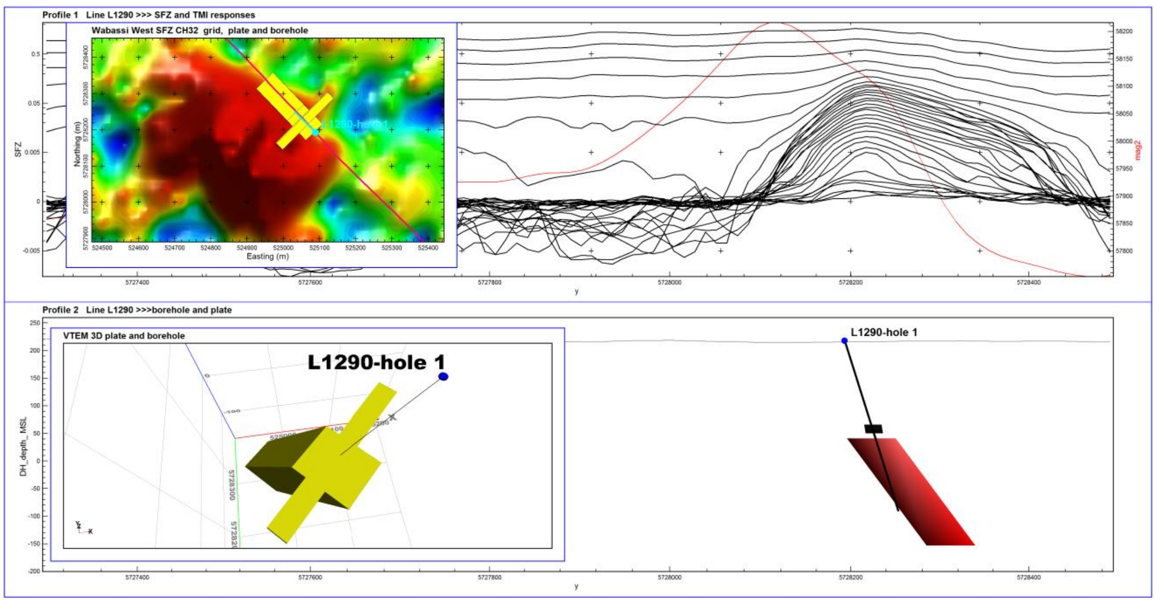

L1290 Two plates return similar fits, a thinner shallower one, and deeper thicker one with significant depth extent. One hole intersects the center of both pates. The hole intercept is the shallow plate, the EOH is out the side of the thicker deeper plate as shown on the lower right panel.

Wabassi West "Subzone 3 L1300"

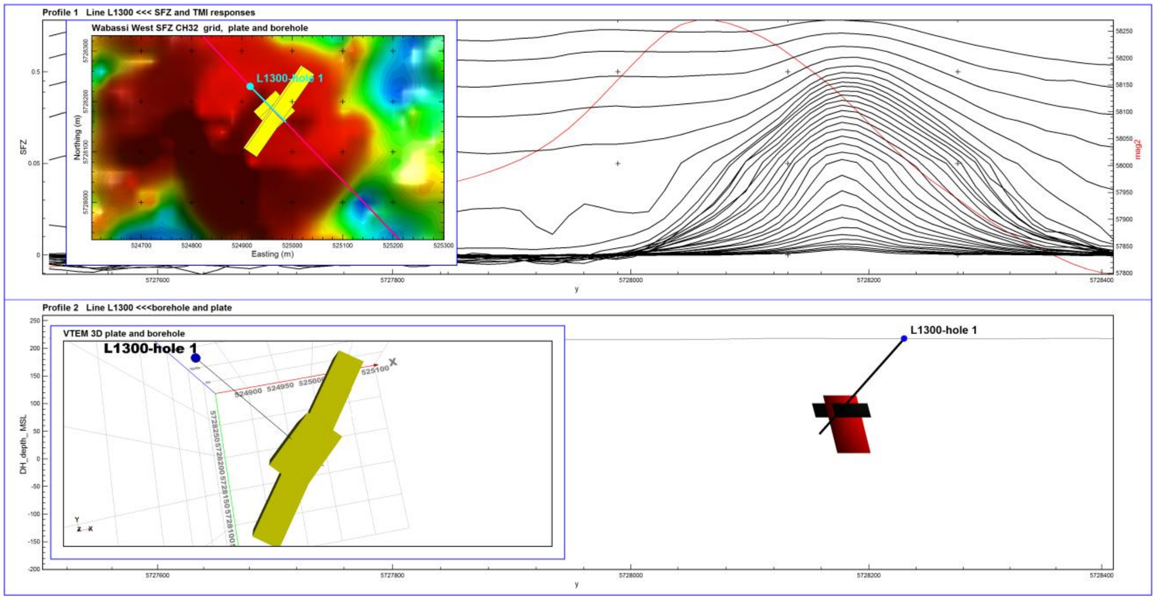

L1300- Two thick plates of different morphology fit the field response, one drill hole provided that intersect the plate centers of both plates. The hole intersects the top center of the deeper thicker plate and exits out its side as shown in the lower right panel.

Wabassi West "Subzone 3 L1310"

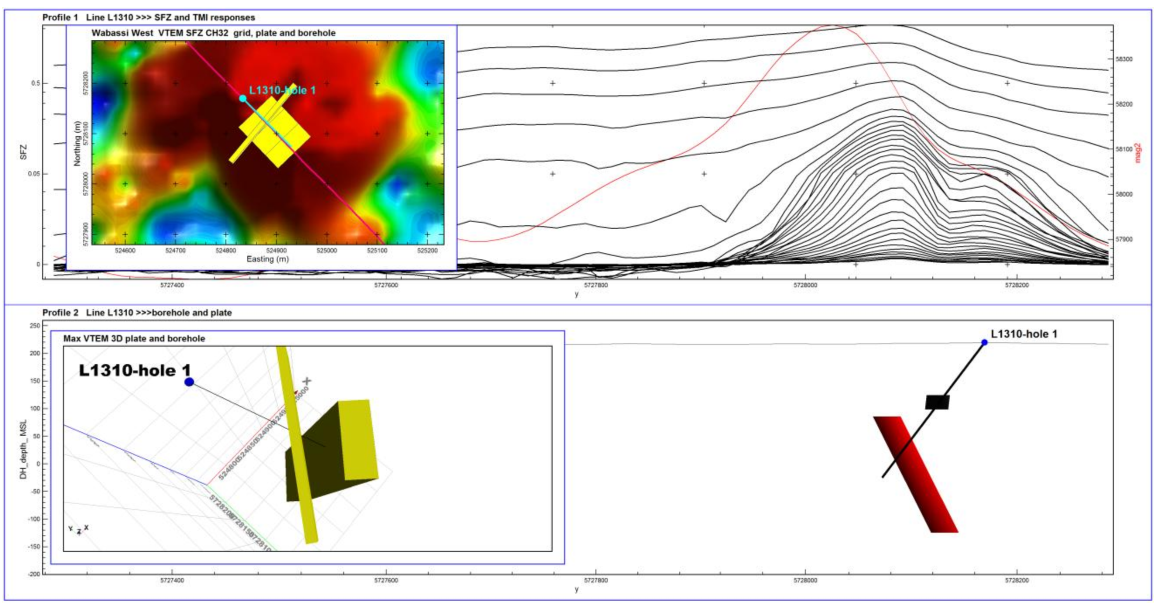

L1310 Two plates, one shallower and thin, one deeper and thick, fit this response. The shallow thin plate returns a better visual fit, though the calculated fit errors are the same for both modeled plates. One hole is provided to pierce both plates, Hole one intersects the center of the thin shallower plate at -110 m, and also intersects the top right side of the deeper plate at -180 m. High priority.

Wabassi West "Subzone 3 L1320"

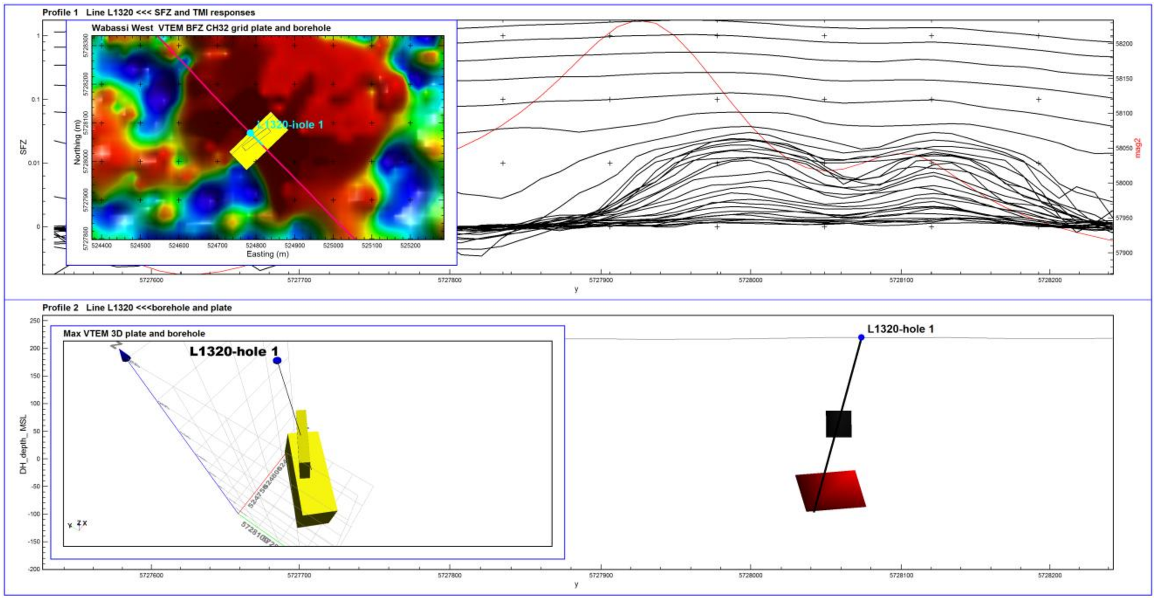

L1320- Two plates, one shallower, one deeper, fit this response. The shallow plate returns a better visual fit, though the calculated fit errors are the same. One hole intersects the center of the thin shallower plate at -140 m, and intersects the deeper plate at -250 m. High priority.

Appendix D-Notes on Magnetic Modeling

Appendix E-Wabassi-Max historic drill hole list

Hole_id	Easting	Northing	Dip	Azimuth	Elevation	Length
10WA-01	527657	5728911	-65	120	212	234.7
10WA-02	531967	5734539	-75	145	204	154.2
10WA-03	527705	5734265	-50	325	217	267.3
10WA-04	525860	5733240	-75	145	218	301.75
10WA-05	525860	5733240	-75	325	218	341.38
10WA-06	525735	5733145	-65	145	217	216.41
10WA-07	525355	5732415	-85	145	216	213.4
10WA-08	525978	5733062	-60	290	219	302
10WA-09	525761	5733141	-60	290	218	192
10WA-10b	525800	5733129	-60	110	218	266
10WA-11	525948	5733287	-68	280	221	288
10WA-12	525896	5733172	-65	290	220	1
08WA-01	521362	5739350	-55	270	226	14.9
08WA-02	522415	5738860	-55	300	220	160.6
08WA-04	518084	5734790	-65	330	223	347.12
10WA-13	525408	5732393	-55	290	215	164
08MX-01	518586	5734504	-55	280	223	426.72
08MX-02	518586	5734504	-75	270	223	502.92
08MX-03	518084	5734790	-70	270	223	362.7
08MX-04	521628	5735853	-55	270	220	207.26
08MX-05	518690	5734200	-75	270	224	787.35
08MX-06	518290	5734200	-70	90	225	739.07

Appendix F- VTEM Target Plate Parameters

File	Plate	x	y	z	Depth	Dip	Dip Dir	Length	De-pExt	Cond-Thick	Cond	Thick
WabWest-L1040	1	527767	5728990	118	-96	74	136	200	55.8	92	12.8	7.2
WabWest-L1050	1	527740	5728900	61	-152	27	136	58	19.8	181	20.7	8.7
WabWest-L1050	2	525071	5731649	38	-178	21	136	72	34.0	105	10.7	9.8
WabWest-L1060	1	527715	5728790	83	-130	23	136	43	42.3	278	33.5	8.3
WabWest-L1060	2	527720	5728780	63	-150	91	-45	200	12.5	1319	59.4	22.2
WabWest-L1070	1	527690	5728660	94	-118	20	136	30	20.3	712	97.6	7.3
WabWest-L1070	2	527695	5728650	76	-136	66	-45	200	6.6	2858	186.2	15.4
WabWest-L1120	1	527335	5728326	59	-155	16	136	35	12.1	780	97.8	8.0
WabWest-L1120	2	527333	5728329	39	-174	58	136	200	11.2	2625	229.7	11.4
WabWest-L1130	1	527238	5728270	78	-136	16	136	38	5.6	754	81.3	9.3
WabWest-L1130	2	527241	5728259	68	-145	74	-45	200	5.7	2531	173.6	14.6
WabWest-L1140	1	527151	5728214	64	-150	14	136	41	5.9	837	80.9	10.4
WabWest-L1140	2	527155	5728215	61	-152	82	-45	200	6.8	3083	205.8	15.0
WabWest-L1150	1	527077	5728153	69	-146	15	136	41	5.1	759	72.2	10.5
WabWest-L1150	2	527083	5728147	59	-156	70	-45	200	5.2	3279	233.8	14.0
WabWest-L1290	1	525060	5728225	66	-150	82	-45	200	16.6	1351	58.7	23.0
WabWest-L1290	2	525059	5728221	40	-176	122	136	64	229.0	152	2.4	63.3
WabWest-L1300	1	524975	5728180	100	-118	80	-55	200	25.7	966	35.6	27.2
WabWest-L1300	2	524970	5728175	115	-103	99	136	60	106.3	331	8.6	38.4
WabWest-L1310	1	524872	5728122	125	-93	95	-50.00	200	26.9	1451	149	9.74
WabWest-L1310	2	524923	5728076	85	-133	70	316	91	222.7	234	6.9	34.1

WabWest-L1320	1	524801	5728059	87	-133	90	143	82	48.8	812	58	14
WabWest-L1320	2	524810	5728050	-25	-245	99	136	150	67.0	647	11.5	56.2
Max-L2180	1	518279	5734800	104	-119	103	270	400	411.1	20	0.5	39.2
Max-L2190	1	518205	5734650	85	-137	133	270	400	426.8	24	1.1	21.1
Max-L2300	1	519029	5733000	23	-201	73	90	200	500.0	18	0.3	51.7
Max-L3280	1	521464	5718305	23	-192	86	270	177.9	378.7	64	2.143	29.9
Max-L3280	2	522695	5718300	40	-174	119	90	177.9	283.8	161	3.4316	46.9
Max-L4080	1	519705	5717342	176	-45	102	179	400	94.6	249	na	na
Wabassi-L4380	1	526035	5733510	96	-132	86	130	42	36.4	4696	871.1	5.4
Wabassi-L4390	1	525975	5733320	-5	-227	116	135	69	273.4	431	10.4	41.4
Wabassi-L4400	2	525631	5733560	35	-182	46	135	200	8.7	3003	353.3	8.5
Wabassi-L4420	1	525685	5732970	99	-117	64	135	100	11.6	2236	430.4	5.2
Wabassi-L4420	2	525555	5733150	63	-153	90	135	51	7.3	76245	1,863.3	40.9
Wabassi-L4450	1	525462	5732497	97	-120	86	53	27	213.0	351	27.3	12.9
Wabassi-T4780	1	525355	5732445	119	-97	28	135	63	3.8	2411	169.4	14.2

Appendix G- VTEM Target Drill Hole Parameters

Grid	Hole_ID	Easting	Northing	Dip	Azimuth	Elevation	Length	Intercept
Wabassi-West	L1040-hole 1	527835	5728952	-60	300	212	170	140
Wabassi-West	L1050-hole 1	527798	5728844	-65	315	213	200	170
Wabassi-West	L1050-hole 2	525145	5731583	-66	316	217	220	200
Wabassi-West	L1060-hole 1	527757	5728747	-73	315	212	190	160
Wabassi-West	L1070-hole 1	527720	5728629	-76	315	212	160	145
Wabassi-West	L1120-hole 1	527353	5728301	-80	325	215	200	180
Wabassi-West	L1130-hole 1	527208	5728302	-71	135	214	170	160
Wabassi-West	L1140-hole 1	527134	5728235	-80	135	215	170	155
Wabassi-West	L1150-hole 1	527055	5728181	-75	136	215	170	155
Wabassi-West	L1290-hole 1	525089	5728193	-75	315	218	320	160
Wabassi-West	L1300-hole 1	524917	5728230	-60	135	218	200	130
Wabassi-West	L1310-hole 1	524834	5728170	-61	135	220	280	110
Wabassi-West	L1320-hole 1	524786	5728074	-82	136	220	320	140
Max	L2180-hole 1	518390	5734800	-60	270	224	250	170
Max	L2190-hole 1	518332	5734650	-60	270	223	240	190
Max	L2300-hole 1	519190	5732998	-60	270	225	350	260
Max	L3280-hole 1	521325	5718300	-60	90	217	330	260
Max	L3280-hole 2	522540	5718301	-60	90	215	300	230
Max	L4080-hole 1	519699	5717390	-60	180	220	110	80
Wabassi	L4380-hole 1	526090	5733435	-60	323	233	200	180
Wabassi	L4390-hole 1	525859	5733445	-60	137	216	350	280
Wabassi	L4400-hole 1	525616	5733585	-80	145	217	200	190
Wabassi	L4420-hole 1	525734	5732913	-60	320	216	160	145
Wabassi	L4420-hole 2	525536	5733173	-80	145	215	180	160
Wabassi	L4450-hole 1	525530	5732420	-60	320	216	250	180
Wabassi	T4780-hole 1	525403	5732481	-60	233	216	120	110

Appendix H- InfiniTEM Target Plate and Drill Hole Parameters

Plates

File	Plate	x	y	z	Depth	Dip	DipDir	Length	DepExt	Cond-Thick	Cond	Thick
Wabassi-L300utm	1	525845	5733220	97	-118	93	271	400	40.8	2774	na	na
Wabassi-L400utm	1	525850	5733110	109	-106	89	269	200	34.8	3538	231	15.3
Wabassi-L500utm	1	525925	5732975	-68	-283	92	265	200	216.4	853	28	31.1
Wabassi-L600utm	1	525592	5732969	203	-12	40	265	200	98.7	23289	na	na
Wabassi-L1200utm	1	525360	5732435	170	-45	101	315	200	15.1	8914	2408	3.7

Drill Holes

Grid	Hole_ID	Easting	Northing	Dip	Azimuth	Elevation	Length	Intercept
Wabassi	L300-hole 1	525770	5733245	-60	110	217.91	200	165
Wabassi	L400-hole 1	525780	5733136	-60	110	219.21	170	135
Wabassi	L500-hole 1	525730	5732980	-60	90	219.6	450	360
Wabassi	L600-hole 1	525530	5732967	-60	90	215.25	90	55
Wabassi	L1200-hole 1	525390	5732424	-60	290	215.78	75	65

Appendix I-Archive DVD